UNIVERSIDAD POLITÉCNICA DE MADRID
Escuela Técnica Superior de Ingenieros de Caminos, Canales y Puertos

Predicting the fire performance of flame retardant polymer composites with data-driven approach

DOCTORAL THESIS

Submitted for the degree of Doctor by:

Junchen Xiao
Diplom-Ingenieur

Madrid, 2024

UNIVERSIDAD POLITÉCNICA DE MADRID
Escuela Técnica Superior de Ingenieros de Caminos, Canales y Puertos

Doctoral Degree in Engineering of Structures, Foundations and Materials

Predicting the fire performance of flame retardant polymer composites with data-driven approach

DOCTORAL THESIS

Submitted for the degree of Doctor by:

Junchen Xiao
Diplom-Ingenieur

Under the supervision of:
Dr. De-Yi Wang

Madrid, 2024

Title: Predicting the fire performance of flame retardant polymer composites with data-driven approach

Author: Junchen Xiao

Doctoral Programme: Engineering of Structures, Foundations and Materials

Thesis Supervision:

Dr. De-Yi Wang, senior researcher, IMDEA Materials Institute, Madrid, Spain (Supervisor)

External Reviewers:

Dr. Raquel Sánchez Diáz, Senior Scientist, Zoetech SL

Dr. Guang-Zhong Yin, Researcher, Francisco de Vitoria University

Thesis Defense Committee:

Thesis Defense Date:

Acknowledgement

I am delighted to express my emotions here, to all my friends that lend me helping hands in my PhD study. First and foremost, I would like to show my sincere gratitude to my professors: Prof. De-Yi Wang and Prof. Maciej Haranczyk. I appreciate their collaboration in this field, giving me the opportunity to play with data-driven technique and material investigation. Not only did they impart a wealth of knowledge to me in the fields, but they also greatly assisted me in learning how to express my views, complete a project, collaborate and share with others, and approach life and work with the right attitude. I am truly grateful to have encountered two outstanding and dedicated mentors during this important phase of my doctoral studies.

Also, I would like to extend my appreciation to my colleagues for their helpful guides and suggestions in writing programs, solving problems, doing experiments and spending the four years joyfully. Special thanks to Giulia for her help in programming the machine learning codes, which lays the foundation of my work. I am grateful to our "secretary" in HPPN group, I would do nothing without Jimena's help. I also appreciate the help from Jose, Xiang and Xiaolu, for their assistance is essential to finish my work. Similarly, I cherish and appreciate the time spent with my other friends. I don't want to list everyone's names, as that would resemble a roster. Therefore, I will simply say that I am grateful for your companionship, I enjoy working with you, and I will never forget your support.

Additionally, I am grateful to those who helped me in dealing with the paper works in IMDEA materials. Without their help, the Spanish documents and forms could drive me crazy.

Thank you for your companionship; I will never forget the time we spent working together and enjoying weekends and holidays!

Abstract

Since we have stepped into the 21st century, new materials and technologies play more and more significant roles in the construction of human civilization. The flame-retardant polymer composites (FRPCs) have found various applications in human society due to the versatility, ease of processing, customizability, cost-effectiveness and safety. Nowadays, traditional research workflow has been integrated with modern computational technology. It has widely spread and emerged in various traditional disciplines that utilizing high-performance computers to construct the digital models for complex humanities and social sciences, physical and chemical systems, as well as engineering technologies. In the field of materials science, by using machine learning (ML) models, the data-driven method has been used to predict the thermal, mechanical and combustion-related properties of different materials, and recognize the type of polymers and phase of physical/chemical processes, which effectively enhances the research process, reduces the cost and lower environmental impact.

In this study, we employed various ML algorithms to develop accurate, robust, and generalizable models for predicting the results of cone calorimeter test (CCT) and mechanical performance of FRPCs. Initially, we compiled and collected 828 data of related formulations from approximately 150 publications, involving the types of raw materials, selection of processing parameters, and final properties. Based on different flame-retardant (FR) mechanisms, we divided FRPCs' data by the FR additives: inorganic metal hydroxide (MH), metal-organic framework (MOF) and layered double hydroxide (LDH), marked as different FR-systems. Mainly, the Random Forest (RF), Support Vector Machine (SVM) and their linear combination were used to build ML frameworks to predict the target properties of FRPCs in different FR-systems.

In the MH-system, RF models achieved coefficients of determination (R2) of over 0.81 in all test sets. Feature screening indicated that the distribution and amount of MH in polymer composites had the greatest impact, followed by the content of effective FR elements in other synergists. The models in MOF-system had predictive accuracy generally exceeded 80%. Model interpretation showed that not only the structure and type of MOFs significantly influenced the performance of FRPCs, but also the properties of polymer matrix and incorporation methods of FR additives were important. At last, LDH models exhibited good predictive accuracy, particularly in predicting Time to Ignition (TTI), where the R2 reached 0.9 and the

Area Under Curve (AUC) was also 90%. The feature analysis revealed the key features as organic modification and interlayer spacing of LDH strongly affecting the heat release in CCT. Besides the prediction of separate values, the simulation of HRR development presented the potential of ML framework to replace the physical experiments. The simplified HRR curves containing important development tendencies have been predicted accurately, restored the heat release of FRPCs in CCT qualitatively and quantitatively. Meanwhile, the predictive performance of final ML models involving all kinds of FR additives, including MH, MOF, LDH, intumescent FRs, and other organosilicon, nitrogen-containing chemicals, exhibited the potential of the construction of a comprehensive, all-FR-systems-contained and prediction-oriented big-data model.

Resumen

Desde que hemos entrado en el siglo XXI, los nuevos materiales y tecnologías desempeñan roles cada vez más significativos en la construcción de la civilización humana. Los compuestos poliméricos retardantes de llama (FRPCs, por sus siglas en inglés) han encontrado diversas aplicaciones en la sociedad humana gracias a su versatilidad, facilidad de procesamiento, personalización, rentabilidad y seguridad. Hoy en día, el flujo de trabajo tradicional de investigación se ha integrado con la tecnología computacional moderna. Esto se ha extendido y emergido ampliamente en diversas disciplinas tradicionales, utilizando computadoras de alto rendimiento para construir modelos digitales de sistemas complejos en humanidades, ciencias sociales, sistemas físicos y químicos, así como tecnologías de ingeniería. En el campo de la ciencia de materiales, mediante el uso de modelos de aprendizaje automático (ML, por sus siglas en inglés), el método basado en datos se ha utilizado para predecir propiedades térmicas, mecánicas y relacionadas con la combustión de diferentes materiales, además de identificar el tipo de polímeros y las fases de procesos físicos/químicos. Esto mejora eficazmente el proceso de investigación, reduce los costos y disminuye el impacto ambiental.

En este estudio, empleamos varios algoritmos de ML para desarrollar modelos precisos, robustos y generalizables que predigan los resultados de las pruebas de calorímetro cónico (CCT) y el desempeño mecánico de los FRPCs. Inicialmente, recopilamos y reunimos 828 datos de formulaciones relacionadas de aproximadamente 150 publicaciones, abarcando tipos de materias primas, selección de parámetros de procesamiento y propiedades finales. Basándonos en diferentes mecanismos de retardancia de llama (FR), dividimos los datos de FRPCs según los aditivos FR: hidróxido metálico inorgánico (MH), estructuras metal-orgánicas (MOF) y hidróxido doble laminar (LDH), marcados como diferentes sistemas FR. Principalmente, utilizamos Random Forest (RF), Support Vector Machine (SVM) y su combinación lineal para construir marcos de ML que predijeran las propiedades objetivo de los FRPCs en diferentes sistemas FR.

En el sistema MH, los modelos RF lograron coeficientes de determinación (R^2) superiores a 0,81 en todos los conjuntos de prueba. El análisis de características indicó que la distribución y la cantidad de MH en los compuestos poliméricos

tuvieron el mayor impacto, seguidas por el contenido de elementos FR efectivos en otros sinergistas. Los modelos en el sistema MOF tuvieron una precisión predictiva que generalmente superó el 80%. La interpretación del modelo mostró que, además de la estructura y el tipo de MOFs, las propiedades de la matriz polimérica y los métodos de incorporación de los aditivos FR también influyeron significativamente en el rendimiento de los FRPCs. Finalmente, los modelos LDH exhibieron una buena precisión predictiva, particularmente en la predicción del Tiempo de Ignición (TTI), donde el R^2 alcanzó 0,9 y el Área Bajo la Curva (AUC) también fue del 90%. El análisis de características reveló que las modificaciones orgánicas y el espaciado interlaminar del LDH afectaron fuertemente la liberación de calor en el CCT.

Además de la predicción de valores individuales, la simulación del desarrollo de la HRR presentó el potencial del marco de ML para reemplazar los experimentos físicos. Las curvas HRR simplificadas, que contenían tendencias importantes de desarrollo, fueron predichas con precisión, restaurando cualitativa y cuantitativamente la liberación de calor de los FRPCs en el CCT. Mientras tanto, el desempeño predictivo de los modelos finales de ML, que involucraron todo tipo de aditivos FR, incluidos MH, MOF, LDH, FR intumescentes y otros químicos organosilícicos y nitrogenados, mostró el potencial para construir un modelo integral, orientado a la predicción y que abarque todos los sistemas FR.

Table of Contents

List of Figures

List of Tables

Abbreviations and Acronyms

UPM	Universidad Politécnica de Madrid
CCT	Cone calorimeter test
FR	Flame-retardant
FRPC	Flame-retardant polymer composite
ML	Machine learning
RF	Random Forest
SVM	Support Vector Machine
MH	Metal hydroxide
MOF	Meta-organic framework
LDH	Layered double hydroxides
TTI	Time to ignition
pHRR	peak heat release rate
THR	total heat release
FRI	flame-retardant index
ROC	Receiver operating characteristic
AUC	Area under curve
MDH	Magnesium di-hydroxide
ATH	Aluminium tri-hydroxide
PBU	Primary building unit
SBU	Secondary building unit
ZIF	Zeolitic imidazolate framework
MIL	Materials Institute Lavoisier
UIO	University of Oslo
SDBS	sodium dodecyl benzene sulfonate

IFR	intumescent flame retardant
FEM	finite element method
DFT	density functional theory
DT	decision tree
kNN	k-nearest neighbours
ANN	artificial neuro network
FI	feature importance
EVA	ethylene vinyl acetate
LOI	limiting oxygen index
SDS	Sodium dodecyl sulphate
APP	ammonium polyphosphate
EP	epoxy resin
CBC	cobalt basic carbonate
TPU	thermoplastic polyurethane
PE	polyethylene
LDPE	low density PE
MDPE	Medium density PE
HDPE	High density PE
PLA	Polylactic acid
oMMT	Organic-modified montmorillonite
VTES	Vinyltriethoxysilane
DDM	diamino diphenyl methane
PER	Pentaerythritol
TGA	thermo gravimetric analysis
SMOTE	Synthetic Minority Over-Sampling Technique
MLP	multi-layer perceptron
RFE	Recursive Feature Elimination
CV	Cross-validation

MAE	Mean Absolute Error
RMSE	Root Mean Square Error
R2	coefficient of determination
SHAP	SHapley Additive exPlanations
PA6	polyamide 6
CM	confusion matrix

Data-driven investigation of FRPCs

1. Introduction

1.1. Flame-retardant polymer composites (FRPCs)

The history of humankind is critically influenced by the application and technology of materials. Seen from the earliest stone age to our modern society, the innovation and development of materials has not only contributed to the blossom of technologies, but also delivered the profound impact on the economic, social and cultural evolutions. The usage of metal materials has enabled the occurrence of diverse and complex structures and constructions. However, as we step into the new century, new requirements and challenges are being posed to the materials. Polymer materials, which have attracted significant attention and achieved artificial synthesis after the industrial revolution, have been widely researched by a considerable number of individuals and organizations from both scientific and commercial fields due to their special advantages in material properties. [1,2] Compared to metallic materials, polymers are light-weighted, flexible and highly processable, which contribute to lowering the cost of production and transportation. [3] Polymers are widely used in packing materials, medical apparatus, buildings and infrastructure, and daily supplies, as in Fig. 1-1. [4–6] Furthermore, polymer materials are highly customizable through the addition of different functional components to adjust the chemical and physical properties and be competent to in specific applications. At the same time, the development of science and technology has inspired creativity and innovation of polymer materials in recyclability, environmental-friendliness, and novelty. [7]

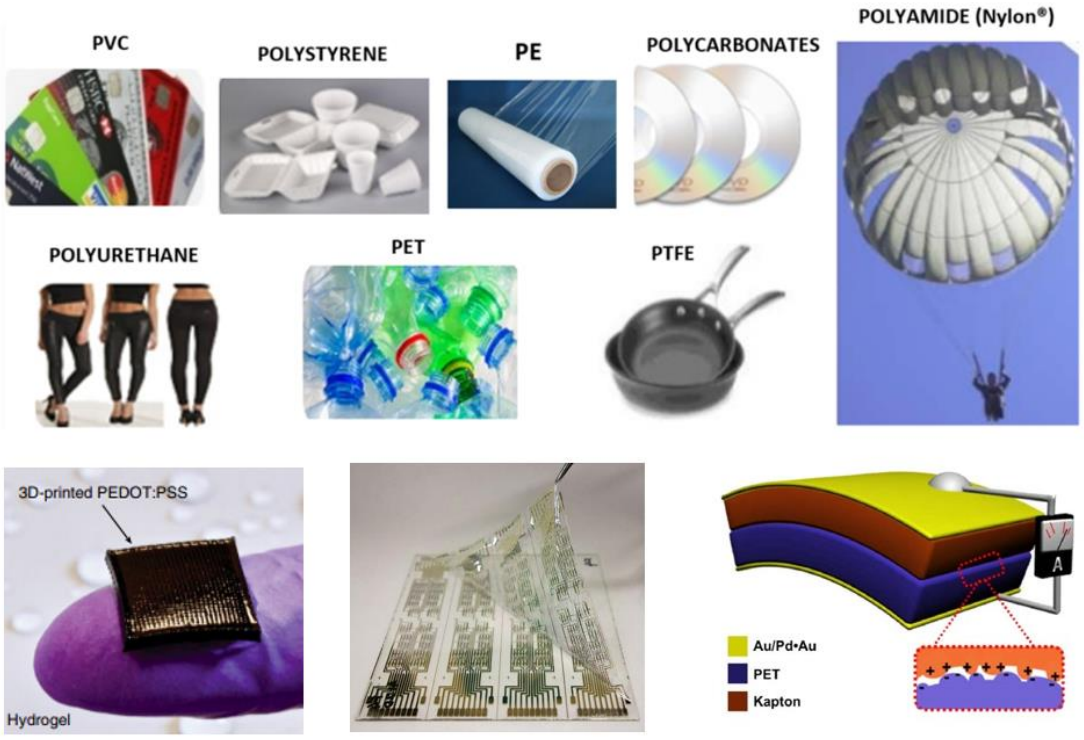

Fig. 1-1 Application of polymer materials

There are, of course, problems which should be addressed in the application of polymer materials. The first famous synthetic thermoplastic "celluloid", invented by Alexander Parkes in 1855, has been greatly used in staple goods, and photographic films in particular. [8] But this polymer is prone to aging and is highly flammable: exposing to temperature > 150 °C leads to spontaneous ignition. After celluloid, other synthetic polymers like Bakelite, Nylon, Teflon, and many polymer materials have been pioneered and employed in almost every aspect of our lives. A critical problem, however, still remains unsolved: how to protect the polymeric parts from the high temperatures and flames so that they shall not develop into hazards for humans?

With the rapid increasing in the number of applications of polymer materials in the living environment, there are more and more fire hazards occurring in different sizes and shapes every year, which lead to great damage to properties, human health, environment, economy and society. [9] However, the development of polymer materials always follows this principle: identifying problems during the usage and optimizing materials throughout these problems; They are intrinsically complementary, just like spears and shields. In the early stage (before 1950s) of flame-retardant polymer materials, traditional method to prevent the fire hazards was to use inorganic materials like asbestos. Later, the investigation of FR

additives became a key area of FR polymer materials, aiming to improve the fire performance of the polymers through physical, chemical mechanisms and their interactions. [10,11] Since 1980 [12,13], metal hydroxides are considered a good choice attributed to its smoke-suppression [14], nontoxicity [15], and low cost [16,17]. Meanwhile, the FR additives that contain halogen, phosphorous and nitrogen are highly effective in preventing the development and spread of flames. However, with the increasing concern about the environment and human health, the investigation of low-toxic, eco-friendly FR additives is crucial in recent years.

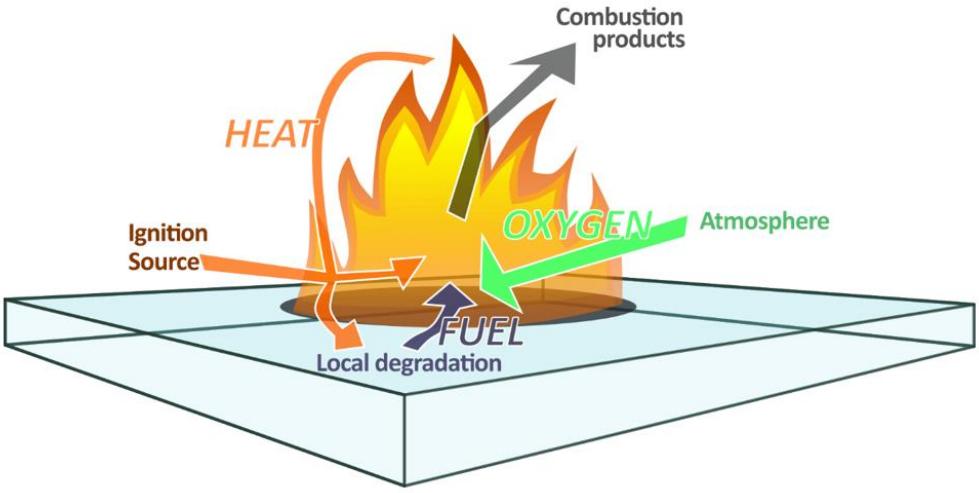

Fig. 1-2 Combustion of a flammable sample, fire growth on the surface.

The combustion is a complex process involving various chemical and physical reactions between the three fundamental elements of fire: fuel, oxygen and heat. It is usually featured with released heat, unhealthy smoke and strong fire. As shown in Fig. 1-2, the flammable matter, e.g. polymer matrix, is exposed to an external heat source, which leads to increased temperature of the surface area. In the classic Cone Calorimeter Test (CCT), this ignition source is electric spark, combined with the heating cone upon the sample surface. After reaching certain degree of the local temperature, the degradation and melting begins. With the support of oxygen from the external atmosphere, thermal oxidation reactions occur in the combustion front, together with the release of energy and reaction products in both solid and gas phases. In return, released heat also contribute to the temperature rise of the sample. With the development of fire, the flame front spreads to other area and in the direction of depth, till the whole flammable sample is engulfed in fire. In this process, the transfer of heat and materials is the key to

the development of combustion. As a consequence, all FR effects can be attributed to giving impact on the one or more part of this burning cycle.

Up to now, there are many types of flame retardants, induvial or combined used in polymer composites. [18] The well-known halogen flame retardants have high FR efficiency and moderate cost. Halogen additives decompose at the temperature around 200 – 300 °C, releasing plenty of free radicals (halogen) that can capture the free radicals produced by the decomposition of polymer combustion. These reactions break down the reaction chains of combustion, thus postpone and suppress the development of fire. At the same time, the reaction product (halide) is difficult-combustible, diluting the oxygen content in the environment. However, a crucial disadvantage makes this type of flame retardants nor recommended: the burning products are toxic, can greatly harm the health of humankind and environment.

As a popular flame retardant in many kinds of polymers, the metal hydroxides are simple and easy to use. [19] This inorganic filler is simply inflammable, can directly decrease the fuel content of polymer composites. Furthermore, hydroxides tend to lose their water under moderate temperatures as in equation (1), usually around 200-350 degree Celsius. This decomposition reaction is endothermic with a positive decomposition entropy, that is to say, some heat will be absorbed leading to a cooling effect of the surrounding environment. Meanwhile, the released water can dilute the concentration of the flammable matters in the combustion area, containing the spread of fire. In addition, the metal oxide produced by the decomposition reaction also plays a role in the flame retardancy: a sufficiently strong and dense physical barrier is able to slow the development of flame effectively. Due to the simple mechanisms, the MH-system of flame retardants is a proper choice to be started with in the machine learning modelling.

$$Me(OH)_y \xrightarrow{\Delta} \frac{1}{2}Me_2O_y + \frac{y}{2}H_2O \qquad \Delta H > 0 \tag{1}$$

The types of metals in MHs are diverse. Common MHs consist of magnesium, aluminium and calcium. Zinc hydroxide is occasionally used too. Magnesium di-hydroxide (MDH) and aluminium tri-hydroxide (ATH) are the most popular inorganic fillers added into the polymer matrix. MDH will start the decomposition when the temperature reaches 330 °C. In this process, 1300 kJ of heat is absorbed by every 1 g of MDH, producing 0.31 g of water and 0.69 g of MgO. ATH, compared to MDH, has a much lower initial decomposition temperature of 190 °C, and

decomposition entropy is 1050 kJ/g. Except for these two typical MHs, other similar hydroxides are also used, which properties are listed in Table 1-1.

However, precisely because of such simple FR mechanisms and the way they work, the main drawback of using MHs as flame retardants lies in their high loading. Their FR-efficiencies, compared to some organic additives, are not so satisfied to high requirements in certain applications. In addition, high loading leads to the deterioration of other properties of polymer composites, especially the mechanical properties. Also, the processability is strongly influenced by the addition of high melting point materials, increasing the difficulty and cost in production chain.

Table 1-1 Properties of typical metal hydroxides

MH Name	Chemical components	H2O*1	Oxide*1	E-dec*2	Tini*3
MDH	$Mg(OH)_2$	31.03	68.97	1300	330
ATH	$Al(OH)_3$	34.61	65.39	1050	190
CDH	$Ca(OH)_2$	24.33	75.67	986	300
HM	$4MgCO_3{\cdot}Mg(OH)_2{\cdot}4H_2O$	28	46	800	200
CHD	$Ca(OH)_2{\cdot}Mg(OH)_2$	27.27	72.73	1062	370
sHD	Ca(OH)2·yMg(OH)2·(1-y)MgO	16.89	78.59	685	320
U	MgO 37.5%, CaO 7.5%, SiO_2 0.6%; final loss 52.5%	1.93	45	1150	210
ZH	$Zn(OH)_2$	18.2	81.8	-	125

**1: equivalent content of water or metal oxide in weight percent in MHs*

**2: decomposition entropy in kJ/mol*

**3: initial decomposition temperature of MHs in °C*

Taking the limitation of single flame retardant into account, the usage of a combination of multiple FR additives with different focuses is the trend. Multiple types of flame retardants can sometimes have exceeded effect compared to the sum of individual contributions. Thus, our second FR-system is focusing on usage of a novel material: metal-organic framework (MOF), which is widely used in many fields and has demonstrated excellent universality in the polymer composites. [20,21]

The MOF, as the name means, is a combination of metal nodes with organic ligands, which contribute to forming a porous, organized crystalline structure in the microscale. The coordination of metal ions, also called the primary building unit (PBU) and organic molecules (secondary building unit, SBU) delivers a highly tuneable pore morphology and rigid scaffold for supporting or encapsulation of synergic flame retardants. [22] In addition, the organic components indie MOF enables better dispersion of the FR additives in the polymer matrix. Based on above-mentioned advantages, researchers have done many works on MOF-loaded polymer composites. Although researchers use primarily the typical MOFs, such as zeolitic imidazolate frameworks (ZIFs), MILs (MIL for Materials Institute Lavoisier) and UiOs (UiO for University of Oslo), there are many other types of MOFs due to the adjustability of the building units. Compared to inorganic fillers, the FR mechanisms of MOF along is considered to be attributed to the good dispersion of nano- or micro-sized particles, catalytic effect of metal atoms and additional reactions between organic ligands and polymer matrix. However, MOF is commonly combined with other flame retardants. In this situation, the second FR additive can be encapsulated into the pores of MOF structures or grafted onto the MOF skeletons. Sometimes, MOF is grown on the surface of other flame retardants to achieve a special structure.

Another "carrier" that is widely used as flame retardants is the layered double hydrate (LDH). Just as the name means, LDH consist of two-dimensional layers, in which different types of anions exist. Its structure is shown in Fig. 1-3. General formula of LDH can be described as $[(M^{II})_{1-x}(M^{III})_x(OH)_2]^{x+}(A^{m-}_{x/m})\bullet nH_2O]$, in which M^{II} and M^{II} are divalent and trivalent metal ions. Divalent ions are commonly Mg^{2+}, Ca^{2+}, Mn^{2+}, Fe^{2+}, Co^{2+}, Ni^{2+}, Cu^{2+}, or Zn^{2+}, and the trivalent ones are Al^{3+}, Fe^{3+}, Co^{3+} or Ni^{3+}. The anions in the interlayer spaces are typically CO_3^{3-},NO_3^- and Cl^-, which are balanced with the positive charges. Similar to MOF, the modification on LDH is suggested before being used as the FR additive. [23,24] In general, the anions are replaced with some big organic molecules, like sodium dodecyl benzene sulfonate (SDBS). This modification will not only introduce organic parts that containing FR elements into LDH, but also change the interlamellar distance between two neighboured layers.

Data-driven investigation of FRPCs

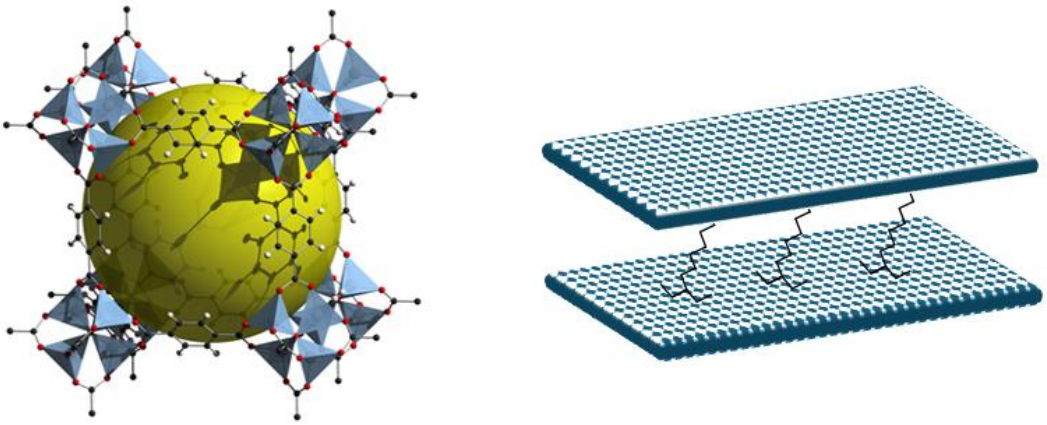

Fig. 1-3 Structure of flame retardants: MOF (left) and LDH (right)

The last typical FR additives are the intumescent flame retardants (IFRs), which has three main components: a carbonizing agent as carbon source, a carbonization catalyst as acid source and an expanding agent as gas source. [25–27] When the IFRs are heated to certain temperature, a series of physical and chemical reactions are activated, including the production of inorganic acid, catalytic carbonization of carbon-rich substances, formation of intumescent, porous carbon layers through the water vapor or other non-flammable gases. Once the physical barriers are formed, they are able to resist the fire attack, weaken the heat transfer between the undamaged polymer and fire front, and prevent the diffusion of gases. When the combustion area lacks the heat and oxygen, the fire of fuel will extinguish.

There are, of course, a lot of influence factors that affect the formation of a stable and strong barrier. [28] These factors come not only from the FR additives themselves, but also from the chemical structure and physical property of polymer matrix. The activation conditions of those reactions and their rates have also impact on the construction of carbon layer. As a result, the thickness, porosity, stability and strength of the layers decide the thermal protection effect. IFR can also be used together with other flame retardants due to its high FR efficiency. Less than 10 wt-% of IFRs can effectively improve the fire performance of the majority of polymer composites. [29] Accompanied by a small amount of other functional additives, polymer composites can reach more comprehensive improvement of performance in fire and mechanical aspects.

1.2. Fundamental of materials informatics

Traditionally, researchers conduct the trial-and-test method to develop new materials and improve the old parts. From this empirical science, we can already find that there is an intrinsic relationship between the raw materials, parameters of production processes and final properties of designed products. In 1997, G. B. Olson discussed the three-link chain model connecting science and engineering in material research. He built up an ascensive scientific link between Processing-Structure-Properties. [30] This deductive flow precisely describes the progressive cause-and-effect relationship from ingredients to produced samples. Typically, there are various phases appeared in the forging of metal or metal alloys. Different quenching methods or rates lead to different metallographic phases, which can be directly observed with optical microscope. This is the same in the production of polymeric samples, although their structural changes are difficult to see.

Based on this chain of causation, researchers now have different approaches to realize their goals. From the early empirical rules to the model-based theoretical science [31], to the mathematical simulation with computational techniques [32,33], to the (big)data-driven science in modern age [34], four research paradigms are summarized. With the development of high-power computers and mathematical fundamentals in simulation and modelling, the investigation of materials is accelerated. It is very helpful to use the finite element method (FEM) and density functional theory (DFT) to simulate a physical or chemical process occurred in a special sample or reaction. Through the simulation, the whole micro-scale process is visualized. They also reveal the possible results of the materials or reactions that are not tested. But a disadvantage of the computational simulation lies in the high requirements of corresponding acknowledges. It is necessary to have full understanding or, at least proper hypothesis, of the simulated processes for the setting of boundary conditions, development equations and mathematic limitations. This leads to a fact that the computational simulation is not well suited to a complex system, the combustion behaviour in particular.

Complicated processes, like the combustion of polymer composites with various flame retardants inside, have plenty of physical and chemical reactions happened simultaneously or successively. For such complex process, it is hardly to find the mathematical equations to describe and solve them. Despite this, we can go directly to the data themselves: the process-structure-property can be encoded or decoded into useful data, and the relationship between them is then converted into

the relationship between input and outcome data. Considering the inherent real-world connections, the transformed data is bound to retain the analogous characteristics. Investigate the patterns among these data from the statistic perspective becomes a promising way to enhance the understanding of the mechanisms behind the processes.

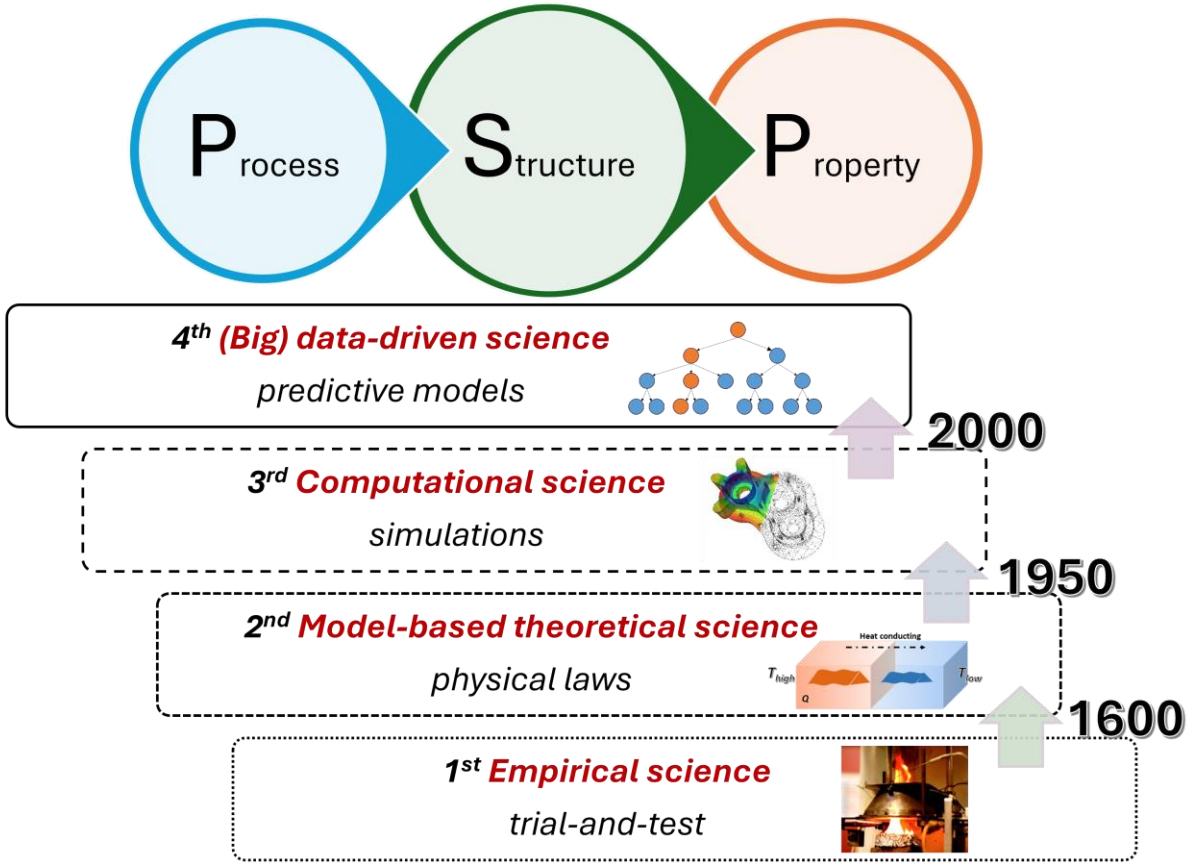

Fig. 1-4 Process-Structure-Property chain and four research paradigms in material science

In the data-driven approach, a complete and comprehensive dataset is the foundation. With this dataset, we are able to build a machine learning "black box", which can give predictions of the target properties, as shown in Fig. 1-5. To build the model, a machine learning algorithm is necessary. There are many kinds of algorithms based on various mathematical fundamentals, using different strategies to process and analyse the data, establishing corresponding models to make predictions. [35] The typical supervised algorithms include linear regressing, decision tree (DT), k-nearest neighbours (kNN), random forest (RF), support vector

machine (SVM) and artificial neuro networks (ANN) etc.. They can be explained with the same equation (2). The target properties are either numerical, physical or chemical results from experimental measurements like density, tensile strength, pH-value and solution conductivity, or categorical qualities like solubility, flammability and reactivity. Based on their intrinsic, natural relationships between materials and properties, these results can be described as a function of various independent variables indicated as the following X_1 to X_n. Due to the difficulty in understanding all the mechanisms and influencing factors behind the complicated systems, it is convenient to build the machine learning models for these systems on the basis of collected dataset. These models are acting like black boxes, providing the final predictions and analysing results through the ingestion of the input dataset, assessment of suitable models and optimization of hyperparameters. The judgements, decisions, classifications are then made to concrete questions and systems.

$$\vec{y}_{target\_properties} = f(X_1, X_2, \dots, X_n) = f\left(\vec{X}_{input\_features}\right) \tag{2}$$

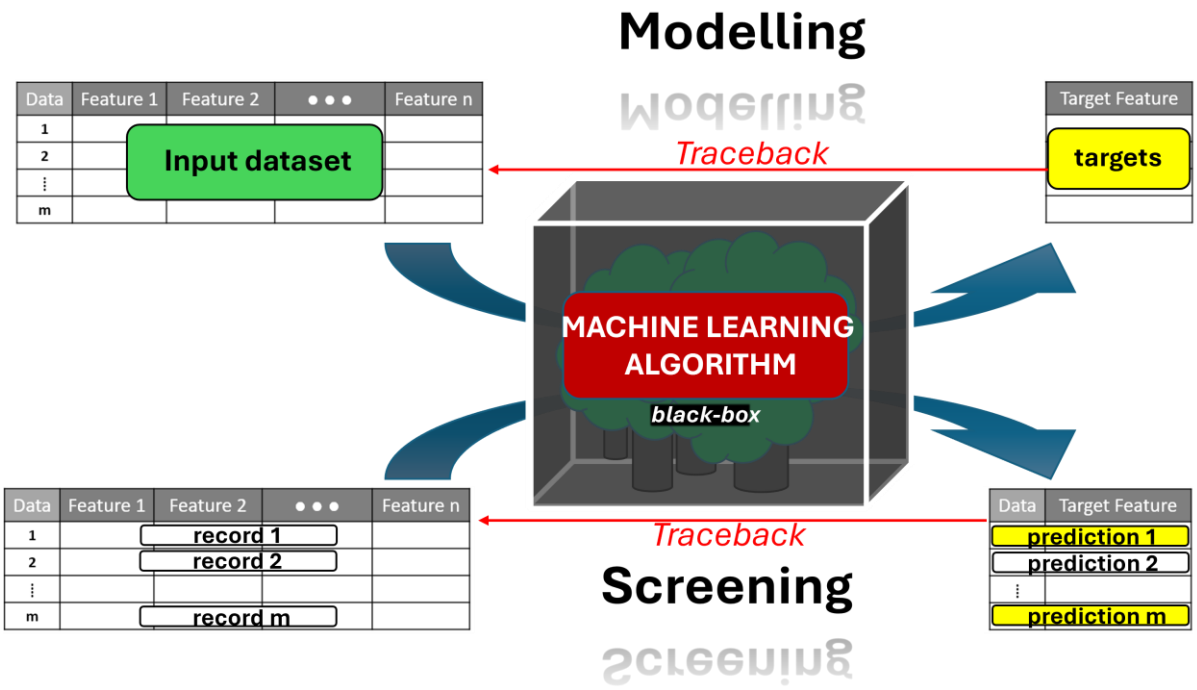

Fig. 1-5 Machine leaning "black box": training with input dataset and target feature to build proper models; making predictions with provided dataset to screen the formulations with wanted properties

The RF is a widely used method developed by Leo Breiman and Adele Cutler. [36,37] It is a tree-based ensemble method, in which thousands of decision trees "grow" randomly to make decisions. The prediction of DT follows the logistic

thinking: it walks through all necessary conditional control statements, reaches the end node along the correct route and returns the node as the decision, as illustrated in Fig. 1-6 (a). The final decision made by RF is obtained by averaging the results of all sub-estimators, usually the mathematical mean value. RF has the advantages of high accuracy and low overfitting. Moreover, it is beneficial to use the build-in function of feature importance (FI) to analyse the significant influencing factors. Through the FI, the RF models can be further improved, explained and used to screen wanted features and values. Meanwhile, researcher can gain deeper insight into the relationship between specific features and target properties. [38]

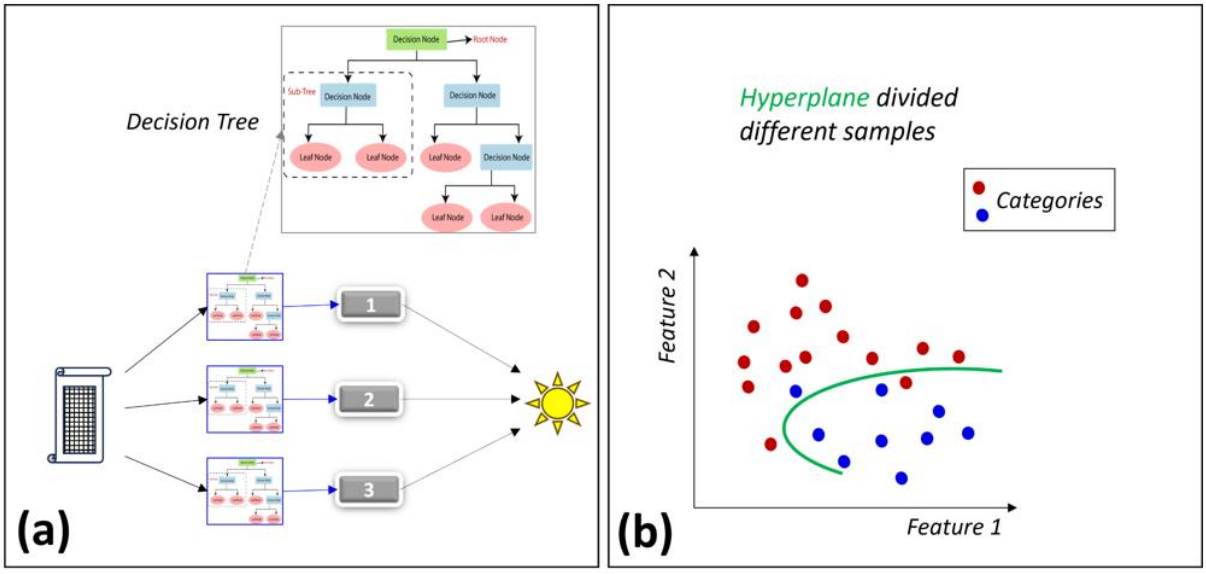

Fig. 1-6 Random Forest (RF) and Support Vector Machine (SVM)

Another algorithm, Support Vector Machine (SVM), is advantageous in dealing with complex dataset, and have sometimes better performance than other techniques due to many features like various kernel functions and capacity control brought by margin optimization etc. In SVM, a hyperplane with certain margin. Which can be adjusted depending on the situations, is constructed to classify the data points of different categories. [39,40] This algorithm and the variants have been widely applied in image classification like biological and medical studies, military application, hydrological science, agriculture sector, remote sensing etc.

Except for the individual algorithms, a third modelling method, which is actually built upon the former models, is constructed, called linear combination. It is in fact similar to RF, except that RF is the ensemble of many DTs, whereas the linear

combination is based on RF and SVM. In general, the performance of a predictive model is strongly related to the characteristics of dataset, complexity of research purpose and iterative process of this model itself. In some cases, a single model fails to live up to expectations due to certain limitations. In view of such facts, combining machine learning models is an effective strategy to improve predictive accuracy. All these algorithms will be explained in detail in the section or methodology.

2. State of the art

2.1. Flame retardants in FRPC

From the market research in 2020 [41], the worldwide consumption of all flame retardants amounts to over 2.39 million tons in 2019. Classified by the type of flame retardants, aluminium hydroxide takes the highest percentage of consumption with 38% as the single flame retardant in the worldwide. The second largest consumption of single additive is the organophosphorus type with 18%. However, the halogenated FR systems consisting of the brominated and chlorinated FR additives, have still compromising high percentage in consumption. This halogenated system is usually used together with the antimony oxides and has a part of 30% in total in the market. At last, the other FR additives, including inorganic phosphorus compounds, nitrogen and zinc-based flame retardants make up the remaining 14%.

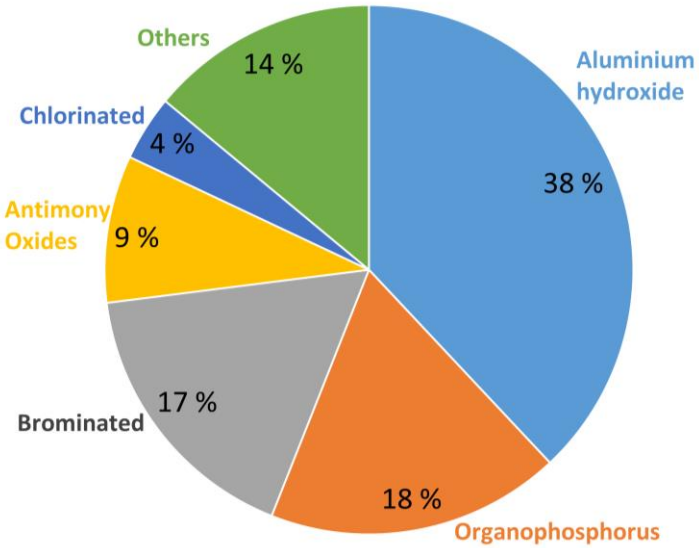

Fig. 2-1 Worldwide consumption of flame retardants by type, 2019 [41]

Seen from the research results, MH as the FR additive has significant enhancement in the fire performance of polymer composites, making it a widely used components in the FRPC. The analyse results of searching results of "Metal hydroxide" in the Web of Science™ shows the published works during the last two decades in Fig. 2-2. Till now, MH is still an effective additive in the competition

with other new kinds of FR additives, but the research focus has gradually shifted towards various modifications upon MH or using MH as kind of modifier.

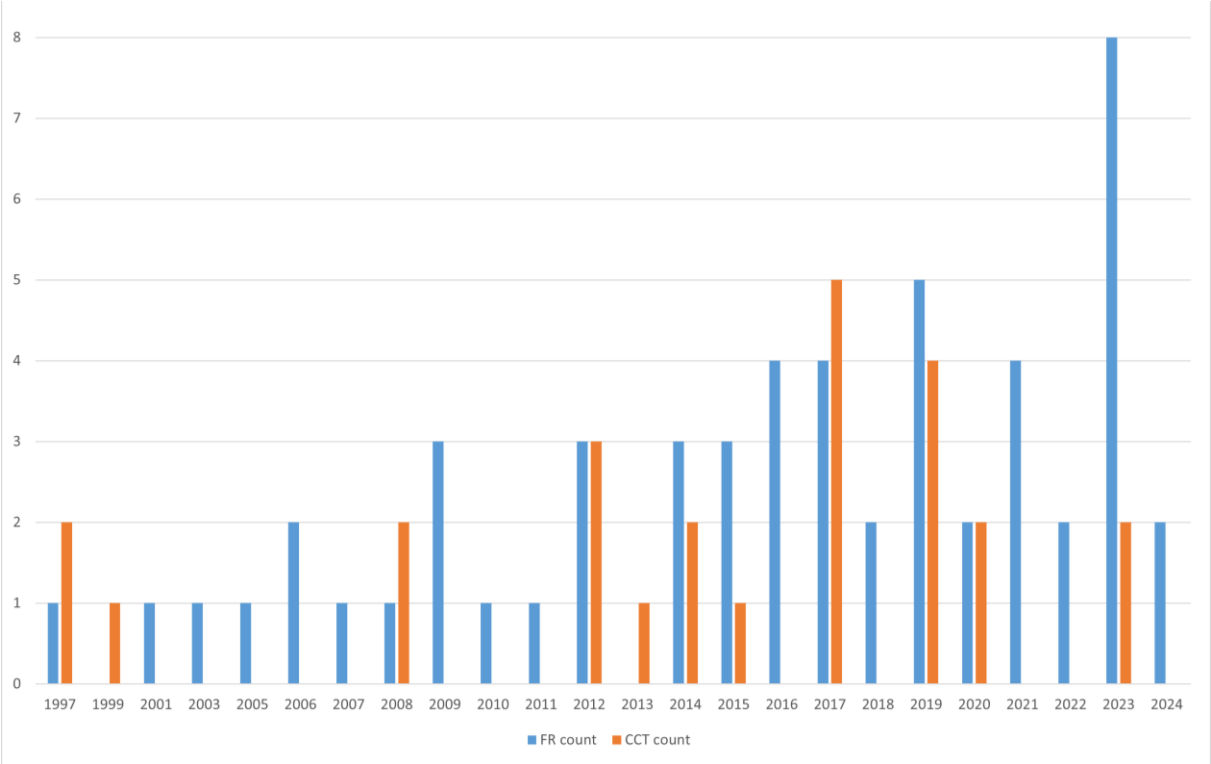

Fig. 2-2 Analyse results of yearly publications of searching the "metal hydroxide", extra keywords is applied: "flame retardant" in blue and "cone calorimeter" in orange from Web of Science

With high loading of inorganic MH in polymer matrix, the spread of fire, release of smoke and heat are all suppressed to some degree. It is glaringly obvious that its effect gets higher with increased mass fraction. Kalali et al. [42] demonstrated a high reduction of peak heat release rate (pHRR) of an ethylene vinyl acetate (EVA) composite with a loading of ATH in 50 wt-%. pHRR decreased to 581 kW/m2 from the 1020 kW/m^2 of neat EVA. Besides, the Young's modulus also increased by 160%, limiting oxygen index (LOI) value increased to 25.5 vol-%. In 2022, Ma et al. [43] added 55 wt-% of MDH into EVA and achieved prolonged time to ignition (TTI) of 51 s, pHRR reduction of almost 80%. Although the UL-94 rating stayed unrated, its LOI increased to 41.4 vol-%.

Unlike the dominant market share of MH in worldwide consumption, how to use the MOF-system efficiently is currently under investigation. In the past works, adding MOF as individual flame retardant shows unstable influence on the fire performance. Considering the special characteristics of MOF, encapsulating other FR additives into MOF is a promising way. The Table 2-1 presents the cone results

and mechanical performance of polymer composites with MOF-system. The mass fraction of MOF in these composites are normally below 5 wt-%, and the total loading of all additives generally does not exceed 20 wt-%.

Table 2-1 Results of some research works of MOF-loading polymer composites*

Polymer matrix	MOF type	Synergist	year	Mechanical performance	CCT results
TPU	Co-DdmSa	APP	2019	Tensile strength decreased from 24.3 MPa to 17.3 MPa	TTI slightly lower, pHRR reduction of 80% (257 kW/m2), THR decreased by 20%
UP	HKUST-1	DMMP	2019	Storage modulus @25C raised to 2.3 GPa	TTI lowered by 40%, pHRR reduction of 70%, THR halved compared to neat polymer
PC	UIO-66		2019	Both tensile strength and storage modulus increased by 10%	TTI was prolong, pHRR halved to 316 kW/m2 and THR decreased
EP	UIO-66	SiO2	2019	Storage modulus slightly increased to 2.1 GPa	pHRR and THR decreased by 30%, TTI stayed the same
PLA	Ni-SaTr	APP	2020	Storage modulus significantly increased to 2 GPa	TTI was prolonged to 97 s, pHRR reduction of 28%, and THR decreased by 22%
PS	Co-BDC	PCT	2020	Storage modulus increased from 2.6 to 3.6 GPa	TTI stayed the same, but pHRR reduction of 40%
EP	UIO-66	PA + β-CD	2021	Tensile strength slightly decreased, but storage modulus was improved to 1.9 GPa	TTI was the same to neat EP of 60ss, pHRR reduction of 50% (675 kW/m2)
EP	ZIF-67	PA	2022	storage modulus increased by 50% to 0.33 GPa	TTI was shorter but pHRR reduced to 645 kW/m2

**: The data are excerpted from the collected data tables, and all the references involved are listed at the end of the document*

Due to the special double-layer structure, LDH is commonly used after being modified. Through the intercalation of different anions, the distance between the layers can vary from 0.5 to 3.5 nm. [44] Furthermore, different combination of the di- and trivalent metal ions also lead to the change of charge density, or have extra property, like the activation of sulphur crosslinking around Zn^{2+} ions [45]. In general, the anions that occupy the interlay space after modification have many

choices. SDBS and the Sodium dodecyl sulphate (SDS) are commonly used. [46–48] Besides, acids like e.g. benzoic acid, oleic acid, borate acid and many saturated fatty acids, and self-synthesised salts also exist. In these modifiers, the majority is organic molecules and elements including N, P and S are frequently observed. On one side, organic modification promotes the compatibility between additives and polymeric surroundings; on the other side, these elements can make contributes to the improvement of fire performance of polymer composites.

Shao et al. coprecipitated the Fe-Zn-LDH with ammonium polyphosphate (APP) in-situ to form a hybrid additive and added into epoxy resin (EP) as flame retardants in 2022. [49] With the mass fraction below 5 wt-%, the LOI values and UL-94 ratings of polymer composites exhibited quite an improvement. The pHRR from CCT also had a reduction of over 55%, compared to neat EP. In 2023, Song et al. demonstrated a reduction of 25 % in pHRR of EP composites with only 2 wt-% loading of Co-Co-LDH. Moreover, the well-shaped hybrid from Co-Co-LDH and cobalt basic carbonate (CBC) improved this reduction to 38.5 % with the same loading. The smoke suppression also decreased by 44.2 %. [50]

As mentioned in Introduction part, IFR is usually mixed-used with other FR systems except for the MH-system. The P-containing flame retardants share the same FR mechanisms of the formation of char layer in the combustion of polymer composites. In MOF- and LDH-systems, loading of small amount of P-containing substance leads to further improvement in fire performance of the samples.

2.2. Materials informatics

With the development of information technology, high-performance computers and the matched modelling software proliferate rapidly. Skipping over the computational simulation, the data-driven approach to establish proper models for complex systems has attracted numerous pioneers. In general, machine learning (ML) is the main topic of data-driven technique. The utilization of ML has already spread to image/speech recognition, content recommendation [51], spam filtering, process optimization [52,53] and property prediction [54,55] etc..

In the last 5 years, numerous works about the usage of machine learning in predicting wanted properties and performances have blossomed. In 2019, Rong et al. predicted the effective thermal conductivity of composites using the recognition of sections images. [56] The same year, Moosavi et al. used the adaptive genetic algorithms in the synthesis of MOF. [57] Sabiston et al. built an ANN model to

predict the orientation tensors of Sheet Moulding Compound composites with respect to charge size and placement. [58] Wang et al. integrated the bibliometric analysis, computational toxicology techniques and *in vitro* analysis to construct hypothesized toxicity pathway of lipid metabolic disorders induced by typical replacement flame retardants (TPP). [59] In 2021, Mendikute et al. applied various ML models to predict the filling quality of resin transfer moulding, trying to diagnose the composite quality and optimize the strategies. [60] Erps et al. built the data-driven multi-objective optimization framework to accelerate the discovery of 3D printing materials, more specifically, how to mix primary formulations to create better-performing materials. [61] Humfeld et al. presented a novel ML framework to optimize the air temperature cycle in the real-time active control of manufacturing. [62] Kang et al. integrated a ML model to predict the mechanical properties of epoxy-silica composites. [63]

The data-driven approach can not only be used in the science and engineering, but also blossom in the fields of social sciences. Taking the harrowing crisis of COVID-19, there are many researchers made contributes to resisting this disaster using their own methods. [64] Mendels et al. developed and evaluated the accuracy and performance of a mobile application named xRCovid to support the identification of SARS-CoV-2 serological rapid diagnostic tests, which had improved accuracy compared to eye reading. [65] Derek et al. investigated a multimodal approach to the diagnosis and prognosis of patients with COVID-19. [66] Fusco et al. reported an overview on AI-supported diagnosis and treatment based on chest computed tomography scan and chest X-ray images, in which twenty-two studies met the inclusion criteria, potentially be used in the identification of disease clusters, monitoring of cases, prediction of future outbreaks, mortality risk, COVID-19 diagnosis and disease management. [67]

In the field of fire safety, Chen et al. used machine learning to analyze the experimental data of FR polymers, explore the relationship between limiting oxygen index (LOI) and components. [68] Fang et al. developed the image recognition model for identifying the combustion stages of fire development in residential room fires. [69] Naser from Clemson University utilized the ANN to evaluate the fire resistance of timber structures based on over 12000 data points. [70] Wang et al. predicted the real-time heat release rate (HRR) by flame images and deep learning algorithms. [71]

2.3. Objectives

In this work, we aimed to build accurate ML models to predict the properties of polymer composites that contain various flame retardants. The FRPCs are primarily consisting of common polymers and different FR systems to improve their fire performance. In the data collection, the polymer matrix was not restricted in only one type, but varied in EP, EVA, thermoplastic polyurethane (TPU), polyethylene (PE) with different density from low (LDPE), moderate (MDPE) to high (HDPE), Polylactic acid (PLA) etc.. These polymers occupied different physical and chemical properties and required different processing methods. The FR additives matching these neat polymers were correspondingly different. The kinds and amounts of the FR additives were also unlimited. That was to say, there could be numerous formulations that were in accord with the FRPCs we wanted to include in our dataset. However, it was definitely impossible to collect all data due to the facts that: a). There was no specific database of FRPCs led by reliable and powerful organizations or entities. b). Dataset for machine learning was done by single person, and research group, thus the scale of the work was limited, and the collection source was solely the public literature, from which the data was processed and comprehensively filtered up to the standards. And for such reasons, the data-driven approaches were limited to be used for specific FR systems, which would be explained in detail in next section.

As our goals, we planned to achieve the following millstones:

1. Successfully assessment of ML models predicting the CCT results of MH-integrated FRPCs. As the main characteristics in CCT, the time to ignition (TTI), peak heat release rate (pHRR) and total heat release rate (THR) were the most typical and important values to estimate the fire performance of FRPCs under certain combustion condition. These values were normally numerical varying from 0 to over thousand. But due to fact that these values fluctuated strongly depending on the measuring environments, operation conditions and device situations, sometimes these numerical properties would be transformed to categories to be predicted.
2. Expand the optimisation and building of ML models to other FR-systems: FRPCs involving MOFs, LDHs and IFRs (or similar phosphorous-containing chemicals). These systems had more complicated FR-mechanisms than that of MHs, leading to more complex physiochemical reactions in the combustion of FRPCs. In addition to CCT results, the storage modulus

measured from DMA test was an extra target feature in ML model for MOF-added FRPCs. Since it was very attractive to know if and how the addition of MOF could enhance their mechanical properties of FRPCs. Another characteristic was the LOI of FRPCs.

3. Evaluation and explanation of ML models with promising predictive performances. The models were to be rated with the unseen data coming either from the divided data not used in training and testing the models, or from additional experiments. Furthermore, through the significance of input features, usage of different explanations and screening the feature values, we are able to find out the relationships between important descriptors and the composites' properties. We can obtain the tendencies how and how much do these influence factors affecting the CCT and DMA results. Also, through the feature importance and screening of virtual dataset, we can find suitable formulations that meet the requirements for specific applications.
4. In addition to individual values of TTI, pHRR and THR, an attempt to predict the development of heat release rate (HRR) against time is also demonstrated in the work. We segmented the temporally developing HRR by cutting the curve across the time, preserving the key features of HRR, and meaningfully dividing its development stages in the whole combustion phase. Ultimately, we transformed the time series into the predictions of individual targets with the ML framework, which was consisting of unified but chained models.

Data-driven investigation of FRPCs

3. Materials and methods

3.1. Experimental formulations

Apart from the ML part, some experimental results that are used to evaluate the model performance is necessary. In the prepared samples, three kinds of commercial EVAs containing 28 wt-% vinyl acetate (VA) content were bought from Repsol Co., Ltd, and DuPont Company and Hanwha Company, respectively. HDPE was obtained from Sabic Innovative Plastics Co., Ltd. EP (Epoxydhedraz C) was provided by R&G Faserverbundwerkstoffe GmbH, Germany. The MDH organically modified with montmorillonite (oMMT), vinyltriethoxysilane (VTES), and diamino diphenyl methane (DDM, ≥97.0%) were purchased from Sigma-Aldrich Química SL. Pure MDH and ATH also came from the same source in analytical standards. Ammonium polyphosphate (APP) was provided by Clariant AG, marked with Exolit AP 750. Pentaerythritol (PER) was purchased from Sigma-Aldrich Química SL. POH-C12 was a self-synthesized organic additive containing phosphorus of about 10 wt.-%. MOF-1 was obtained from the company MOF Technologies (Fe-BTC with 262.96 g/mol molecular weight) and UIO-66(-NH2) was synthesized by published method cited in article.

The preparation methods of polymer composites vary with different types of polymer matrix. For EP-based composites, the FR additives are directly mixed into weighted Epoxy-C with hand, and then, depending on the type of additives, using the magnetic stirrer or three-roll mill to homogenize the mixture. When using the magnetic stirrer C-MAG HS 7 from IKA ®, the pre-mixed viscous solution was heated to 75 °C and stirred with 1000 revolutions per minute (rpm) for 30 min. With the triple roll mill EXKAT 80E, the viscous fluid was milled and collected at room temperature. The gap between apron and centre rolls decreased from 20 to 15 to 10 μm gradually, with the feeding gap kept 5 μm wider than that. The homogeneous solution consisting of neat polymer and FR additives was then mixed with curing agent DDM under continuously stirring at 1200 rpm at 75 °C for 5 min. The final mixture was transferred to a silicon mould pre-heated at the 80 °C and was degassed for 20 min at the same temperature. Finally, the degassed fluid samples were cured in two steps: placed at 110 °C and 150 °C for 2 hours,

respectively. The weight ratio pure EP to DDM was fixed at 78:22 for all EP-samples.

For the preparation of EVA, HDPE and PLA samples, the mixing of all raw materials was done through compounding. Depending on the size of products, there were two compounder with different size used in this work: a small micro compounder branded with MC 15HT from Xplore Instruments, and a twin-screw extruder named KETSE 20/40 from The Bartender Company. Different polymers had their own proper operation temperatures, which were 180 °C for EVA and HDPE, and 175 °C for PLA pellets. The well-mixed extrudates were filled into stainless stell moulds and delivered to the programmable hot press from JUMO GmbH.

Fig. 3-1 lab devices. Above: from left to right are magnetic stirrer, three roll mill and vacuum over; below: from left to right are micro compounder, twin-screw extruder and hydraulic hot press

The polymer composites were formed to different shapes and sizes for different characterization methods. Their components are listed in following tables. These samples are all the formulations used in this work, but specifically used in individual parts, which will be distinguished in results sections.

Data-driven investigation of FRPCs

Table 3-1 Formulations used for validation tests of ML models (part 1)

Sample label	Polymer matrix (wt-%)			FR additives (wt-%)							
	EVA	HDPE	EP	MDH	ATH	APP	oMMT	VTES	POH-C12	UIO66	MOF-1
EVA01	45	-	-	51	-			4	-	-	-
EVA02	45	-	-	52	-	-	-	3	-	-	-
EP01	-	-	90*1	9	-	-	-	-	-	1	-
EVA03	70	-	-	25	-	-	5	-	-	-	-
HDPE01	-	70	-	25	-	5	-	-	-	-	-
EVA-1	45	-	-	53	-	-	-	-	2	-	-
EVA-2	75*2	-	-	25	-	-	-	-	-	-	-
EP-3	-	-	83	17	-	-	-	-	-	-	-
EP-4	79	-	-	-	20	-	-	-	-	-	1
EP-5	78	-	-	-	20	-	-	-	-	-	2

**1: Mass fraction EP includes the weight of curing agent*

**2: EVA used in this sample is different from other EVA samples*

Table 3-2 Formulations used for validation tests of ML models (part 2)

Sample label	Polymer matrix (wt-%)		FR additives (wt-%)			
	EP	PLA	ATH	APP	PER*1	MOF-1
M0	71	-	29	-	-	-
M1	70	-	29	-	-	1
M2	69	-	29	-	-	2
A0	88	-	-	9	3	-
A1	87	-	-	9	3	1
A2	86	-	-	9	3	2

**1: Intumescent flame retardant (IFR) was mixture of APP with PER in a ratio of 3:1 in mass fraction.*

3.2. Characterization of FRPCs

As mentioned above, we take the measured results from CCT and DMA as the target properties in our ML models. The cone calorimeter test (CCT) adopted by the International Organization of Standardization (ISO 5660-1) collects essential characteristics like the heat release rate per unit (HRR) while burning well-prepared samples. [20,72] The calculation of HRR is based on oxygen consumption and illustrated against the time as the HRR curve. [20,73] It provides considerable insight into the physical-chemical reactions, transfer of heat and mass, and occurrence of possible burning instabilities during combustion This makes the HRR curve very sensitive to the experimental environment and specimen conditions. The shape, fluctuation and peak positions of curves have certain connections to the existence of different FRPCs. [20,20,74,75]

In CCT, sheet-like samples are placed in a sample holder, usually wrapped in aluminium films to avoid the burning remains damaging the device, as shown in Fig. 3-2 (a). Under the sample holder is the weighting unit, monitoring the weight change in the whole burning period. Before the normal test begins, the calibration is necessary to keep the cone calorimeter in good condition. While the normal test,

the sample is exposed to certain heat flux produced by the cone heater and ignited with a spark ignitor. The TTI is then recorded when obvious fire appears. With the combustion going on, the gas exhaust collects the gas to analyser, calculating the production of carbon monoxide, carbon dioxide and release of heat. The combustion is covered by glass to avoid the external influence.

The heat released from combustion is an important characteristic to evaluate the scale of burning. In the Fig. 3-2(b), a typical HRR curves is shown. From the initial of HRR (TTI), to the first local maximum and steadies for a while, then to the global maximum (pHRR) and decaying to the extinguishing of fire, HRR develops with time, differing in different FRPCs. Although our targe properties, including TTI, pHRR and THR can usually be obtained from the tables in publications, there are still many missing data in the figures, in which we need to use the Digitalizer in Origin to read the values. In this situation, TTI value is no longer the time point that the operator sees the fire occurring on the sample surface, but the time when HRR reaches certain value, e.g. 25 kW/m^2 in our work.

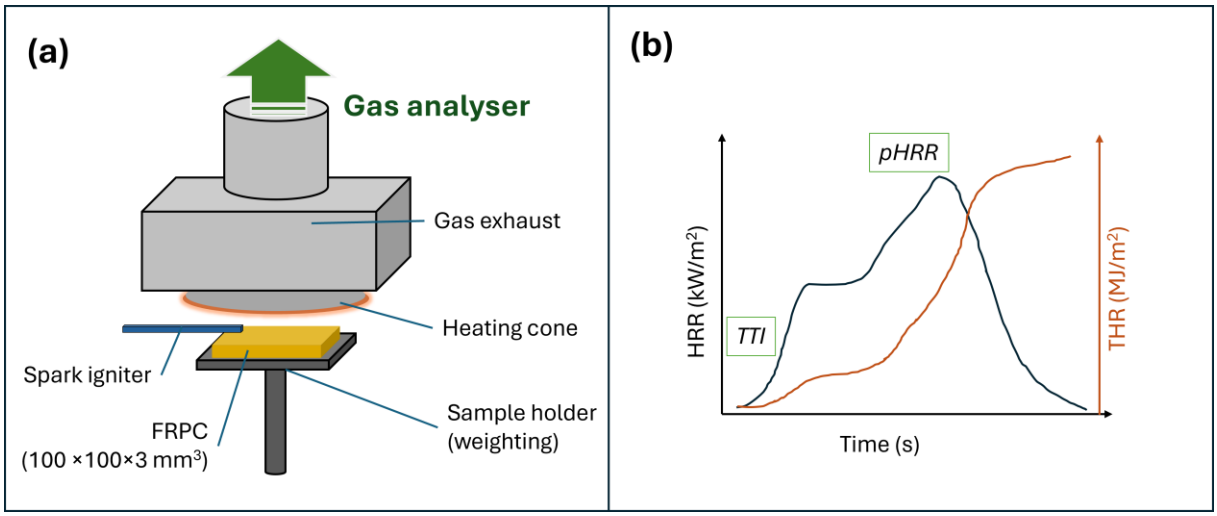

Fig. 3-2 (a) Schema of Cone calorimeter; (b) typical curves from CCT, HRR (kW/m2) and THR (MJ/m2) against time (s)

Except for the single values of TTI, pHRR and THR, the development of HRR, namely the whole HRR curve, is also one of our target features to be predicted with ML models. As a result, understanding the HRR in CCT is indispensable for accurate prediction of HRR development with a limited dataset. Calculation of HRR based on oxygen consumption is in accordance with Thornton's rule: the energy released by fire is nearly proportional to the corresponding oxygen consumed as equation (1), in which $\dot{q}$ is the heat released, $\dot{m}_{O_2}$ means the oxygen in incoming air and output gases, and E is the proportionality coefficient. Most fuels

generate 13.1 kJ of heat on average per gram of oxygen, and this formula is used as the theoretical basis of the oxygen consumption calorimeter. [76]

$$\dot{q} = E \cdot \left(\dot{m}_{O_2}^{in} - \dot{m}_{O_2}^{out}\right) = 13.1\, \Delta\dot{m}_{O_2} \tag{2}$$

The change of HRR over time represents not only the combustion stages of samples in a given circumstance but also reveals the influence of possible interior processes occurring in a burning scene. The compositions, thermal properties and sample sizes significantly impact the shape of HRR curve. Many researchers have divided the HRR curves into different parts, indicating different burning behaviors or mechanisms behind. Still, in general, there are three fundamental phases distinguishing the fire behaviors as shown in Fig. 3-3(a) [77,78], except for the incipient time before ignition:

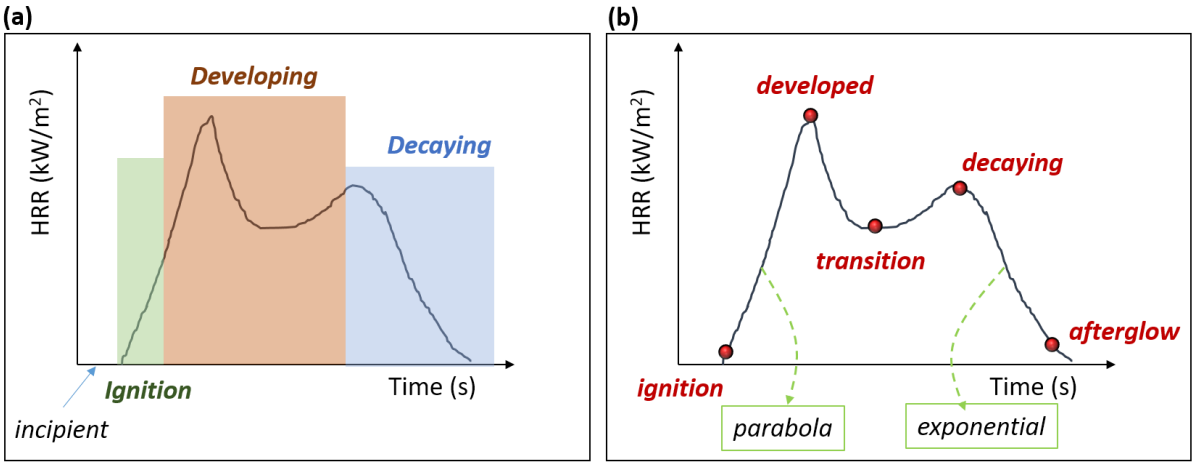

Fig. 3-3 Heat release rate (HRR) curves in CCT. (a): 3 main combustion phases of HRR over time; (b): key anchor points representing significant features of HRR.

(i). The initial phase is recognized by the increased composition of flammable small-molecule gas produced by pyrolysis in high ventilation. Local temperature rising leads to the ignition of sufficient fuels and the sample surface. [79] Usually, the parabola (t^2 fire [80]) is used to describe the increasing heat release rate.

(ii). In the second stage, the fire develops. The growing amount of heat released by combustion, in turn, raises the temperature and promotes flaming. HRR reveals a general trend of fast increase as a joint result of growing fire density and continuing ventilation. [81] Neat polymers generally show a single peak of HRR in this phase. However, taking the possible flame-retardant (FR) effects into consideration, HRR changes may be greatly influenced: strong fire-hindering effect shall suppress its growth and make HRR curves low and prolonged in time; FR

additives that are not efficient enough can temporally restrain HRR growth, but the second peak is still possible.

(iii). The last stage is the decaying of fire density with HRR decrease, which is basically caused by the lack of fuel. In general, the exponential decaying function is applied to describe the HRR decrease with the reduction of fuels in this stage. Related equations are shown in (3) to (5), in which H_{rr} is the heat release rate, $\frac{dW}{dt}$ the mass loss of sample, h the equivalent heat capacity of fuels, $\frac{d\alpha}{dt}$ the conversion of fuels from the sample and k, k_1, k_2 the constant coefficients in fuel-limited burning. [82,83]

$$H_{rr} = h\frac{dW}{dt} \tag{3}$$

$$W^{"} = k_1\frac{d\alpha}{dt} = k_2\frac{dW}{dt} \tag{4}$$

$$\frac{dH_{rr}}{dt} = kH_{rr} \tag{5}$$

In light of this, we have conducted the simplification of HRR curves by choosing five key anchor points to make the prediction of HRR possible, as shown in Fig. 3-3(b). Each point is featured with specific pairs (t, hrr) with units of s and kW/m^2. Not all values are listed in public papers. In order to gather data that has high confidence and good operability, the start- and endpoints are concluded with HRRs equalling 25 and 50 kW/m^2 separately. In most cases, polymer composites show complex changes in HRR in the second phase due to their FR additives. These transitions indicate different FR effects occurring in CCT, as mentioned above. The critical point of the transition phase is then established to mark different transition trends. The transition point (t_{trans}, hrr_{trans}) either locates in the inflection point or is calculated as the middle point of (t_{devlp}, hrr_{devlp}) and (t_{decay}, hrr_{decay}). These key anchor points are the important strategies to predict the HRR curves in the ML modelling, listed in Table 3-3.

Table 3-3 Five key anchor points to simplify measured HRR curves

Key anchor point	Format	Interpretation
Ignition	$(t_{ignit}, 25)$	Ignition point, sample begins to burning when measured HRR reaches 25kW/m^2.

Developing	(t_{devlp}, hrr_{devlp})	Developing points, previous parabolic burning slows down, new combustion phase dominated by HRR or ventilation begins.
Transition	(t_{trans}, hrr_{trans})	Transition point, HRR changes also depending on the FR effect of composites composition.
Decaying	(t_{decay}, hrr_{decay})	Decaying point, HRR starts to decrease due to fuel limitation.
Afterglow	$(t_{after}, 50)$	Afterglow point, flame faints till HRR reaches 50kW/m^2.

Another testing result named storage modulus comes from DMA test. This is a technique used to measure the dynamic modulus and mechanical loss of a prepared sample under programmed temperature controlling and alternating stress, with respect to temperature or frequency. Under this periodic stress (usually sinusoidal), the samples have the corresponding vibration strains, which are in general delayed in phase compared to the given stress. According to the physical law, a complex modulus is obtained through the strain (ε) and stress (σ), as calculated by equation (6). From the complex modulus, two components can be distinguished as storage modulus M' and loss modulus M''. Unless the sample is perfectly elastic, there is always the loss modulus, which means the viscoelasticity of the sample.

$$M^* = \frac{\sigma}{\varepsilon} = \frac{\frac{F_A}{A}}{\frac{L_A}{L_0}} = \frac{F_A}{L_A}\frac{L_0}{A} = \frac{F_A}{L_A}g \tag{6}$$

The F_A and L_A are the amplitudes of force and displacement of the testing sample; A and L_0 are the equivalent area and length of the sample, which are combined to the geometry factor, differing in different testing modes. There are in total 6 testing modes illustrated in Fig. 3-4, in which the samples have also varied shapes and sizes, and different sample holders are used to fix them. The difference is not only in the fixing, but also the calculation of geometry factors varies due to the change of geometries of samples.

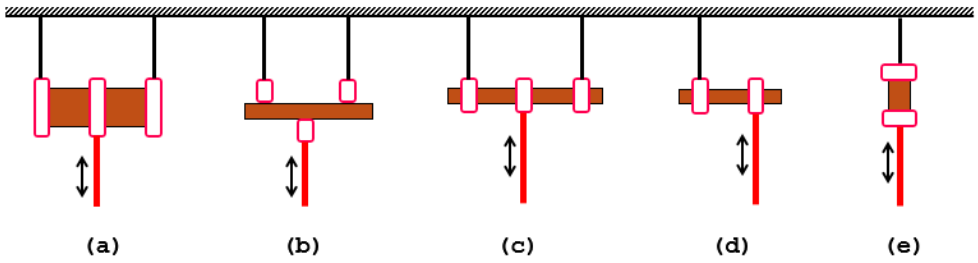

Fig. 3-4 DAM testing modes, in which the brown parts are samples and red for fixtures: (a). Shear; (b). Three-point bending; (c). Double cantilevers; (d). Single cantilever; (e). Stretch or compress

3.3. Data preprocessing and feature engineering

The dataset for statistical modelling was completed by retrieving data from publications in recent years and experiments. Each record, much like the formulation of the polymer composite, is marked as unique through the combination of features containing the information about the type of polymer matrix, loading of the FR additives, and operation parameters in both sample preparation processes and characterization methods. To begin with, 3 basic datasets are produced facing the challenges of building the ML models for different FR-systems. Their sources, which are more than 100 references, are listed in the annexes.

A dataset is a two-dimensional collection of data, in which the columns are the descriptors or features, and rows are the corresponding values. As detonated above, each row refers to a formulation of polymer composites. Through the column names and the values in this row, we can easily know what the components in this sample are and how this sample be produced and tested to get the target properties. For example, the Table 3-1 is a rough dataset, in which we can know how the EP-composites are consisting of. The datasets for ML modelling are certainly not so simple. They contain not only the name of each chemicals inside the composites, but also important, from empirical rules, descriptors that could give impact to their CCT or DMA properties, as demonstrated in Fig. 3-5. As we used the supervised ML algorithms, the input data should not only have the influence factors (the input features) but also the target properties (also target features) as the answer to this question.

Data-driven investigation of FRPCs

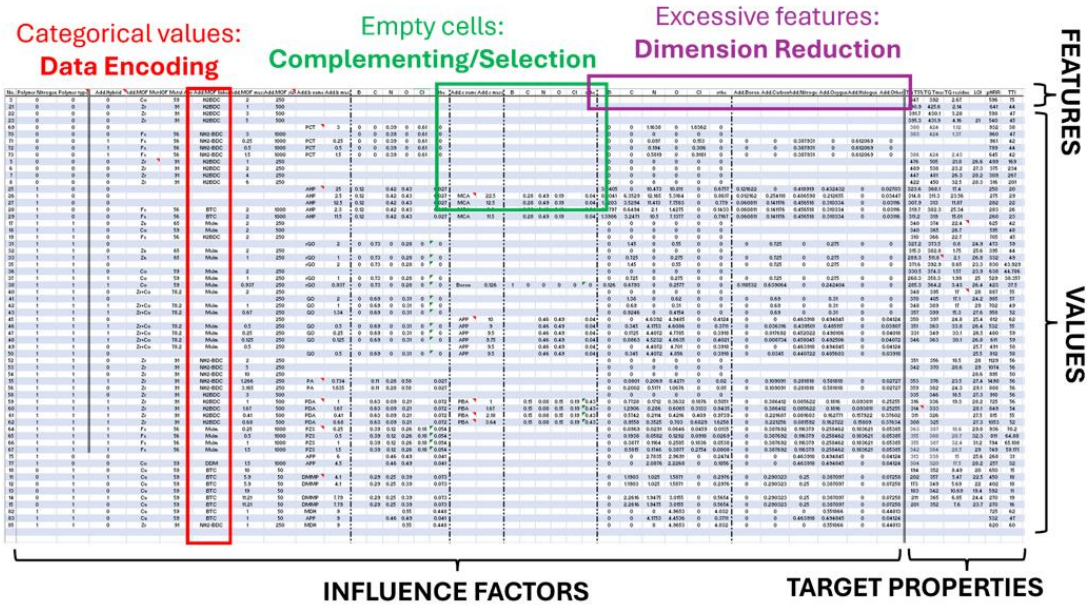

Fig. 3-5 Schematic illustration of the data operation in dataset, including the descriptors of formulations (influence factors) and properties to be predicted (target properties)

3.3.1. Input features in groups

Since the majority of our dataset for statistical modelling is completed by retrieving data from publications, the accessibility, generalizability and usefulness of the wanted features are significant. Firstly, we shall make clear that the ML models are designed to predict the properties (measured by certain testing methods) of polymer composites with certain additives. So, the key points in this problem are quite obvious: how are these FRPCs prepared and characterized throughout the whole process. Think back, the polymer matrix (pure or mixture from plural polymers) and functional additives (usually multiple chemicals that have different amounts, types and numbers) are well-mixed through the above-mentioned methods, then the mixtures are prepared to standard size and shape for following characterization. Taking the FR mechanisms into consideration, we have marked the dataset with the combination of descriptors containing the information about these groups: properties of raw materials, important parameters in the sample production and essential parameters of characterization methods.

The raw materials, including the polymer matrix and FR additives, are described with their chemical and physical properties. due to the large variety of the

polymers and additives, this group is divided into group of polymer matrix (labelled as "Polymer_Matrix"), group of functional FR additives (referring to the specific additives like MDH, MOF or LDH, labelled as "MH/MOF/LDH_Materials") and group of other additives (labelled as "Main_FR", because these additives are the main chemicals affecting the composites' FR performance). The parameters during the sample preparation and characterization are merged into one group labelled as "Other_Parameters" in the modelling. These features are explained in detail as follows and listed in Table 3-4:

1) Properties of polymer matrix ("Polymer_Matrix"): Features related to neat polymer are bound to this group, consisting of the density, thermal conductivity and decomposition temperatures; results of corresponding characterization of neat polymers are also included; in some cases, multiple polymers are mixed in the formulation, treated as one polymer matrix in the dataset.

2) Functional FR additives ("MH/MOF/LDH_Materials"): the reason why we should take these functional additives separated from other FR additives is that these additives have their special functions in the polymer composites and usually/sometimes used along in the formulation. At the same time, the selection of features of them are quite different from that of the next group. For the MH-system, the thermal decomposition properties, particle size and loading amount are the main features in this group. For the MOF-system, we consider the types of metal ions and organic ligands, represented mainly by their atomic numbers and molecular weights; MOF's thermal decomposition properties, micro-structures, type of the building units and mass fraction are also collected; For LDH-system, the interlayer distances varied due to different intercalations are recorded. Also, the types of anions, metals in the structures and their loading amount are important.

3) Other FR additives ("Main_FR" or "Synergists" depending on the FR system): in this group, the other FR additives besides MH, MOF and LDH are marked with selected features. They can be any kind of compounds, chemicals or even inorganic fillers that provide additional synergistic functions/main FR effects depending on the formulations. The main features in this group include their elemental composition and mass fractions.

4) Other parameters ("Other_Parameters"): This group focuses on the parameters in sample preparation and performance testing that possibly have an impact on the composites' properties. Significant features, e.g., the operation temperatures, mixing ways, forming methods and devices used in the production of samples, their shapes and sizes in the characterization, as well as the methodological parameters in thermo gravimetric analysis (TGA), DMA and CCT, are documented.

Table 3-4 Input features of the dataset

Polymer matrix	Loading of MH	Synergists besides MH/MOF/LDH	Process parameter
Type of neat polymer	Mass fractions	Type of chemicals	CCT: Heat flux
LOI value	MOF: Metal type	Mass fraction	CCT: Sample thickness
decomposition temperatures in TGA (initial, 50% and max-weight-loss)	MOF: molecular weight, elemental contents of organic ligands	Contents of elements listed below:	processing temperature while producing composites
Molecular structure	MOF: classification of MOF types	Phosphorus	Mixing method
Temp. of melting /glass-transition	MOF: decomposition temperatures	Nitrogen	Forming method
Density	MH: Metal type	Silicon	Geometry factor in DMA
Storage modulus measured by DMA	MH: Equivalent content of H2O and Oxide	Boron	DMA testing mode

TTI, pHRR and THR from CCT	MH: Particle size d50	Carbon
	MH: Enthalpy of decomposition	Oxygen
	MH: decomposition temperatures	Metals
	LDH: types of bi- and trivalent metals	
	LDH: intercalation molecules	
	LDH: interlayer spacing	

Although we have selected so many features out as the input data, there are still challenges in dealing with the features. It is very difficult, almost impossible, to obtain the values of some features, like the molecular structure of neat polymers, which are complex properties unable to be described with simple words. It is also hard to find the values of describing how big the pores are and what they look like in the pore morphology of MOFs. Besides, how to exhibit the dispersion of FR additives and compatibility between matrix and additives are difficult, which gives serious impact on the performance of polymer composites in turn. In these cases, we intended to add some indirect descriptors to compensate for the information loss. For example, the particle size of functional additives (MH, MOF and LDH) and organic modifications should give additional information about the dispersion and compatibility from the experimental experience. The types of metal, the used organic ligands and synthesis process usually decide the micro- and macro-structures of MOFs. Using these features also supports the ML modelling to some extent. Based on these ideas, we have finally constructed the data structure of our datasets for further analysis.

In addition to the above features, we also collected the information of FRPCs including their decomposition properties from TGA and LOI values, too. These

features are not intended to be used in ML modelling predicting the CCT and DMA results but used to pre-learn the relationships between the properties of composites, supporting the further investigation of FR effect of corresponding additives.

All the feature values are collected from corresponding publications. However, there are always values missing in our dataset because not all authors would accomplish or publish the data about all raw materials, parameters in measurements like the thermal conductivity and density of polymer matrix, surface area and pore distribution of MOFs, decomposition properties of MHs, intercalation/modification percent of LDHs, the decomposition details of the additives and detailed molecular formulas of the chemicals. These data are not essential to evaluate their research activities in the articles but may play an important role in building elegant models. As a result, there could be many vacancies in corresponding columns in our dataset. In general, for those features containing vacancies below 20% in the dataset, we attempt to keep these features in order to not lose information. To complement these blanks, either the theoretical values from other literature or released values from authorities, or mathematical averaged values from the whole dataset are inserted into the dataset. However, if the features have too many vacancies, we must drop them to keep the dataset clean and trustable.

In addition, another question in the data collection is the reliability of the data. There are several situations throwing doubt on the reliability of the data. The first case is the reading of graphs. In some papers, the authors have conducted a large number of experiments, and thus have numerous tables and figures shown in the publication. In general, there are only prat of the samples showing their results in the tables due to the limitation of numbers of samples. The results of the rest of samples can only be obtained from the figures, which lead to some problems: a). The graphs are quite blurry in some parts since the paper was published long ago. b). The results in the graphs are not fully displayed, and the required data is not included in the ranges. c). The styles of curves in graphs are not suitable for precious reading of values, the markers in the curves are too dense and big, and curves overlap with each other, making it too difficult to read the values. Another situation that leads to a trust issue is the abnormal descriptions in the paper. Researchers who have been working in a particular field for a long time often develop fairly accurate experience in judging the performance of products. In the

comparison of different articles, for the similar formulation, some authors have reported the results that are unusually low. The reduction in pHRR of their polymer composites can reach over 60% even with relatively small amounts of FR additives. Also, there are sometime inconsistent descriptions in figures or results and discussion parts of the paper, making the results doubtful. These records are marked in our dataset, which would be distinguished whether to keep or drop in the following modelling part.

3.3.2. Target properties of FRPC

The to-be-predicted target properties of FRPCs in this work come from the results of CCT and DMA, more exactly, the four properties: TTI (s), pHRR (kW/m^2), THR (MJ/m^2) and storage modulus (GPa). These features are numerical values and labelled for all formulations in the dataset. In some cases, these numerical values would be converted to categories for classification.

Different FR-systems have slight variations due to the time scale and research progress. For the FRPC with MH-system, the target features include TTI, pHRR, THR and a researcher-defined index named flame retardant index (FRI). FRI is actually a combined number of the three important values calculated with equation (7). The target features of ML models in MOF-system are the above-mentioned four characteristics. For LSH-system, there are only TTI, pHRR and THR as the targets. Except for the prediction of single property of FRPC, we also constructed models to predict the whole HRR curves to comprehend and confirm the ability and limitation of ML models, which is illustrated in following section in detail.

$$FRI = \frac{\left[THR \times \frac{pHRR}{TTI}\right]_{polymer\_matrix}}{\left[THR \times \frac{pHRR}{TTI}\right]_{composite}} \quad (7)$$

Table 3-5 Conversion of numerical values to categories in the dataset of MH-system

Target property	pHRR → D-pHRR	TTI → Lv-TTI	THR → D-THR → Lv-THR	FRI → Lv-FRI
Level/Ratio	Composite / Neat polymer	10 (s)	Composite / Neat polymer;	0.1

Example 1	Values of D-pHRR obtained by the ratio between composites' pHRR and that of neat polymer	< 20	(Lv) 0	D-THR same as D-pHRR, but levelled as Lv-TTI with a level of 0.1	0 – 0.1	(Lv) 1
Example 2		100 - 110	(Lv) 9		0.4 – 0.5	(Lv) 5
Example 3		> 200	(Lv) 19		> 1	(Lv) 11

In addition to the original values of composites' properties, the target features also contain the ratios of normalized, matrix-independent values obtained by dividing the composites' properties by the corresponding values of neat polymers. Through this transformation of values, we can reveal the changing of properties caused by the hybrid with FR additives, representing the influence of FR additives separately. These target features are marked with "D-" or "_d" like "D-pHRR" in MH-system and "TTI_d" in MOF-system. In addition, all these numerical values of target features are also categorized into distinct classes to enhance the performance of predictive models. These categorical features are then marked with "Lv-" or "c", e.g. "Lv-TTI" and "TTI_dc". All four target properties were classified in several categories, decided by their value ranges. The difference between the neighbored categories represents a numerical difference typically around 10%. This conversion is on the grounds of the fact that the measuring errors are inevitable in practice. On the one hand, categorization with a relatively less interval could minimize the noise of data reducing the influence of measuring errors; [84–86] on the other hand, we are able to achieve better predictive performance of machine learning models on categories than that on numeric values. Under the limitation of size of dataset, using classifiers to replace regressors has the potential to improve the predictive accuracy of our target features. Different ML systems have different conversion strategies. In Table 3-5 are the transformation in MH-system, and Table 3-6 are the results of MOF- and LDH-systems.

Table 3-6 Conversion of numerical values to categories in the datasets of MOF- and LDH-system

Target	Categories							
Modulus_dc	< 1.00	1.00-1.15	1.15-1.35	1.35-1.70	>1.70	-	-	-
TTI_dc	< 0.70	0.70-0.80	0.80-0.90	0.90-1.00	1.00-1.10	1..10-1.20	1.20-1.30	>1.30
pHRR_dc	<0.30	0.30-0.40	0.40-0.50	0.50-0.60	0.60-0.70	0.70-0.80	0.80-0.90	>0.90
THR_dc	<0.60	0.60-0.70	0.70-0.80	0.80-0.90	0.90-1.00	>1.00	-	-

3.3.3. Data pre-processing

Before being put into use, the dataset must be cleaned and processed to be in accord with the requirements of ML: the dataset must be filled with full numbers for machine recognition. For the missing values, we would use the mean values to fill the vacancies as mentioned above. Some features have categorical values, like the metal types of Cu, Co, Ni, Fr etc., or modification of "Yes" or "No". These features should be converted to numbers before training the models. The normal way is to encode them into numerical information. Typically, there are two encoding methods: label encoding and one-hot encoding. Both encoding methods have their own advantages and disadvantages.

As shown in Fig. 3-6, the label encoding changes all the categories into numbers sorted from 0 directly. It is simple and quick, does not increase the number of features at the same time. But this simple conversion to sorted numbers will bring new information into the feature: a magnitude relationship has been added into the original values of "Zr", "Co" and "Cu" due to the fact that 2>1>0. Since the data-driven approach aims to explore the relationships between all kinds of data, this supererogatory information could lead to decreased performance of ML models. In contrast, the one-hot encoding looks similar to binary coding that changing "Zr" to "1000" and "Co" to "0100". This conversion does not give extra information to the dataset and allows for the clear visualization of the features' values. However, through the figure we can see that the number of features has increased from one feature to the number of categories in this feature. Usually, adding the number of features in a dataset is able to improve the model performance. But with increased

complexity of the models, problems like overfitting, less accurate in unseen data or non-convergent calculations, will also happen. As a result, the feature engineering is not a simple work done only once but will be further optimized with the modelling process.

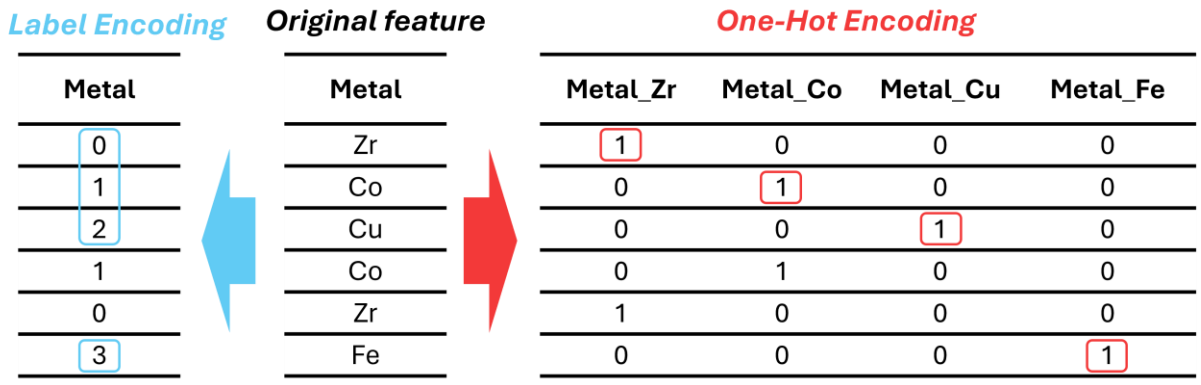

Fig. 3-6 Encoding of categorical features: label encoding (left) and one-hot encoding (right)

Except for the encoding of categorical features, the standardization of dataset is also important. In ML, data standardization is commonly required for many ML algorithms before training. In practice our dataset has normally features with values in different ranges. For example, the values of feature "density of polymer" concentrate around 0.9 to 1.5, but another feature "molecular weight" can vary from 600 to 300000. Since some models have very high sensitivity to numbers, the former feature with such small range may be ignored in the training and building of models. To avoid this, the standardization if necessary and many ML methods benefit from it. In our work, we standardize the data using the tool from scikit-learn, named Min-Max-Scaler. Its function is to set the minimums and maximus of all features to 0 and 1, respectively, and then scale the intermediate values accordingly. Thus, all data in this dataset have the same range. [87]

In addition to the data pre-processing methos mentioned above, there are other modifications required. K-means clustering is used to distinguish the outliers, which are statistically different to other data points. [88] The k-means algorithm is a clustering method measuring the Euclidean distances between sample points and clustering centroids in data space. Using the KMeans-tool from scikit-learn, the points far away from the cluster centroid are considered outliers, which should be used with discretion in model development. [89] Meanwhile, we conducted the Synthetic Minority Over-Sampling Technique (SMOTE) to expand the size of the

dataset for predicting categorical target properties to achieve better performance. SMOTE works by creating new samples based on several of the nearest examples in the feature space. The synthetic samples in the minority class help to balance the class distribution.

3.4. Assessment of ML models

Normally, we import the dataset that contains the input features and target property, into a pre-defined model implemented from the scikit-learn library, train the model with specific settings and obtain the optimized hyperparameters. Then we have the ML model constructed based on the corresponding dataset, predicting the individual property TTI, pHRR or THR specifically. However, models can be combined to get better performance, especially when the performance of single model is not satisfied. In this work, many algorithms have been used to build the ML models, but not all of them achieve good performance. On one side, models like linear regression and decision tree are too simple to undertake the task; on the other side, deep learning methods like multi-layer perceptron (MLP) and neural network often struggle to converge, or even if it does, the results are still not promising. Therefore, the commonly used models are built with RF, SVM and their linear combinations in our work.

The random forest algorithm, as shown in Fig. 1-6 (a), is an ensemble composed of a big collection of decision trees that are randomly grown up from the input dataset. In this forest, each decision tree acts as an individual estimator that makes classifications or predictions based on different features in the dataset. The word "random" in RF represents the key point in the growth of trees: the randomness is introduced not only in the division of sub-dataset (the data points) provided to the tree-growth, but also in the selection of features, which decides the shape and size of a single tree. This helps the RF model avoid the problem of overfitting, which usually happens to a complex model working only for the specific data and reduces the generalization ability on unseen data.

Controlled by the hyperparameters, the forest has varied number (from 100 to 2000 or more) of decision trees. As the forest grows larger, the model becomes more complex, and the time required for training also increases. Generally, a larger forest leads to better predictive performance. However, an overly complex model would reduce its robustness and weaken its generalization ability. In addition to the number of trees, the structure of each tree is controlled by hyperparameters.

Data-driven investigation of FRPCs

Each tree begins by a splitting at the root node (a randomly selected feature), then continues along the trunk to the next node (another feature), branching out as it grows. Whether a split occurs at a particular node depends on the number of data points at that node or whether the tree has reached the size limit set by the hyperparameter. The best split is found through an exhaustive search of all features available to the tree (either all features of the input data or a random subset defined by the hyperparameters). When making predictions with RF model, each tree gives its own probabilistic prediction on all categories. The final output is determined by "averaging" where the result marked with the highest averaged probability is the one the model outputs.

In Fig. 1-6 (b), SVM model constructs a hyperplane, which is the best possible boundary between the data points of different classes. The goal of SVM model is to find out this widest possible gap (or margin) to separate different categories of data. The data points that are closest to this boundary are called support vectors. They are crucial because they help define where the hyperplane should be placed in the data space. However, for non-linear data, a mathematical technique called the kernel trick is used to allow the transformation of the data into a higher-dimensional space, in which a hyperplane can effectively separate the data points. In other words, a two-dimensional data point (x_i, y_i) is transformed into a higher dimension (x_i, y_i, f_i) using a kernel function f((x_i, y_i)). Consequently, a hyperplane that cannot be found in the two-dimensional space can be identified in higher dimension (ranging from three to infinite dimensions, depending on the kernel function used).

In the modelling process, the input dataset is randomly split into training and test sets, corresponding to $\boldsymbol{p}$ and 100%-$\boldsymbol{p}$, respectively. $\boldsymbol{p}$ could be 80% or 85% depending on the size of the dataset. The training set is used to confirm the models' structure and optimize the hyperparameters with a $\boldsymbol{k}$-fold cross validation, followed by the immediate evaluation of predictive performance with the test set. The $\boldsymbol{k}$ is 5 in our work, meaning that the training set is divided into 5 parts and each optimization process takes 4 of them, leaving 1 out for validation. This process is repeated 5 times and final results come from the average of all 5 validations. The train-test split was repeated 100 times randomly to avoid the occasionality, which is usually reflected by the strong up-and-down fluctuations in the determination coefficients R2. Different estimators have usually different parameters. Taking RF-model predicting the target propertied of FRPCs in MH-system as example, the

important parameters are listed in Table 3-7. These parameters control the size of "forest" and the growth of all the trees. After optimization of hyperparameters, they will be filled into the models. Models with optimized parameters are then trained with training sets and the test sets are used to evaluate the predictive performance *in-situ*.

Table 3-7 Best combination of hyper-parameters through grid-searching with 5-fold cross-validation

Hyperparameter	Model for D-pHRR	Model for Lv-TTI	Model for Lv-THR	Model for Lv-FRI
n_estimators	500	100	100	500
ccp_alpha	0	0	0	0.005
max_depth	50	30	30	30
max_features	None	None	Sqrt	Sqrt
criterion	absolute_error	Gini	Gini	Gini
min_samples_split	5	2	2	2
min_impurity_decrease	-	0	0	0

Except for the individual properties, the development of HRR is also one of our aims. Instead of predicting the entire curve, properties from five key points are to be predicted as the target features shown in Fig. 3-3 (b). We chose to employ the Random Forest Classifier (RFC) in our work for several reasons. We use classifier instead of regressor to make predictions of the above-mentioned properties. The main reason lies in the fact that HRR values contain certain errors. As described in the last section, HRR is not directly measurable. The curves concluded from cone tests show clear distinctions in different measurements. [90] These uncertainties come from fuel composition, environmental conditions and instrument accuracy [91], and vary with different flame sizes from 5% to 20% [92,93]. Empirically, we take the assumption of a 10% error in the cone test. In MH-loaded composites, the endothermic reactions of hydroxide decomposition also produce considerable errors to some degree. [94]

In this ML framework to predict HRR curves, 9 different models based on RFC are built. The overall structure of models is illustrated in Fig. 3-7. Model #x is designed to predict the target property listed on the right end. The chained models, i.e.,

model #2 take not only the collected dataset but also the predictive results of model #1 (*t_ignit*) as input. The green lines indicate this extra input for models #2 to #5 and #7 to #8. By collecting the results from Model #1 to #8, we can get the coordinates of all 5 anchor points, which are transformed back to HRR curves as described in section 0.

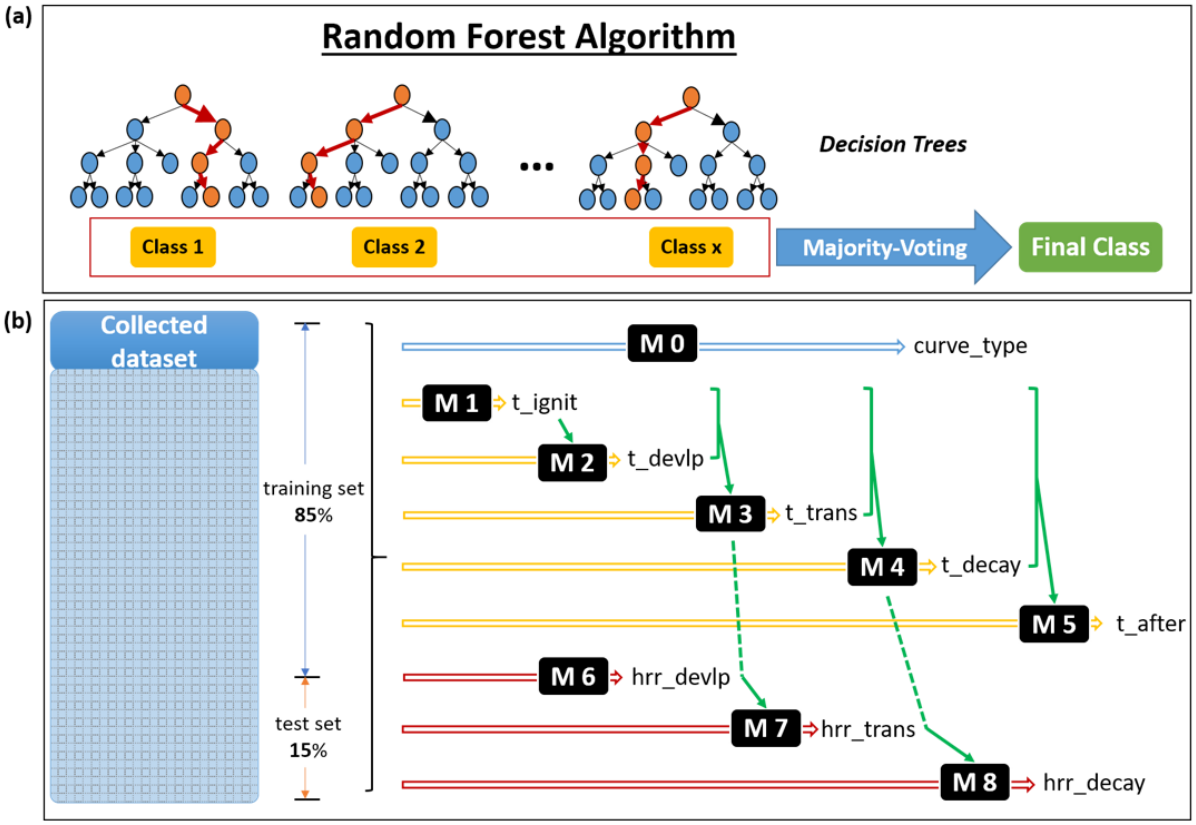

Fig. 3-7 Structure of Random Forest Algorithm (a) and the chained machine learning framework in this work (b).

To optimize model accuracy and avoid fitting effects, the most relevant features were selected via the Recursive Feature Elimination (RFE) integrated with the RF algorithm. A 5-fold cross-validation (CV) was applied simultaneously to achieve better performance. RFE is a type of backward elimination method that removes the least important features iteratively to find the optimal number and combination of features.

3.5. Evaluation and explanation of ML models

In our work, the coefficient of determination (R2), Mean Absolute Error (MAE), and Root Mean Square Error (RMSE) are applied to evaluate the predictive accuracy. The individual indices are defined according to the following equations:

$$R2 = 1 - \frac{\sum(y_i - \hat{y}_i)^2}{\sum(y_i - \bar{y}_i)^2} \tag{8}$$

$$MAE = \frac{1}{m}\sum_i^m |y_i - \hat{y}_i| \tag{9}$$

$$RMSE = \sqrt{\frac{1}{m}\sum_i^m (y_i - \hat{y}_i)^2} \tag{10}$$

Where y_i represents the prediction of i_{th} sample, $\hat{y}_i$ indicates the corresponding real value, and $\bar{y}_i$ represents the mean value. m is the number of samples. The R2 value reveals the accuracy of the predictions, and the other two indices represent the margin of error.

Furthermore, we have presented the confusion matrix, the precision-recall curves (receiver operating characteristic curve, short as ROC) and the area under curve (AUC) to evaluate the predictive accuracy of classifiers. The confusion matrix compares the classification results with the real measurements, visualizing the precision of predictions. Each column in the confusion matrix represents a prediction class, and the total number in this column indicates the number of data instances predicted to belong to this class. Each row represents the actual class of the data, and the total number in each row is the number of data points that are measured to this class. The values within each column represent the number of actual samples that are predicted to the prediction class. In Fig. 3-8 is an example of multi-class problem with 60 data points, in which the predicted classes “Category A”, “Category B” and “Category C” have 20 predictions, respectively. The confusion matrix of the classification results is shown to the left, indicating that 16, 19, and 12 samples are correctly assigned to their respective classes. Meanwhile, there are 6 samples that belong to “Category A” misclassified to “Category C”. Instead of numbers, using grey-scale images to represent the predictive accuracy is exhibited to the right in Fig. 3-8. The whiteness of the blocks indicates the number of misclassifications of the estimators.

	Category A	Category B	Category C
Category A	16	1	6
Category B	2	19	2
Category C	2	0	12

	Category A	Category B	Category C
Category A			
Category B			
Category C			

Fig. 3-8 Confusion matrix of a multi-class classification

The explanation of ML models is performed on the basis of the datasets and ML algorithms. Tree-based models (RF models) provide an integrated tool to calculate the feature importance with respect to the whole model. This feature importance refers to the impurity-based values of this feature in all the nodes of all trees. The calculation of impurity based on the Gini index from equation (11), in which p_i is the proportion of samples of i-th class in the total number of sample within this node, and K is the number of classes. The more frequent this feature is used in the decision trees and higher influence on the change of Gini index, the more importance is this feature in the RF model.

$$Gini = 1 - \sum_{i=1}^{K} p_i^2 \tag{11}$$

For kernel-based models (SVM models), we use the SHapley Additive exPlanations (SHAP) to interpret the outputs. This tool derived from the cooperative game theory attribute the output to the contribution (i.e. the shapely value) of each feature, representing its influence on prediction of target classes. [49] SHAP is an additive feature attribution method, in which the SHAP value of a feature is obtained by the weighted average of its marginal contributions of the predictions' change across all subsets of the feature values. In simple terms, for a given feature, the SHAP value represents how much the prediction of a sample changes when we alter the value of this feature. By aggregating these changes, we obtain the final SHAP value for the feature. Due to the limitations of its mathematical realization, the computation of SHAP values is highly resource-intensive and time-consuming. Generally, approximate methods are used to reduce the computation time and improve calculation efficiency. In this work, we employ the kernel SHAP for this purpose.

The SHAP value provides a consistent and global framework for the interpretation of ML models. The beeswarm plot in Fig. 3-9 (a) exhibits an example of ranked features in pHRR(SVM)-model. It's a clear visualization of the distribution of the

data points and significance across multiple features. As in part (b), the dots distribute horizontally, coloured with red for high and blue for low feature values. The positions of these dots along X-axis refer to their SHAP values, with the middle boundary of zero. Dots distributed to the left or right demonstrate the negative or positive influence on the target property. Through the clustering of sample points, a conclusion can be drawn that the target property will decrease with higher values of the feature "LDH_OrgMod". In this case, it means the organic modification of LDHs enhance the reduction of pHRR of FRPCs. This conclusion is based on the successfully built SVM model, which depends more on the dataset we have retrieved from the literature. With the distribution of SHAP values of all necessary features, we can not only know if the features are significant, but also understand how the features influence the to be predicted target features.

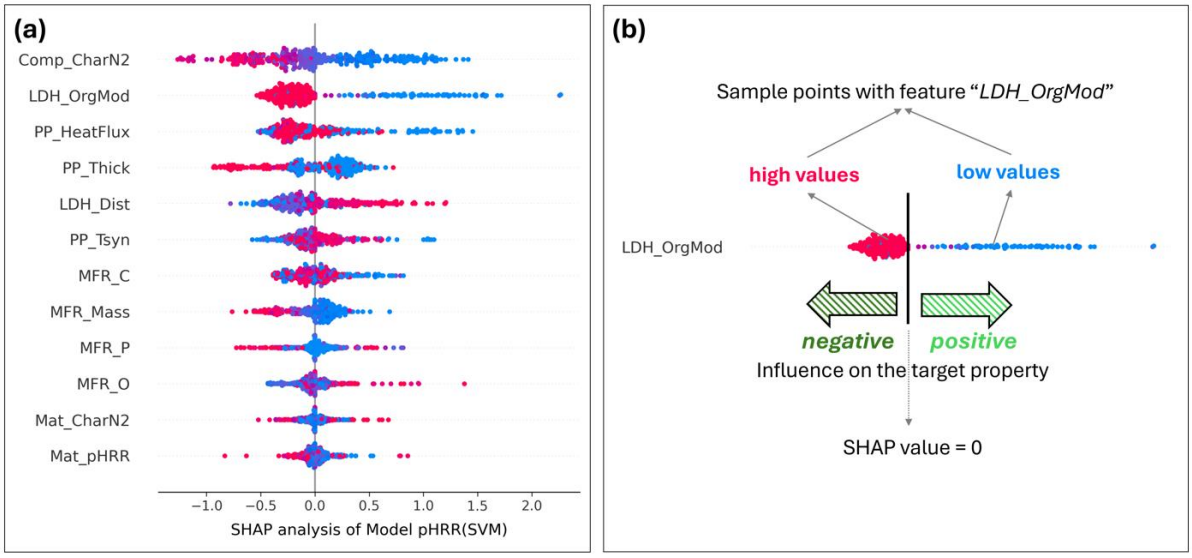

Fig. 3-9 Plot of SHAP values of a model and its explanation of sample points

4. Results and discussion

4.1. ML models for FRPCs in MH-system

As the first ML models, the MH-system has the advantage of simple FR mechanisms. Normally the FR performance of FRPCs is proportional to the mass fractions of MH in the formulations. This is convinced from the relationship between the loading of MH and CCT results in the collected dataset. Also, this is concluded through the feature important analysis of the models.

Data-driven investigation of FRPCs

4.1.1. Influence of MH-addition into FRPCs

The generated dataset consisting of 219 records was used as input in our ML approach. Each formulation was unique due to the combination of the polymer matrix, FR additives, and processing parameters. From the graphic illustration in Fig. 4-2(a), decreasing "D-pHRR" with increasing amount of FR additives was found, corroborating the empirical rules. Interestingly, with increasing the FR loading over 50 wt%, the "D-pHRR" value is estimated to be significantly lower. It should also be noted that the high amount of FR additives significantly enhances the TTI of the polymers from Fig. 4-2(b). Similar decreasing trends in D-THR and FRI in Fig. 4-2(c) and (d) are observed as the behaviour of D-pHRR. However, high filling of inorganic compounds (such as metal hydroxides) lowers the content of flammable polymers as well as provides a cooling function additionally and thereby effectively reduces heat generation [95].

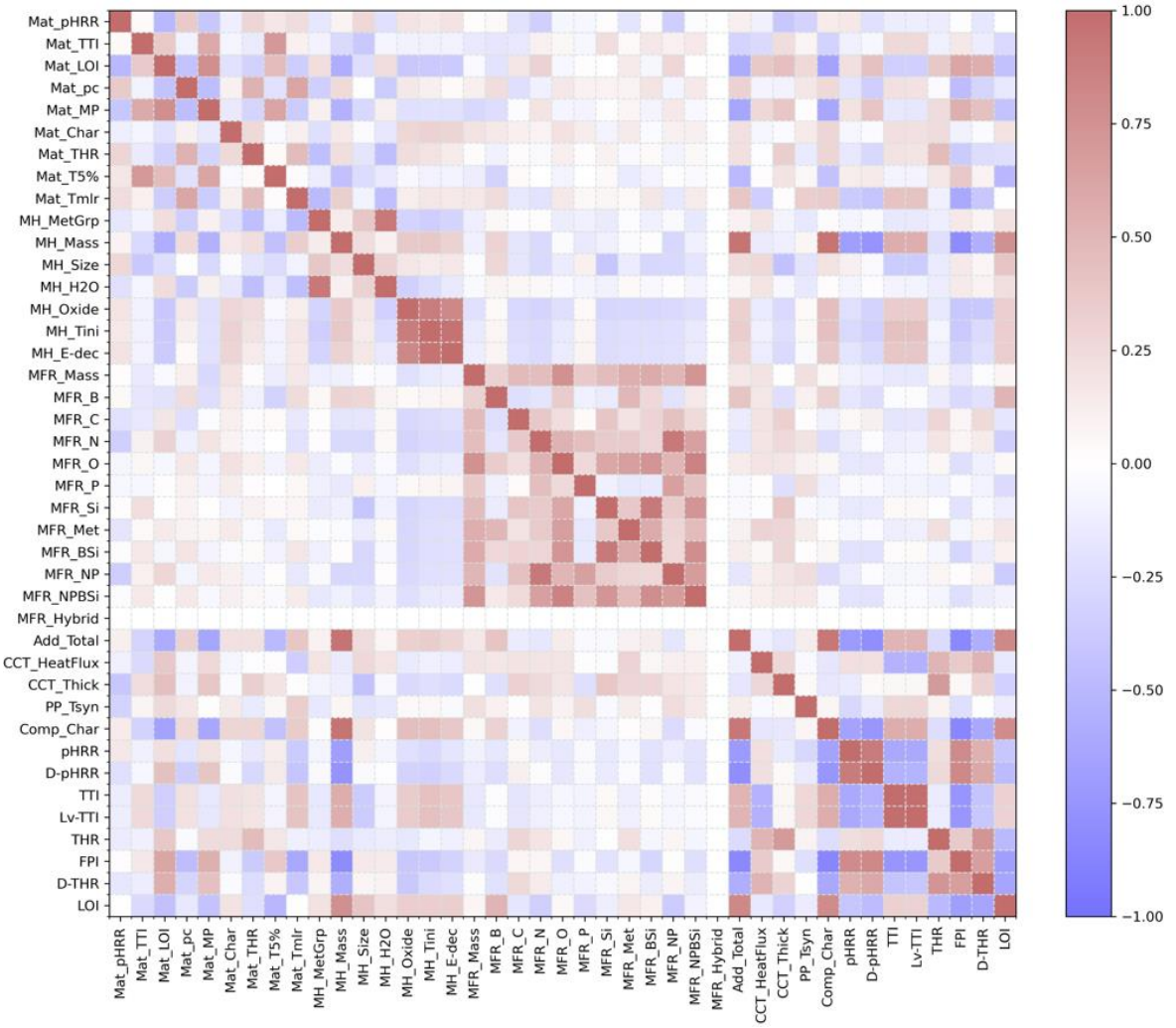

Fig. 4-1 Spearman's correlation map of MH-dataset

This is also observed in the heatmap illustrating the Spearman's correlation between all features in MH-dataset shown in Fig. 4-1. The deeper the colour is, the stronger the correlation between the two features is. Blue and red indicates the dependence is positive or negative. For the modelling, a combination of features that are independent to each other is necessary. In the row of "MH_Mass", the total mass fraction of FR additives, char of polymer composites, pHRR and FPI have all coloured relationships, meaning they are strongly influenced by the mass fraction of MH in polymer composites. Other areas that contain the strongly related features are the features of MFRs (representing the other FR additives except for MH) in the middle and properties of polymer composites themselves at the bottom right. The feature "MFR_Hybrid" is totally white is due to this reason: all the FR additives are physically mixed so that the values of this feature are 0. Although MHs as the key FR components are effective to prolong the TTI and lower the D-pHRR, D-THR and FRI, the influence of other factors including synergists and polymer matrix cannot be ignored. Furthermore, no distinct correlation is observed between the CCT characteristics and the other affecting parameters in the input dataset. Despite the fact that these additional affecting parameters have a certain impact on the combustion process of polymer composites, however, their effects are not as significant as the effect of MHs.

4.1.2. Statistical ML models of fire properties

To evaluate the accuracy of RF models, three common used statistical indices (R2, MAE and RMSE) [96] are calculated in Table 4-1. The R2 scores meet the requirement for precise predictions in test sets: R2 values of 0.81 for prediction of "D-pHRR" and over 0.85 were achieved for classification of "Lv-TTI", "Lv-THR" and "Lv-FRI", respectively. The MAE and RMSE in test sets for all target properties were comparable, relatively small. Such high R2 values indicate that the models match well with the MH-system. Although the R2 in test sets are lower than that of training sets, the models have still promised predictive accuracy.

Table 4-1 Model indices in training and test sets in predicting D-pHRR, Lv-TTI, Lv-THR and Lv-FRI

Indices	D-pHRR		Lv-TTI		Lv-THR		Lv-FRI	
	training set	test set	training set	test set	training set	test set	training set	test set

R2	0.97	0.81	1.0	0.9	1.0	0.84	0.99	0.88
MAE	0.02	0.06	0	0.3	0	0.16	0.02	0.14
RMSE	0.04	0.09	0	1.43	0	0.4	0.16	0.42

Except for the above indices, another direct judgement of accuracy is the Fig. 4-2(e) to (h), in which the predictions are plotted against truly measured values. Blue dots stand for samples in training sets and red stars are from test sets. Because the "Lv-TTI", "Lv-THR" and "Lv-FRI" are integral, categorical values, the dots in these models locate in fixed positions. We can see the distribution of discrete values in the model predicting "D-pHRR". The green lines in the diagonal direction are to indicate the equality of predictions and measurements. The closer the data points are located to the green line, the closer the predicted values are compared to the actual values, indicating more accurate predictions made by the models. In all the plots, blue points of training sets are distributed along the green lines closely, indicating the high equivalence between measured and predicted values. Red marks in testsets spread themselves along the diagonal line but with relatively wider range than the blue dots. Some red stars can be noticed located far away from the green line which are unseen/untrained formulations to the models that lead to high error in predictions. For example, Fig. 4-2(e), 2 samples in testset (22 wt-% synergist without MH and 1.8 wt-% MH with 7 wt-% synergist) locate to the left side due to these rare combinations. These "outliers" can be classified as the minorities in the dataset. [37] Most of the points distribute not far away from the diagonal lines, demonstrating the high predictive accuracy as the high R2 in test sets.

In addition, we prepared the validation samples to evaluate the predictive performance of our models. The red bars in histograms in Fig. 4-2(i) to (l) stand for the measured values into the same format as target properties, and the blue bars are the predictions made by our assembled models correspondingly. In summary, the predictions match the measurements well. Higher accuracy is found in predicting "D-pHRR", "Lv-THR" and "Lv-FRI", where their MAE values remain as low as 0.06, 0.16 and 0.24, respectively. The model for "Lv-TTI" showed inferior performance for some samples, the predicted TTI values are much different from the experimentally measured values. In EVA01 and EVA02 samples, unseen synergists were introduced with varied ratios, which strongly influenced the

ignition properties. Bad performance on HDPE01 sample is attributed to the minority of data featured with HDPE as polymer matrix. Even so, the predictions and measured values are still comparable in most cases. This indicates that the models can be promoted by feeding rare formulations to compensate the inhomogeneity of dataset.

The prime reason for the overfitting can be attributed to the construction of the input dataset. Since most data come from research with high MH-loading to achieve good performance, and published results have commonly similar formulations. Consequently, the predictive performance of such models is inferior for low MHs loading and rare composites. However, the disadvantages during the data collection cannot be ignored. Due to a lack of comprehensive databases on FR polymer composites, our input dataset is constrained in size and feature structure. The information that was retrieved is selective and unable to account for every conceivable type of additive and process. On the other hand, certain errors in characterization are inevitable due to the differences in device conditions, operation skills, and the standard of experimental instruments in labs.

4.1.3. Important MH-properties and effective parameters

RF algorithmic framework allows to calculate importance of every feature based on information gain, aiming to investigate its significance in deciding target properties in our predictive models. All features are coloured into 4 parent groups explained in methodology part.

Unsurprisingly, all target properties are significantly affected by the mass fraction of MH shown in **Fig. 4-3**. The mass fraction of MH in the polymer composites has the importance of 0.14 to 0.35 in all models, taking the first place in the ranking of input features. The difference is that MH mass nearly dominates in deciding "D-pHRR": MH related features (sum of "MH_Mass", "MH_Size" and "MH_E-dec") take 57% feature importance in total. Other features do not have such influence on "D-pHRR" like MH does. In other 3 models, features referring to polymer matrix, synergists and processing parameter still have significate impact. In "Lv-TTI" model, the mass fraction of additional FR additives "Syn_Mass" has the importance of 0.10, taking the third place. The heat flux of CCT follows with 0.08 importance. However, in the model predicting "Lv-THR", the influence of polymer matrix is more important: "Mat_TTI" is ranked in the second place with 0.10 importance, and "Mat_pHRR" takes the fourth place. The purple bars representing

the “Polymer_Matrix” feature group locate themselves more or less at the forefront. Besides, the highest temperature in the sample preparation process is also essential to the THR of polymer composites, in which “PP_Tsyn” has an importance 0.08. The ranking of features in model predicting “Lv-FRI” looks similar to that of the “D-pHRR” model, combining the significant features from “Lv-TTI” and “Lv-THR” models. In a whole, the influence of features in deciding “Lv-TTI” and “Lv-THR” is more multi-dimensional. In contrast, the loading amount of MH in FRPCs has determined the “D-pHRR” and “Lv-FRI” significantly. The size of feature structure increases with higher complexity of target properties: compared to Lv-TTI and D-pHRR, more features are needed to improve the accuracy in predicting Lv-THR and Lv-FRI. This indicates that the features in the figure do not cover all the influence factors that give impact on “Lv-THR” or “Lv-FRI”. More information is needed to improve the predictive performance of these models.

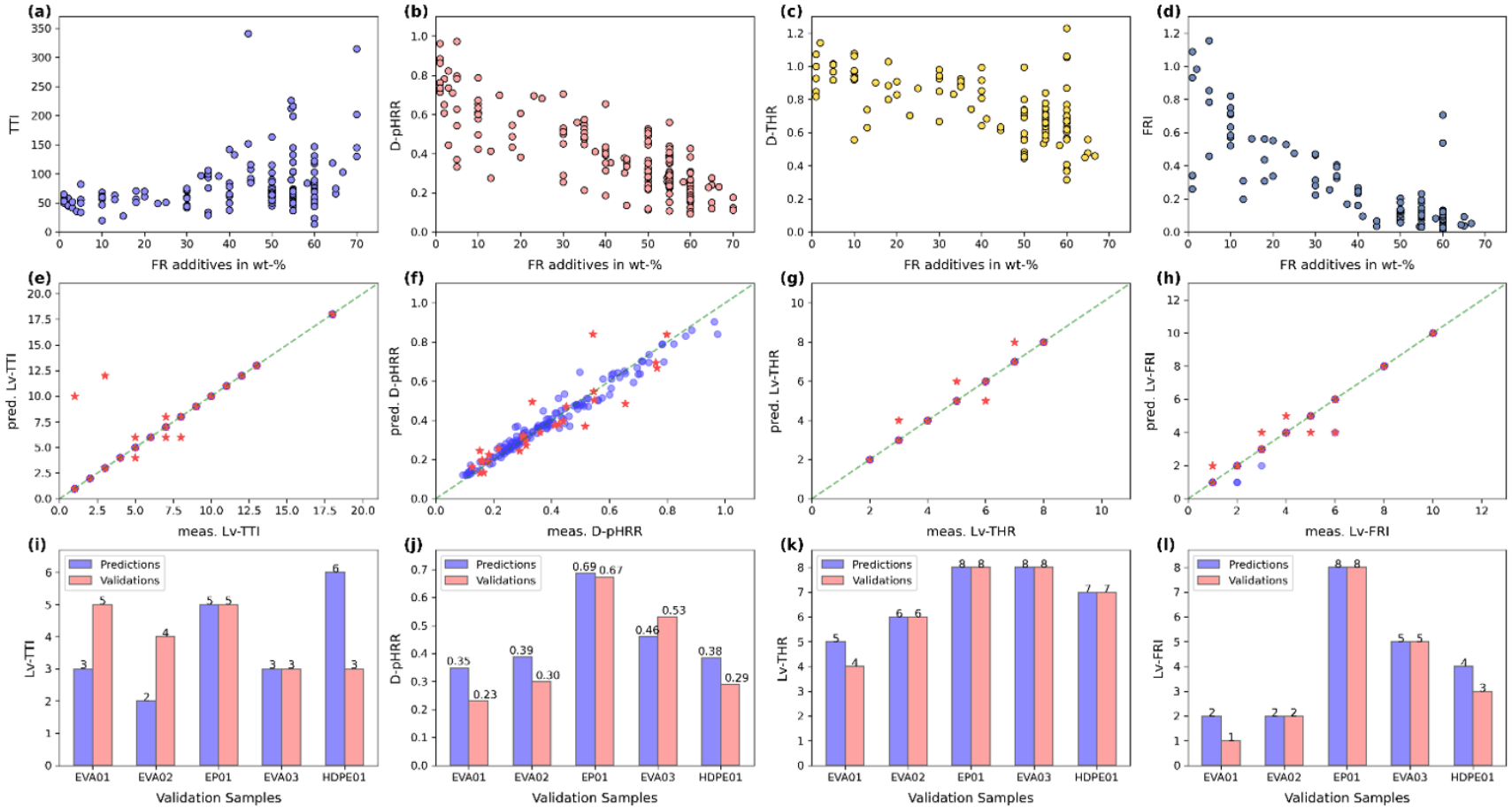

Fig. 4-2 Presentation of dataset and modelling results: Distribution of TTI (a), D-pHRR (b), D-THR (c) and FRI (d) with respect to the mass fraction of flame-retardant additives; different colours stand for different polymer matrixes in the dataset. The size of the dots represents the mass fraction of flame-retardant additives; Predictions versus measurements for Lv-TTI (e), D-pHRR (f), Lv-THR (g) and Lv-FRI (h); Validation in bar plot for Lv-TTI (i), D-pHRR (j), Lv-THR (k) and Lv-FRI (l)

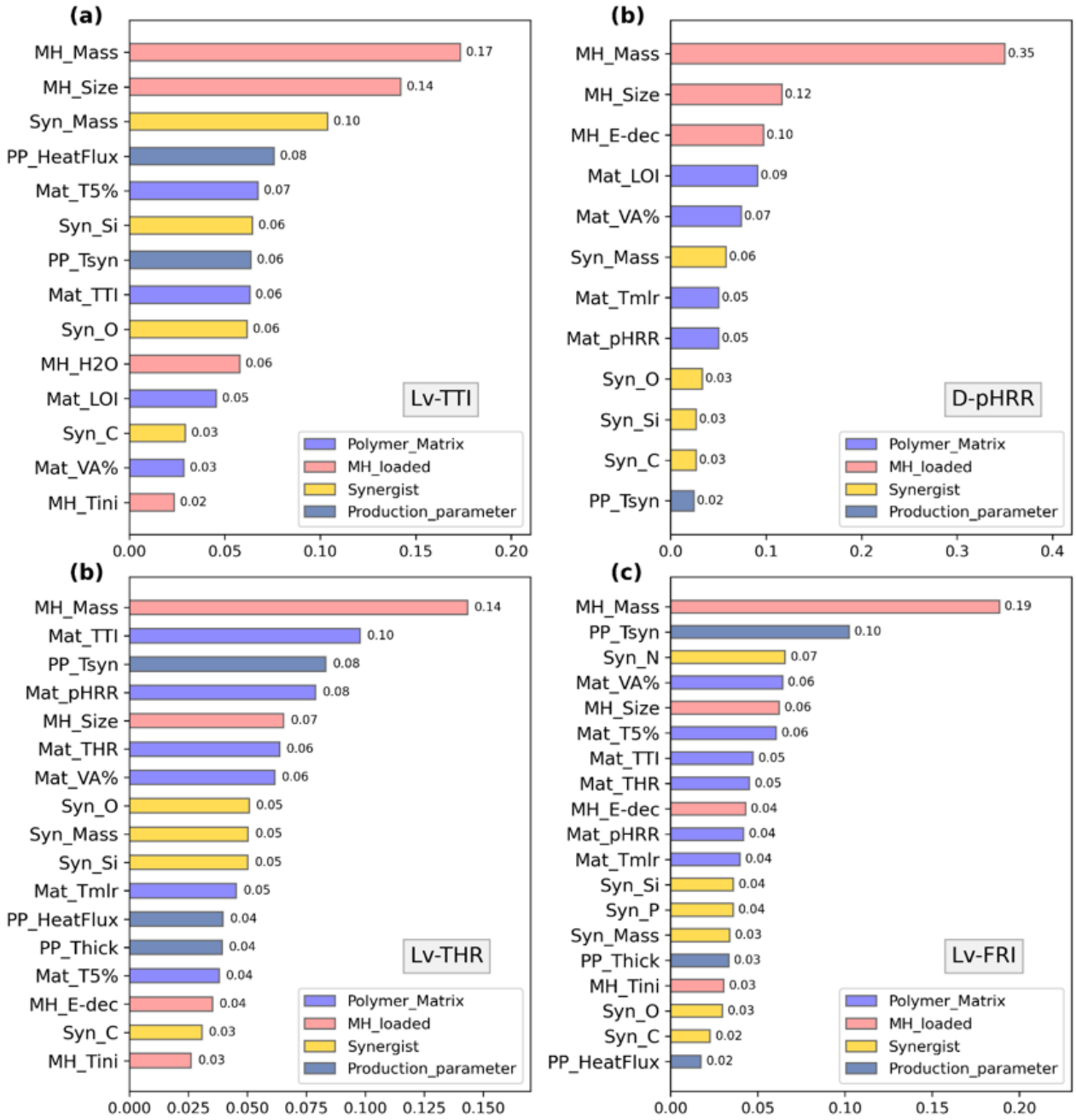

Fig. 4-3 Importance of all features selected to build the random forest models predicting Lv-TTI (a), D-pHRR (b), Lv-THR (c) and Lv-FRI (d); Coloured legends illustrate the parent groups of each feature

4.1.4. Virtual dataset-based multi-objective optimization

To find the optimized formulations for flame retardant polymer composites, virtual datasets featured with the same structures from the original input dataset were generated computationally, in which values were automatically varied in

corresponding ranges (4 grades of 0, 0.33, 0.67, and 1). Due to the limitation of computer performance, the virtual dataset was only imported into the constructed models to predict their D-pHRR and Lv-TTI. Points with D-pHRR < 0.4 and Lv-TTI > 8 are classified into high-performance samples as shown in equation (3).

$$y_{performance} = \begin{cases} high & \substack{D-pHRR<0.4 \\ Lv-TTI>8} \\ low & \substack{D-pHRR\geq 0.4 \\ Lv-TTI\leq 8} \end{cases} \quad (3)$$

As presented in **Fig. 4-4**, Y-axis represents the value range of each feature in the original dataset after label encoding. Each column depicts the individual histograms of feature listed below. Bars in red and blue with different lengths indicate the number of screened formulations with correspondingly low- and high-performance.

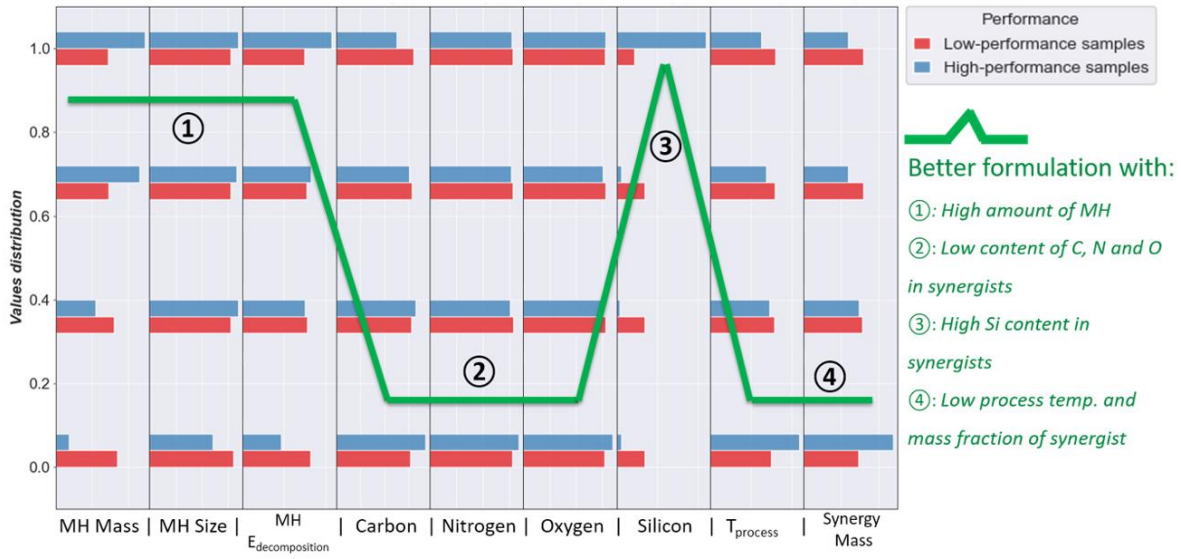

Fig. 4-4 Histograms of values distribution of each important feature, red bars refer to low-performance points and blue bars are high-performance ones; Green segments represent the recommended composition of polymer composites with high performance.

To achieve high performance, the suggested formulation should correspond to the values where the blue bars are relatively long. Along the green line, a large amount of MHs with moderate particle size and high enthalpy of decomposition is preferred. [97] The mass fraction of synergist should be low. The content (atomic percentage) of carbon, nitrogen and oxygen in the synergists should be as much as low, while silicon content is required to be high. Last but not the least, the process temperature required to prepare the samples should preferably be low.

The recommended formulation is constructed according to our models. Consequently, restrictions related to our input dataset exist. For example, the

requirement for high content of Si is partially attributed to the fact that all the Si-containing formulations in the dataset contain high mass fractions of MHs too, resulting in lower pHRR and longer TTI. Such data combination emphasizes a monotonic relationship between the atomic percentage of Si present in the samples and the target features. However, silicon additives have certainly a synergetic effect together with MHs, especially in the condensed phase to facilitate char formation [98].

4.2. ML models for FRPCs in MOF-system

4.2.1. FR effect of MOF and synergists

In the retrieved dataset, formulations of different polymer composites, processing parameters and the measured properties are listed in detail, containing the results from 59 recent papers and past experiments. Among all polymer matrices, the thermoset epoxy (EP) is in the majority with 53%, and thermoplastic ethylene-vinyl acetate (EVA) follows. Other polymers, including polylactic acid (PLA), polyamide 6 (PA6), polyurethane (PU) etc., also appear in the dataset. Over 25 kinds of MOFs are applied in the collected papers, with a mass fraction of lower than 10 wt-% in general. These MOFs include the common types like UIO-66, ZIF-8 or HKUST-1, and also self-synthesised MOFs. Such self-produced MOF generally reference the original synthesis procedures of famous MOFs but undergo partial optimization about the dwell time and temperatures. They utilize different metal atoms or organic ligands, which are either purchased from the market or synthesized by the researchers themselves, featuring with the molecular structures or functional groups that they require for the experiments. Besides, the MOFs are supposed to collaborate with other FR additives to enhance the fire and mechanical performances of polymer composites. Those other FR additives usually contain effective FR elements like phosphorus and varies from commercial products to self-synthesized or modified chemicals. This behaviour is very unfriendly to feature extraction and can even lead to the absence of a large number of values for certain features.

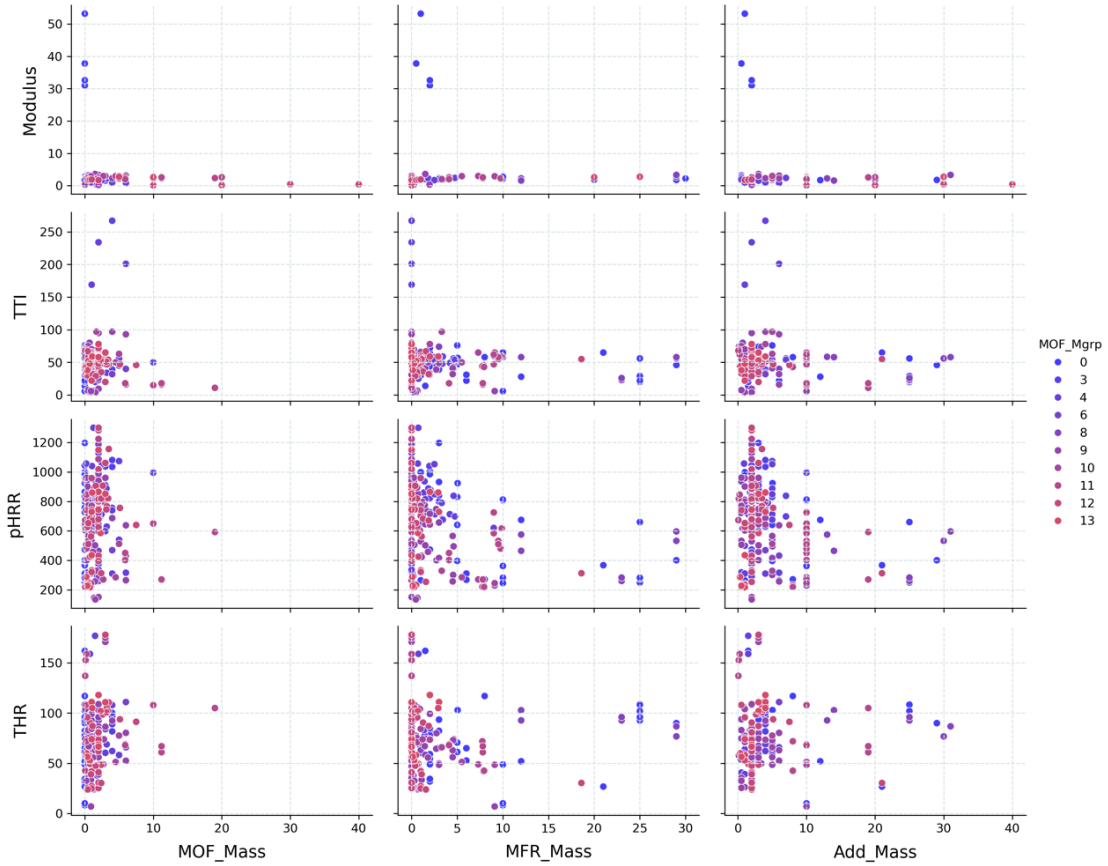

Fig. 4-5 Pairwise plotting of significant features against the target properties of polymer composite: Mass fraction of MOFs or/and other flame-retardant additives as the x-axis; with coloured dots representing the group of metal in MOF

Pairwise scatter diagrams are made through the collected data in Fig. 4-5 and Fig. 4-6, to see if there is similar trend as the MH-system. The data points are coloured from blue to red, representing the group of metal atoms in MOF within the periodic table of elements. Unlike the clear influence of loading amount of inorganic fillers like metal hydroxide [99], although there is approximately a trend of decreasing pHRR and THR with the addition of more additives, it is still difficult to conclude the correlation between MOF/MFR mass and target properties of polymer composites. The metal types in MOF also show less obvious influence on the fire and mechanical properties. Meanwhile, it is obvious that the loading of FR additives in this MOF-system concentrates generally in the small range in Fig. 4-5. The mass fraction below 10 wt-% is the choice of most researchers.

In contrast, the composites' properties exhibit a well-marked semi-proportional relationship to that of polymer matrix in Fig. 4-6, as the dotted lines in diagonal scatters indicating the equivalent values. As the polymer matrix lays the foundation of corresponding composite, such high correlations are apparent to be found. The division of target properties allows us to evaluate the effectiveness of

composite formulations better. In addition, the distribution of data points along the trend lines indicates the inhomogeneity of data in our dataset. Since all formulations are designed to improve the flame-retardant performance of composites, the samples appear to cluster together and shift into same direction (decreasing or increasing the target values), which is especially found in the pHRR- and THR-graphs.

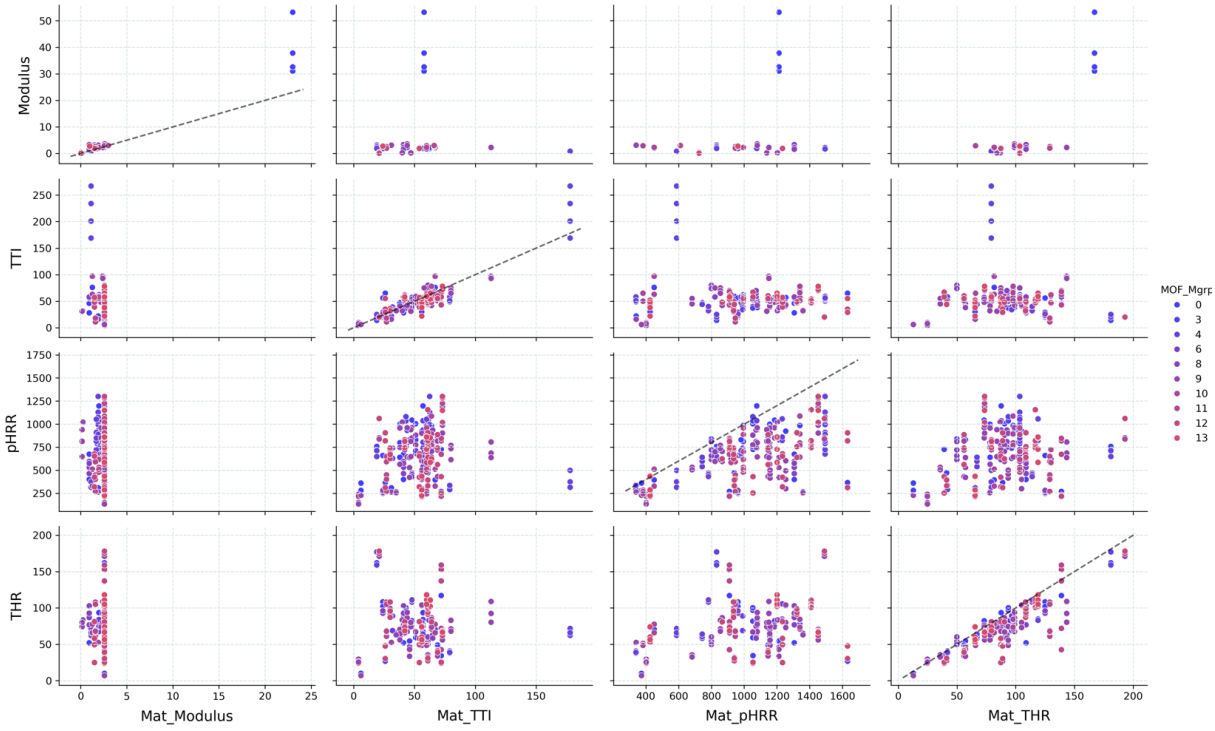

Fig. 4-6 Pairwise plotting showing the relationships between the properties of polymer composites and neat polymers; with coloured dots representing the group of metal in MOF

Seen from the statistical data, it is not only one or two key features that give impact on the target properties of MOF-loaded polymer composites. Over thirty features have been included in our dataset to build the model. Except for the values of matrix, it is vitally significant and essential to select proper combination of features containing the information required for constructing the model. In general, initial selection of descriptors originates from the reaction mechanisms of these additives in polymer composite. Subsequently, the availability of feature values should be considered since we use the publications as our data source. Additionally, calculation of the correlation coefficients between the input features is also important in feature engineering. The Fig. 4-7 highlights the heat map of the Spearman' correlation between every two features, in which the lighter

coloured pairs stand for lower independence between corresponding features. The high correlated features usually focus on the same feature group, forming the clouded areas in the map. The “Moudlus” of polymer composites seems to have a blue correlation with the “MOF_Class”, this relationship is an evidence to the influence of MOFs on the mechanical properties of FRPCs, which is also confirmed in the ML models. However, the columns that are the target properties to the right side of graph are all in white colours, approximately, supporting the conclusions obtained above. Although there are high correlations between the features describing MOF property and other flame-retardant additives, the whole dataset still fits the purpose of modelling.

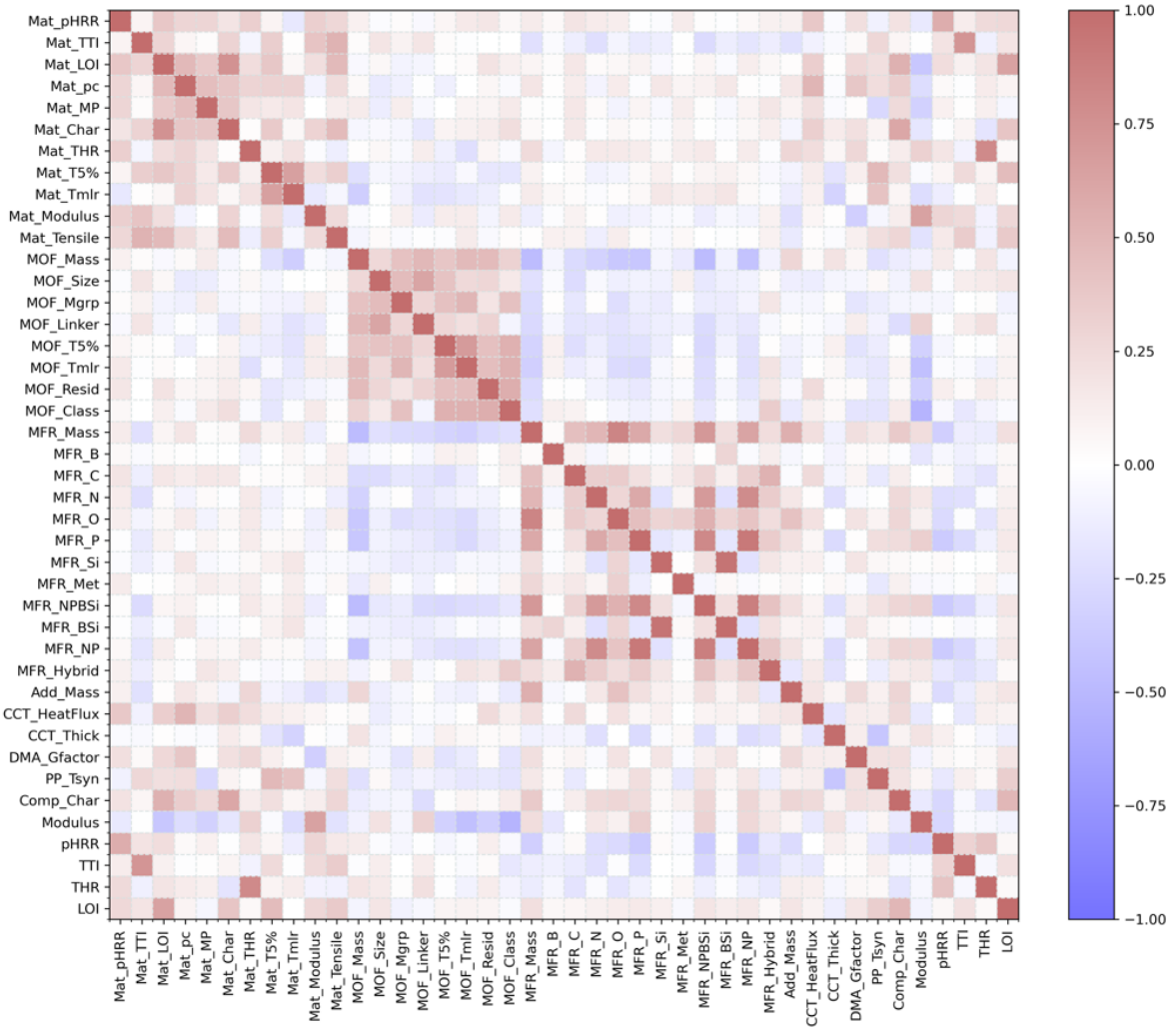

Fig. 4-7 Spearman’s correlation coefficients between input features, the lighter the colour is, the weaker the correlation is.

4.2.2. Mechanical and fire-properties of MOF-loaded FRPCs

As mentioned above, 3 different algorithms were applied in building models that predict the following target properties: "*Modulus_dc*", "*TTI_dc*", "*pHRR_dc*" and "*THR_dc*". The coefficient of determination (R2) and mean errors are listed in Table 4-2. All the models present satisfied accuracy in train sets, with the R2 over 0.87. However, predictions made in testsets are less accurate. In different models, R2 in test sets varies from 0.75 in Modulus(RF) to 0.84 in THR(AVG). The worst models are those predicting pHRR of FRPCs. Although the models built with single algorithm have very low R2 below 0.70, the pHRR(AVG) models have considerable R2 of 0.77. This indicates that the combination of different methods do really improve the predictive accuracy of ML models. Similar behaviour of different magnitudes of errors in train- and testsets is observed. In consideration of the categories of all target properties varying with a gradient of 1, the MAE and RMSE of the predictions in testsets are relatively small. Compared to the other two basic algorithms, the AVG-models have in general higher R2 values, indicating that the combined classifiers have indeed integrated the advantages of both algorithms. However, there are trade-offs. Modulus(AVG) model has slightly higher R2 of 0.77 than that of 0.75 in RF- and SVM-models; but its MAE and RMSE have conversely increased by 30%. This enhancement of R2 of AVG-models is more obvious in predicting pHRR and THR.

Except for the commonly used R2 and mean errors, the confusion matrix (CM) and the area under the receiver operating characteristic (short as AUC for Area Under ROC) values are presented as further judgement of predictive accuracy in Fig. 4-8. This classic metric reflects the classification quality by calculating the number of samples that are misclassified into other categories. In the CM chart, the color of off-diagonal squares exhibits the corresponding number of true or false classifications of the categories in the vertical axis. The whiter the square is, the more samples are incorrectly predicted into another category. We have selected RF-model for predicting Modulus, SVM-model for TTI and AVG-models for pHRR and THR with the overall consideration of R2 and predictive errors. In the Modulus(RF)-model, part of the samples in category ">1.70" was predicted to wrong category "1.35-1.70", indicated by the white square in the last row, which has good agreement with low MAE and RMSE in the testsets. Although the Modulus(RF) shows excellent classification accuracy, this is due to the fact that the number of categories of storage modulus are relatively minimal.

Table 4-2 Determination coefficient, mean absolute error and root mean squared error of selected classification models. See the full table of all 12 models in supporting materials.

Indices of ML models	R2		MAE		RMSE	
	train	test	train	test	train	test
Modulus(RF)	0.87	0.75	0.18	0.42	0.54	0.96
Modulus(SVM)	0.99	0.75	0.01	0.33	0.01	0.5
Modulus(AVG)	0.96	0.77	0.09	0.33	0.3	0.71
TTI(RF)	1.0	0.84	0	0.2	0	0.53
TTI(SVM)	0.96	0.78	0.07	0.32	0.15	0.62
TTI(AVG)	1.0	0.78	0.02	0.51	0.14	1.04
pHRR(RF)	1.0	0.67	0	0.4	0	0.73
pHRR (SVM)	0.97	0.5	0.04	0.93	0.05	2.07
pHRR (AVG)	1.0	0.77	0.01	0.62	0.11	1.07
THR(RF)	1.0	0.76	0	0.37	0	0.85
THR (SVM)	0.99	0.76	0.01	0.33	0.01	0.57
THR (AVG)	1.0	0.84	0	0.37	0	0.7

Unlike the modulus model, the other three models predicting CCT characteristics have more misclassified samples. The inaccuracy of TTI-predictions focuses mainly in the middle categories, i.e. “0.80-0.90”, “0.90-1.00” and “1.00-1.10”. Except for the obvious white blocks, many grey squares are also distributed in between. Predicting the values of samples with relatively greater or smaller TTI-change is more accurate. It is, on one hand, attributed to the lack of key features labelling the physical and chemical reaction on the sample surface under heating. Some researchers think that the flammable organic ligands or other additives with lower decomposition temperature contribute to shortening the TTI of polymer composites. [100,101] Besides, the principle that certain FR additives promote the early decomposition of polymer matrix cannot be adequately summarized using our features. [102] On the other hand, most samples concentrate themselves in the moderate ranges, as shown in Fig. 4-9. Thus, there are more misclassifications in these categories, which is also the joint outcome associated with the insufficient feature mentioned above.

Data-driven investigation of FRPCs

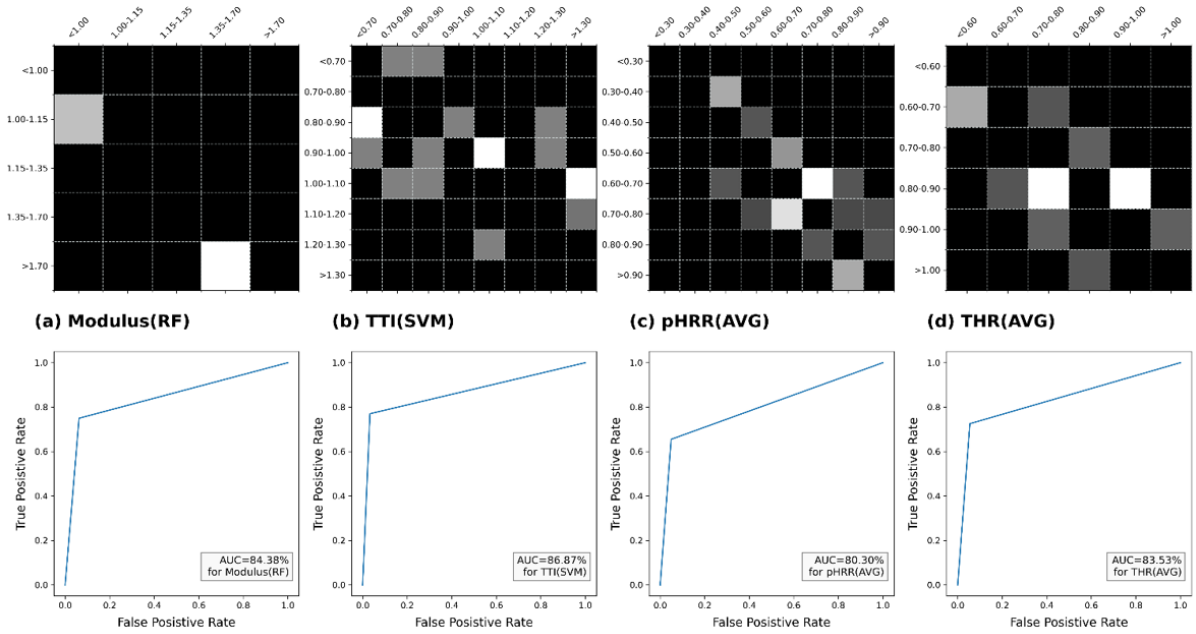

Fig. 4-8 Confusion matrix and ROC curves of selected classifiers predicting "Modulus", "TTI", "pHRR" and "THR"

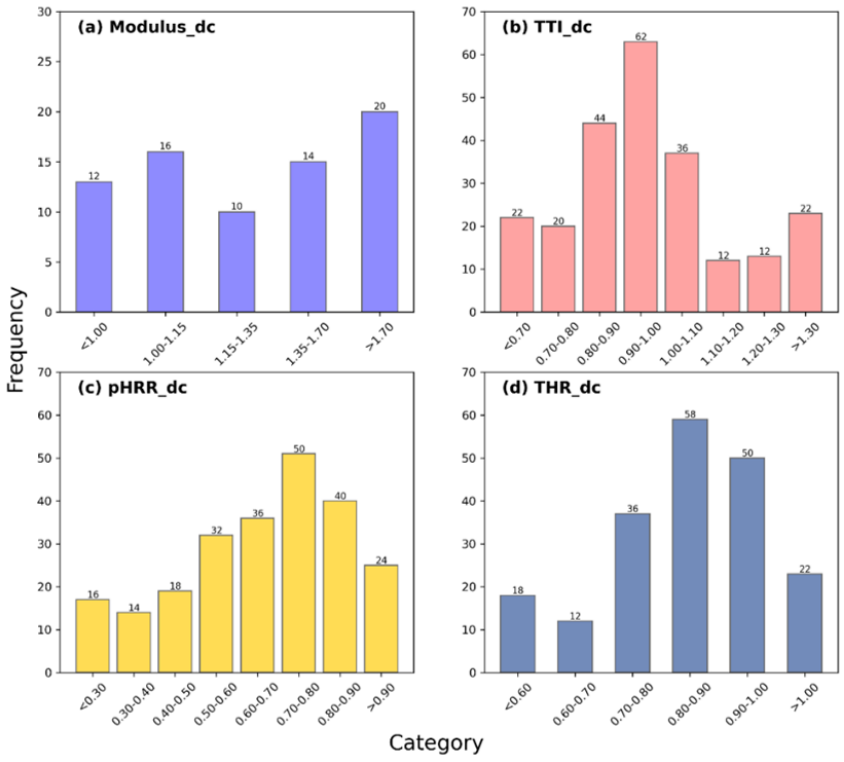

Fig. 4-9 Distribution of all categories of four target properties in our dataset

Compared to the TTI(SVM), the inaccurate predictions in pHRR(AVG) and THR(AVG) models are distributed along the diagonal line. The misclassified data points appear mostly to be distinguished into the neighboured categories.

Furthermore, there are misclassifications across most categories. On the whole, such inaccuracy seems to be more systematic, attributed to the linear combination of RF and SVM models. Likewise, the categories that contain most samples in pHRR and THR (Fig. 4-8(c) and (d)) have the worst performance in CM. In summary, the AUC values of all four models have reached over 80%, indicating that the models have good performance in classification and handling with imbalanced dataset.

In general, a certain amount of data with corresponding features describing the system should be provided to the machine when facing a complicated problem. The required size of dataset is usually proportional to the complexity of question and model. In our case, we collected the data from publications and past experiments due to the lack of reliable and systematic databases. Likewise, the features decoded from the physical properties, chemical components, and processing parameters have involved the generalizability, accessibility, and veracity of their values. Primarily, there are two challenges to be emphasized. Since this work is focusing on the loading of MOF and possible FR additives into various neat polymers, how to summarize the numerous formulations of polymer composites is the first difficulty. The tunability of MOF and abundant kinds of additives leads to highly different chemical compositions, molecular configurations and microstructures, which affect the target properties of polymer composites. Apart from the additives, it is generally accepted that MOF has promoted the char formation by the catalytic effect or surface-distributed nucleation sites. [103,104] However, key features of MOF morphology and molecules is impossible to obtain or quantify from the research articles, leading to the models lacking sufficient information about the promoting effect. Moreover, recent researchers prefer to encapsulate some flame-retardant molecules into MOFs to form various hybrids. The addition of such uniquely designed chemicals makes it more difficult to dig up effective features to cover the possible influencing factors in data space.

Another challenge is the limitation of data. The data-driven investigation concentrates on the interpretation of intrinsic relationships between significant features, abundant data and machine learning models. It is therefore highly required to have systematic databases in material-related fields. However, establishing a comprehensive database, even for a tiny research-line in material science, requires leading promoters and competent organizations. Since the discovery of MOF, it has found many applications as described in the introduction part, and many relevant databases have been created. Although over 160k results

of MOF are recorded in database, the data that are useful for the usage of MOF in the fireproofing polymer composites is still scarce. Relying only on personal work in data collection is not enough. The size limitation makes it difficult to build highly accurate models for the prediction of complicated composite properties.

4.2.3. How do the MOFs affect the properties of FRPCs

The tree-based algorithms (RF models) provide the ability to assign a value of feature importance based on impurity calculation and quantified from the total improvement of the split-quality in modelling. The higher value means that the feature is more important in deciding the final property. Sum of the importance of all features is set to be 1. For the models that are not based on decision trees, we utilized a suitable explanator to produce an interpretable table of feature influence in SVM models: the SHapley Additive exPlanation (short as SHAP) from modern game theory. The Shapley values are attributed to the features of every sample in models, reveal how do the features influence the targets and if they influence the target properties positively or negatively. Although both FI and SHAP reveal the significance of the feature, some features may differ in the ranking since the SHAP calculation is normalized by the samples/predictions separately.

Fig. 4-10 shows the ranked importance of input features in four RF models. The feature combination of input dataset has been optimized and all the four models have different features applied in modelling. Different bar colours indicate the features from different groups described in the methodology part: light purple for the group “Polymer_Matrix”, washed red for “MOF_Material”, yellow for “Main_FR” that is the flame-retardant additives besides MOF and light Prussian blue for “Other_Parameters” involved in sample preparation and characterization process like CCT or DMA test. These feature groups are explained in detail in the methodology part.

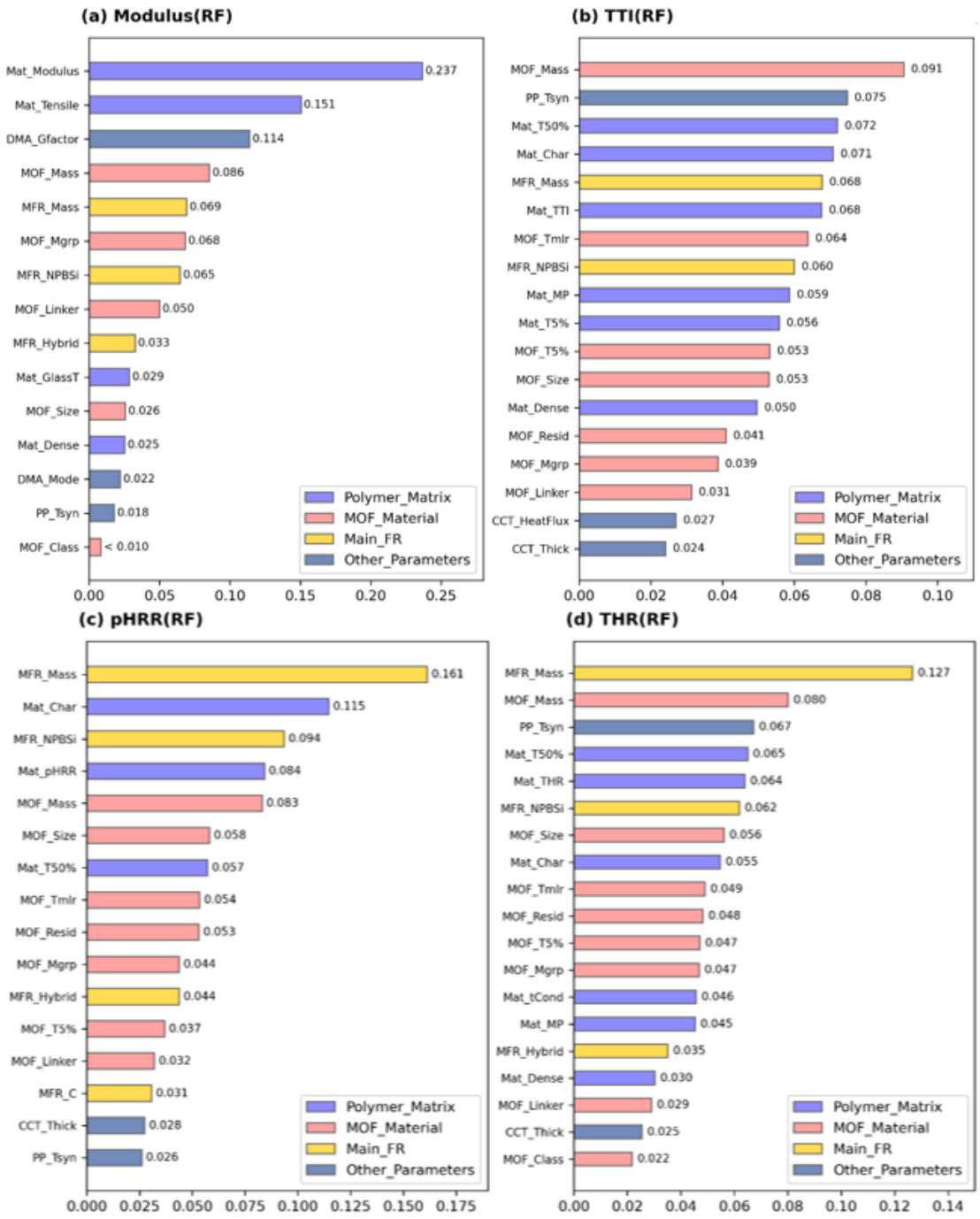

Fig. 4-10 Ranking of feature importance of RF models predicting "Modulus", "TTI", "pHRR" and "THR". Different colors of the horizontal bars represent that the feature belongs to the corresponding feature group.

According to the feature importance (FI), all input features make corresponding contribute to the predicted properties. In some cases, only a few features have considerable importance in the model. In this work, the distribution of FI values of all features has indicated the complexity of the MOF-added polymer composites. Due to the complicated physical and chemical reactions between matrix, MOF and other additives, there are no dominant features in the above models.

The storage modulus of polymer composite depends primarily on the mechanical properties of neat polymer itself, as evidenced by the FI of "Mat_Modulus" and "Mat_Tensile" of 0.24 and 0.15 separately. Moreover, the interaction between the polymer chain segments and the solid filler particles also counts. [105] Since it's difficult to quantify or qualify the interactions between polymer matrix and additives, we have taken many features to describe it indirectly. Although MOF is intended to improve the dispersibility and compatibility of fillers in polymer matrix, and consequently enhances the mechanical performance of polymer composite, the MOF- and MFR-related features in Modulus(RF) model have gradually decreasing importance from 0.09 to 0.03 in the moderate range. The geometry factor in DMA test takes the third place with 0.11 FI is attributed to the great impact of the sample size in modulus calculation.

In the RF models predicting CCT results, the matrix properties are still important but not the most significant features. Under the cone heater, polymer composite is heated uniformly and ignited after certain dwell time. The thermal stabilities of all components inside the composite sample play crucial roles in deciding the TTI. Not only the decomposition temperature, but also the thermal conductivity and viscosity of melting fluid affect the heat accumulation, which leads directly to the ignition of polymer composite. In conclusion, the features influencing TTI are omnifarious and multi-dimensional. More features are necessary to build TTI(RF)-model and they almost have the similar importances below 0.1. The first three features indicate precisely the thermal stability of MOF, matrix and polymer composite.

Conversely, the MFR-related features (mass and elemental contents) have higher influences in pHRR- and THR-prediction than TTI. MFR represents the FR additives excluded MOF in polymer composite and is applied to improve the sample's flame retardancy principally. For that reason, the mass fraction of MFR takes the first place in both pHRR(RF) and THR(RF) models with FI of 0.16 and 0.13, respectively.

The significance of features in SVM models interpreted with SHAP values are shown in Fig. 4-11, constrained with the first twelve features only. Due to different mathematic foundations between SHAP and FI, the ranking of features in Fig. 4-11 is more strongly dependent on the formulations in our collected dataset. Such asymmetrical values in dataset, in which different publications have their

preferred formulations and different number of sample points, leads to many discrete data dots in SHAP diagram and unexpected ranking of features. The data dots are coloured from blue to red in each row represent the values from low to high of corresponding features, with their positions to the left or right of the midperpendicular indicating the negative or positive influence on predictions. In Modulus(SVM) model, "MFR_Mass" is the first feature but with only few dots in red, meaning that the majority of formulations have very low additive mass, and the polymer composites tend to have low storage modulus likewise. Except for this, low processing temperature in sample preparation, encapsulation of additives into MOF and using IRM- or ZEO-type subclasses of MOFs lead to increased storage modulus of polymer composites. In contrast, UIO-type MOF deteriorates the modulus at room temperature. These subclasses have different organic ligands and coordinated metal nodes that form large frameworks with microstructure and pore morphology. To prolong the TTI, polymer matrix with low melting point and char formation is advantageous. Adding more FR additives encapsulated into MOF-skeletons, higher MOF loading and using metals in high groups (group 11, 12 or 13) contribute to reduce the pHRR of polymer composite in CCT.

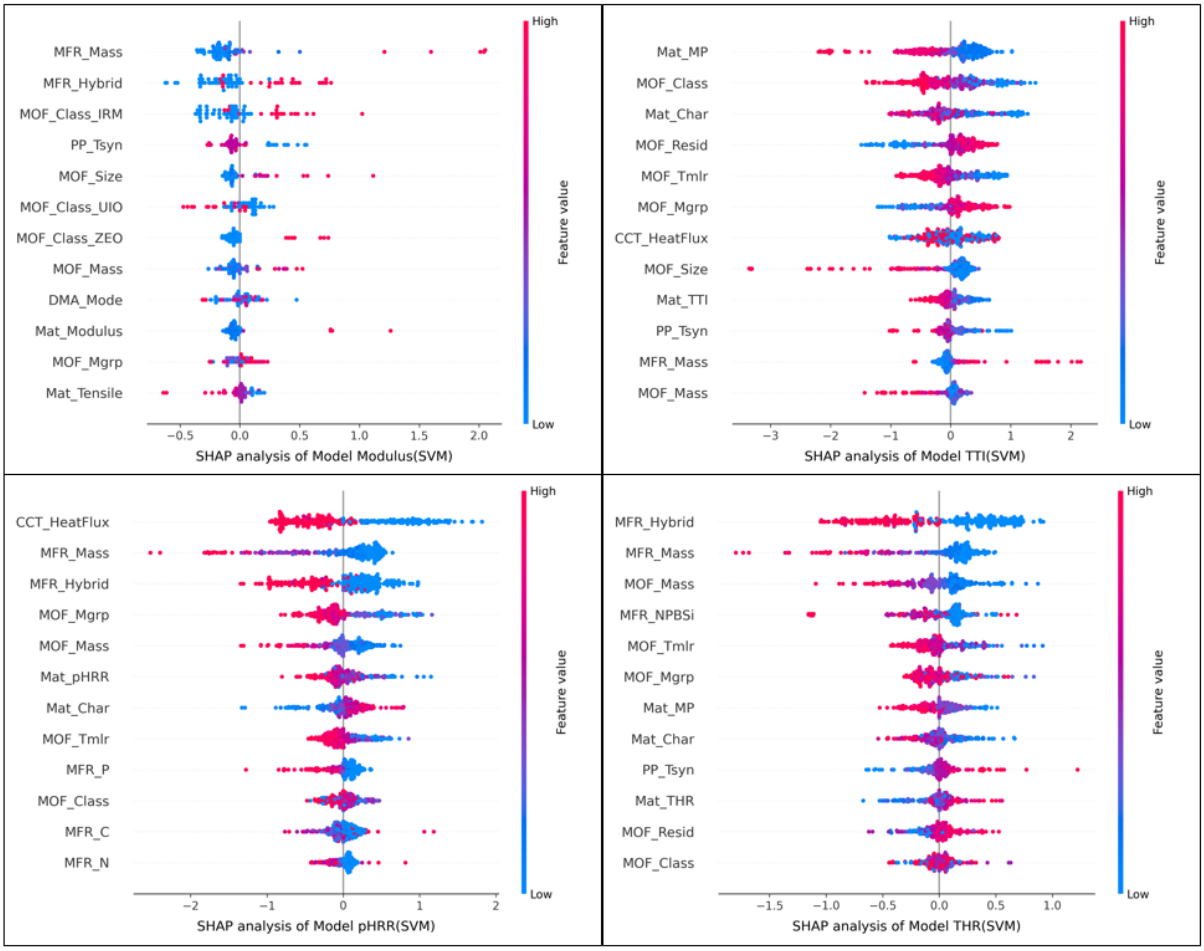

Fig. 4-11 SHAP interpretation of SVM models predicting “Modulus”, “TTI”, “pHRR” and “THR”. Colour stands for the values of features in each row.

MOFs with zeolite-structure is theoretically beneficial to achieve higher dynamic modulus of polymer composite. As for TTI and pHRR of polymer composites, the heat flux of cone calorimeter is the top feature. In a similar way, it affects the TTI easily in the practical CCT. Samples under lower heat flux tend to dwell longer before ignition and hold a less vigorous combustion. Moreover, the MOF prolongs TTI when it is not ZEO- or UIO-types, has high reactive metal nodes and low decomposition temperature. In contrast, the pHRR of polymer composite is negatively influenced by encapsulation of additive in MOF, increased MOF amount, heavy metal nodes, and high decomposition temperature of MOF. To lower the total heat releasing from burning, samples are supposed to have the similar formulation as noted earlier in pHRR-model. Except for the heat flux, the values of input features that have negative influence on pHRR of polymer composite also reduce THR in CCT.

The explanation of features and models is based on the data in our collected dataset. Because of the fact that the formulations in published papers usually have good performance, the majority of our raw data have feature values either concentrated in a narrow range or show only slight difference. Besides, the features describing the nanostructure of MOF, possible synergistic effects between MOF and other additives, and possible reactions between fillers and polymer chains are barely to obtain. Yet these factors are strongly connected to the FR mechanisms of polymer nanocomposite. In our dataset, we selected the indirect features like particle size from SEM characterization, type of building units and synthetic route to represent its structural properties like porosity and specific surface area. Most importantly, the dataset is created from collected publications and experimental works individually, which means its size is limited. Machine learning, as a tool for analysing the internal relationships between the input and output, requires high amount of data to construct a statistical model that enables the prediction of material properties from the production, structure, and measurement. These deficiencies lead to the limited performance of the machine learning models. Conversely, increasing the dimension of datasets is a promising way to improve the accuracy of prediction.

4.2.4. Validation experiments with unseen data

To investigate the predictive accuracy of our models on unseen formulations, we picked out four formulations from the collected dataset and prepared EP composites with Fe-BTC (classified as MIL-type MOF, see supporting information S2 for details) and intumescent flame retardant (IFR, samples labelled with EP-Ax) or metal hydroxide (MH, samples labelled with EP-Mx) for unseen-data validation. In the experimental samples, the mass fraction of FR additive without MOF is fixed at 29 wt-% for ATH and 12 -wt% for IFR. The weight percentage of MOF is marked with "x" in label, varying from 0 to 2 wt-%. As shown in Fig. 4-12, all the composites with FR additives have much lower pHRR compared to neat EP, approximately 50% reduction is observed. This is owing to the effective FR reactions brought by the fillers, which have been confirmed with extensive experiments. Besides, all MOF-added samples have relatively increased TTI, in agreement with the SHAP result: formulation using MIL-type MOF should have longer TTI.

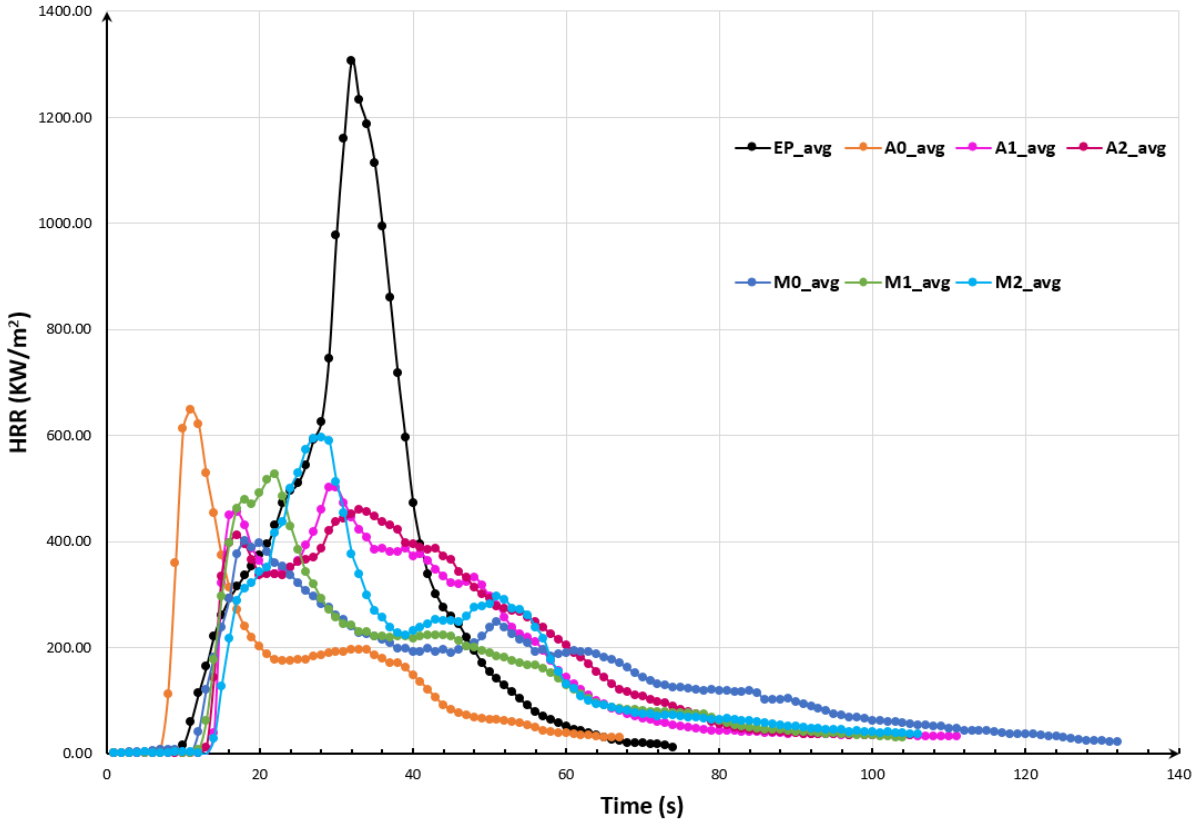

Fig. 4-12 Heat release rate of EP samples measured with heat flux=35kW/m2

Turning back to sole MOF in polymer matrix, the FR performance comes mainly from the type of metallic components and composition of organic ligands. [106]

Data-driven investigation of FRPCs

Seen from the experimental data above, the achieved reduction of pHRR values of polymer composites with only MOF below 2 wt-% varies unexpectedly from 10 - 60%, differing in 16 publications. This result confirms well that the quantitative characteristics of the combustion process in CCT of polymer composites depend not only on the chemical composition and molecular structure, but also the subjective and objective conditions during the CCT. Considering the ventilation situation, atmosphere condition in lab, equipment status and operation habits of researchers, which are barely mentioned in publications, it appears to be extremely challenging to build highly accurate machine learning models by individual researcher or group.

The comparison between the calculated measurements and predictions is shown in Fig. 4-13. In this test, four formulations from publications (marked with "P0" to "P3") and another four EP samples with both MOF and synergists ("M/A1" and "M/A2") are chosen. As mentioned above, we have selected the corresponding model for each target feature: Modulus(RF), TTI(SVM), pHRR(AVG) and THR(AVG). The categories of target properties are presented using bar height with blue for predictions and red for measured values. Along the vertical axis is the category/range of the divided properties listed, which is also numbered from bottom to top as shown upon the bar.

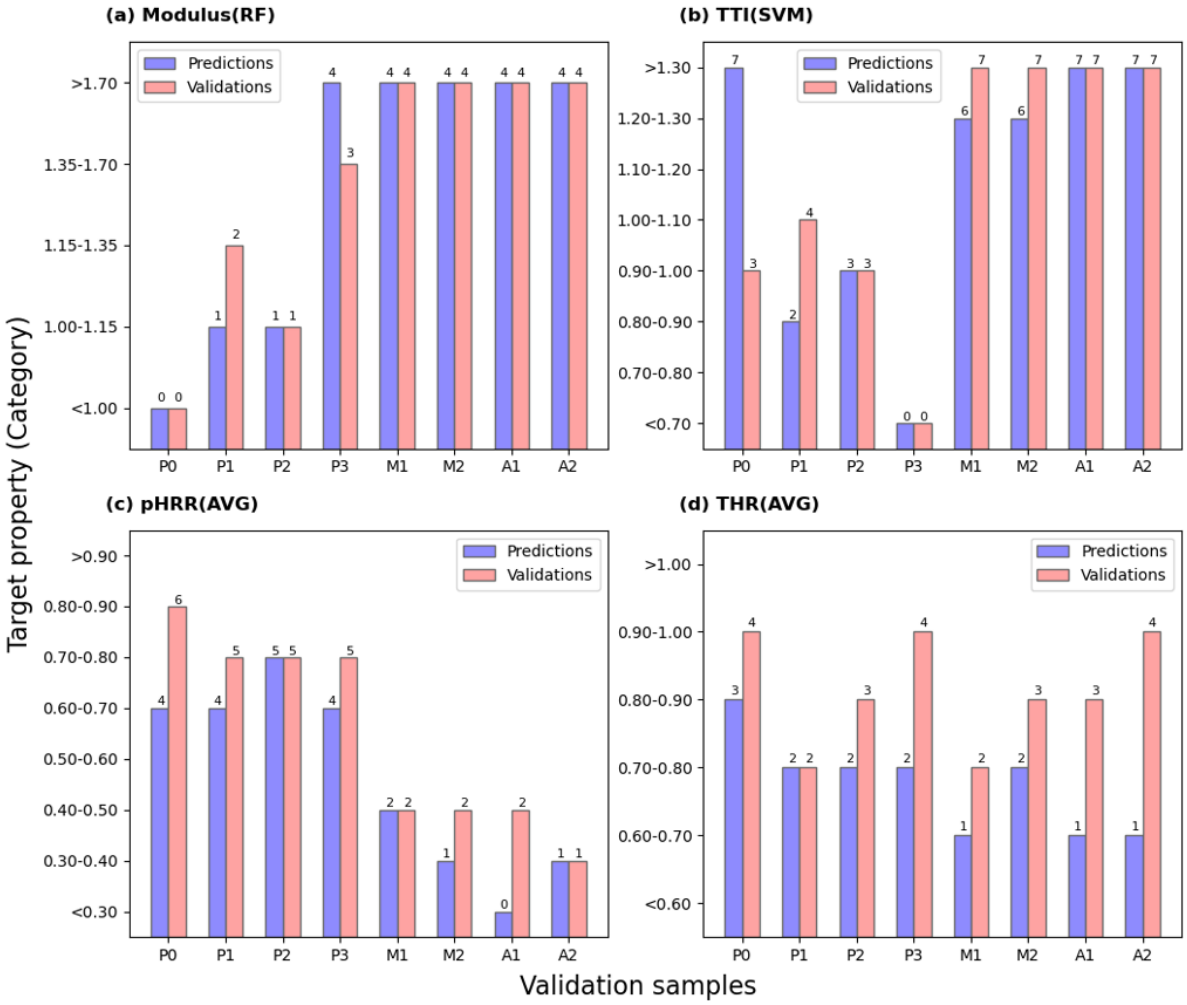

Fig. 4-13 Validation samples of selected models. P0 to P3 are chosen from the publication records; M0 to A2 come from experimental results.

The "in-situ" accuracies of all models are expressed in last section with determination coefficients and confusion matrixes. Observed from the bar plots, similar conclusions can be made that the predictions of modulus and TTI are more accurate than that of pHRR and THR. There are 6 samples of 8 having the same categories in prediction and measurement, and the error of incorrect classifications is not big to accept. In TTI(SVM) model, an obvious misclassification occurs in sample P0, which has the validation value of "0.90-1.00" but the prediction of ">1.30". In this formulation, 0.5 wt-% of self-synthesized Co-MOF was added into EP matrix with pHRR=800kW/m² and TTI=80s. The other two models pHRR(AVG) and THR(AVG), however, exhibit prediction errors in most samples, and all the misclassified samples are underestimated compared to their measured values. Although we selected the validation formulations varied in polymer matrix, additives and the loading, an evident tendency should be noticeable: apart from

the modulus and TTI, all formulations in the published works are designed to lower the pHRR and THR, at least theoretically. In the dataset retrieved from open publication, the divided pHRR is invariably below 1, meaning that the polymer composite has reduced heat releasing compared to neat polymer. Another reason for the underestimation, which is more possible in the AVG-models, is that the averaging operation always returns the smaller integer due to the default rounding down in python calculation.

4.3. ML models for FRPCs in LDH-system

4.3.1. Interconnection between descriptors and FRPCs' properites

The LDH-dataset is consisting of 264 rows from 33 public literature. In this dataset, there are almost 62 kinds of LDHs, which differ in metal ions, big-molecule-intercalations and organic modifications. Due to the variety of anions, the interlayer spacing of LDHs changes from 0.77 to 3.80 nm. Most of the intercalated molecules contain the long carbon chains to widen the distances between LDH layers. Similarly, the loading mass of LDHs in these FRPCs is at the same level as that of MOFs. Thus, the addition of other FR chemicals appears to enhance the fire performance of the polymer composites, generally. Types of these additives vary from normal phosphorus-containing chemicals to reduced graphite oxide, to various organic acids or self-synthesised big-molecules.

From the collected data, there is no obvious trends observed between the input features and target properties (TTI, pHRR and THR). As a kind of inorganic fillers, LDH has the similar FR functions of MH, but is more attractive due to its double-layered structure. Since the dispersion of inorganic additives is always a problem in organic polymer matrix, the modification on LDH can not only improve the dispersion of FR additives, but also provide synergistic effects to enhance the fire performance. From the heat map illustrating the Spearman's correlation between all features, there are only weak dependencies between target properties (pHRR, TTI and THR) and other descriptors. The mass fraction of LDH does not have as significant impact on the target properties of FRPCs as the mass fraction of MH does in Fig. 4-1. Only the corresponding properties of neat polymer have certain positive influence marked with red squares in the heat map.

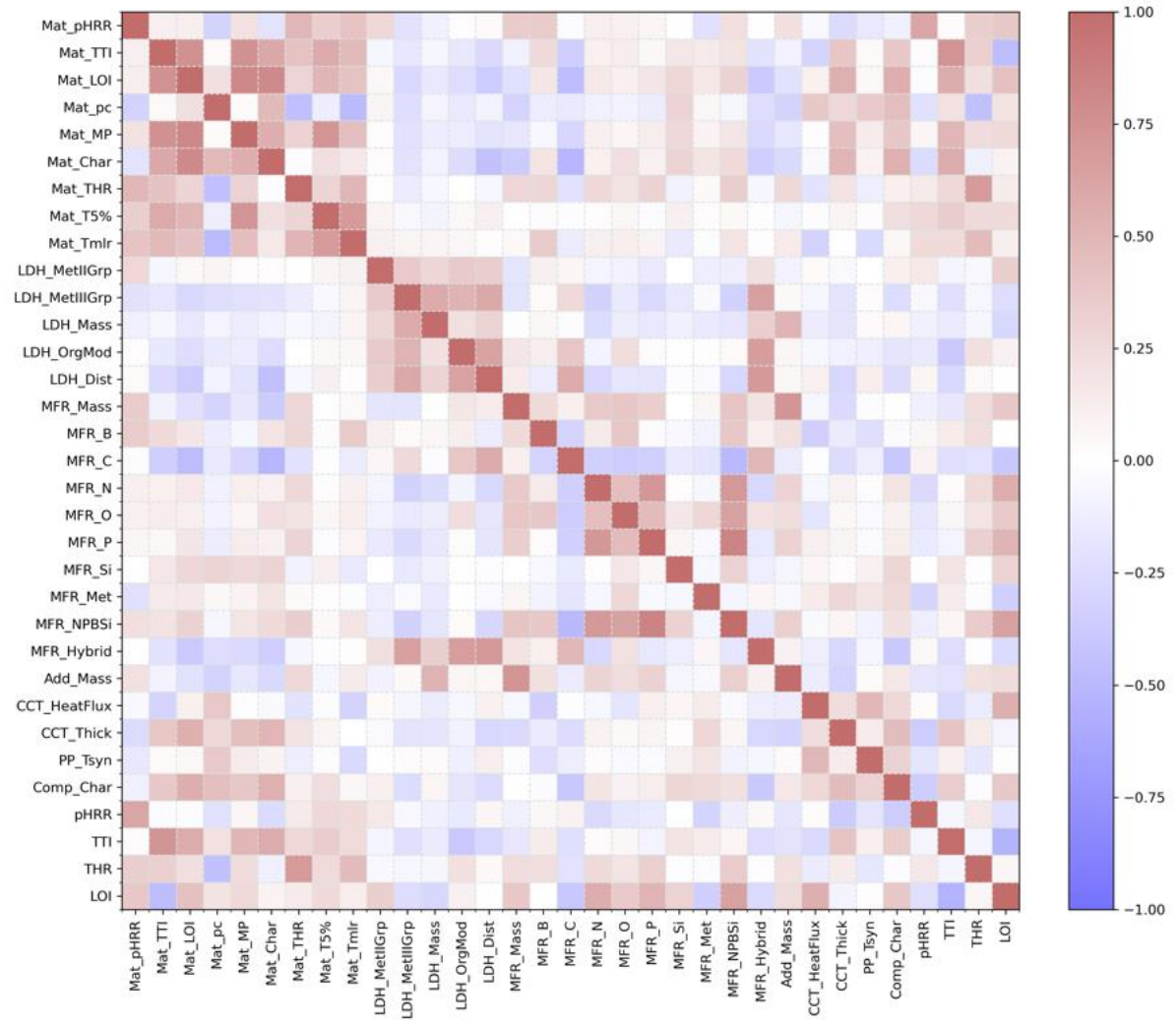

Fig. 4-14 Spearman's correlation heat map of LDH-dataset

4.3.2. Classification accuracy of LDH-models

To evaluate the predictive accuracy, determination coefficient R2 is a good tool for instant judgement. There are 9 models to predict TTI, pHRR and THR in total. Since we are using the classification, the predictive performance in all models is satisfied marked by the red lines in Fig. 4-15. The R2 in trainsets are over 0.90, meaning that the models fit well in the training. The fluctuated red lines represent the R2 in the testsets of randomly splitting. The testing R2 values are normally lower than that in training, especially in pHRR(RF) model, in which R2 in test sets keeps around 0.70. Nevertheless, the performance of combined models (AVG models) exhibit increased R2 compared to single-algorithm models. For both three target properties, the R2 values of AVG-models in test sets have reached over 0.80, slightly lower than that in trainsets.

Data-driven investigation of FRPCs

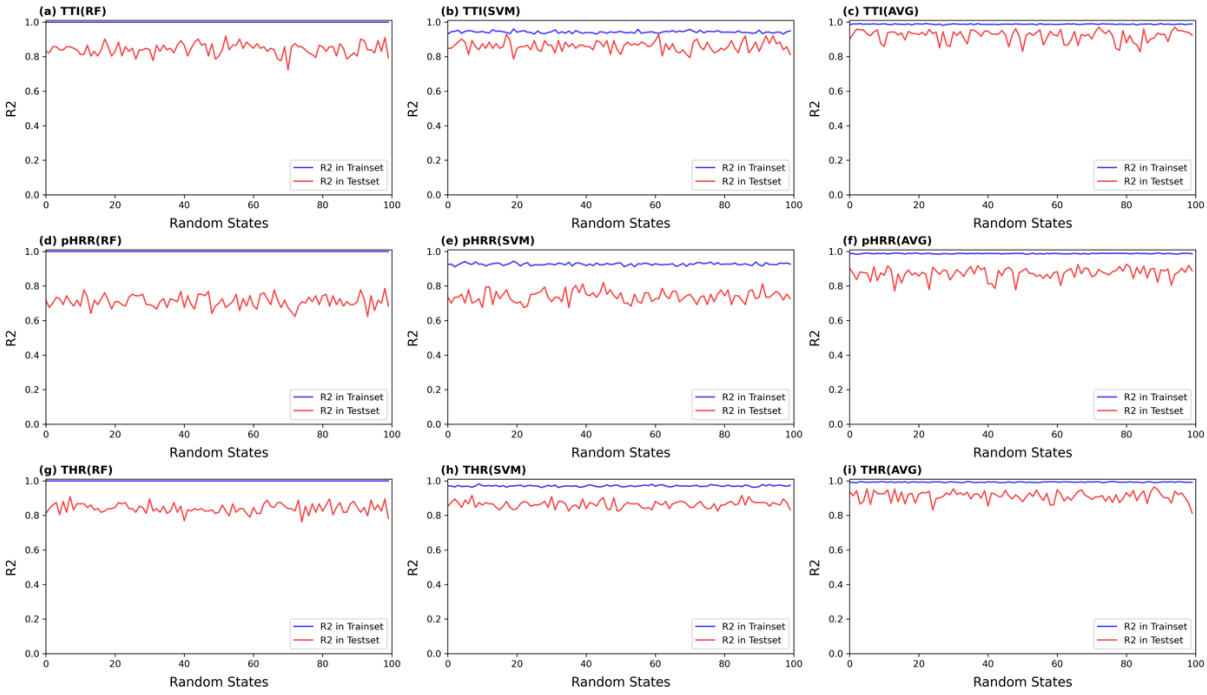

Fig. 4-15 R2 of all 9 models predicting the CCT characteristics of LDH-loaded FRPCs, from left to right are RF, SVM and AVG models

The accuracies of classifications are also in agreement with the high R2. The misclassified classes in Fig. 4-16 is in minority. Wrong predictions of TTI appear to the samples with short TTI below 35 s. Although the samples with the TTI between 55 to 65 s are also partially misclassified, the number of misclassifications is low. The models predicting pHRR and THR performs slightly worse than TTI-models. These models predict not the true values of polymer composites, but the ratio between composites' pHRR (or THR) and polymers' pHRR (or THR). The false classification of the pHRR-ratios concentrates on the moderate class like "0.60-0.75". THR-models' misidentifications are around the class "0.95-1.1" at the same time. Similarly, the AVG-models have higher predictive accuracies, demonstrated by the lower number of light-coloured squares in confusion matrixes. The values of ACU for these three models TTI(AVG), pHRR(AVG) and THR(AVG) are 90%, 83% and 89%, respectively.

4.3.3. Feature importance and model explanation

As usual, the ranking of feature importance from the RF models help to learn the significant factors that influence the target properties of FRPCs. In predicting TTI, the TTI of polymer matrix takes the first place with 0.16 importance, followed by

the char formation of neat polymer. Furthermore, except for the interlayer distance of LDHs, the features in "Polymer_Matrix" group occupy all the five top positions. The mass fractions of LDHs and other FR additives come after them in the feature importance ranking.

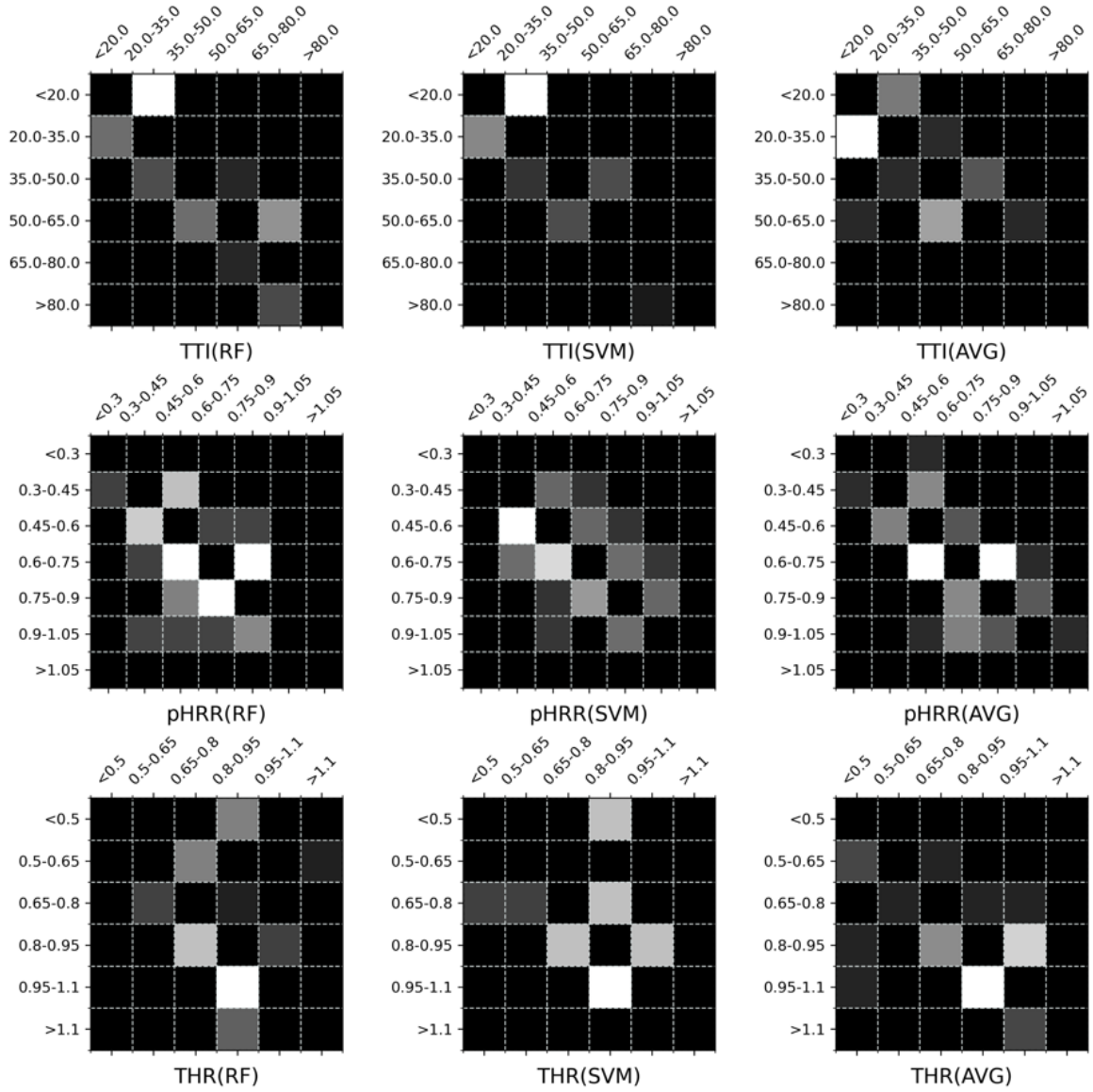

Fig. 4-16 Confusion matrix of misclassified classes in all 9 models, white means the misclassification of class (row) into class (column)

Unlike the TTI-prediction, the pHRR(RF) and THR(RF) models have both the MFR-related features as the most significant ones. The mass fraction of FR additives is very essential in deciding the pHRR reduction of polymer composite with an importance of 0.25 in total. Although the "Mat_pHRR" takes the third place, the influence of all polymer-related features are not comparable to that in TTI(RF). Following the interlayer distance of LDHs, the highest operation

temperature in sample preparation has an importance of 0.07. Because the determination of operation temperature of a polymer is dependent on its thermal and physical properties, this temperature, to some degree, indicates the stability of polymers at high temperature. The elemental content of oxygen in FR additives is more essential than other FR elements like N, P B and Si. The reason may be attributed to the existence of metal introduced by inorganic LDHs. The oxygen content is also the most important features (in MFR feature group) in deciding the pHRR of MH-loaded polymer composites (Fig. 4-3(b)). Higher content of oxygen leads to increased amount of metal oxides, which enhances the formation of physical barriers together with the catalytical carbonization of organic components in FRPCs.

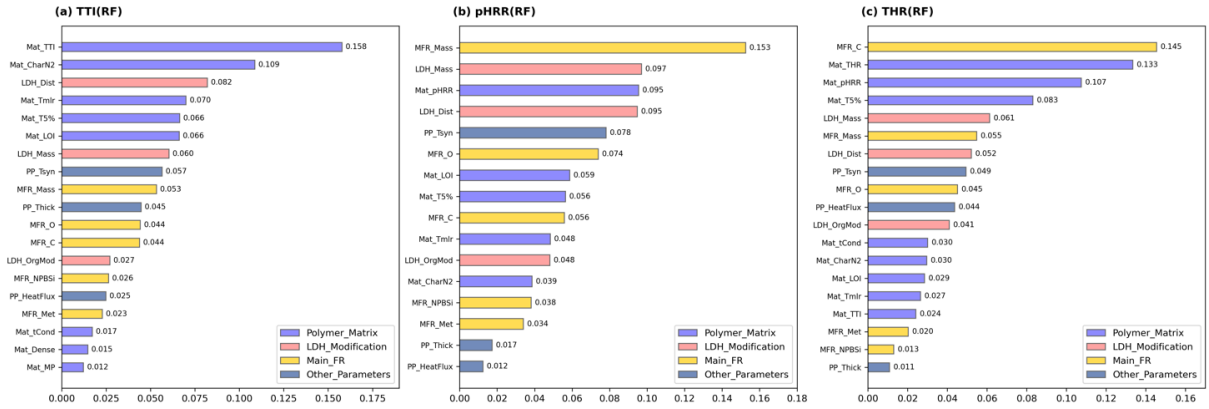

Fig. 4-17 feature importance of RF models predicting TTI, pHRR and THR

The THR(RF) model, however, show different rankings compared to both RF models predicting TTI and pHRR. The carbon content of MFR is in the first position with an importance of 0.15, and the THR, pHRR and initial decomposition temperature of neat polymers follow with high significance. The essentiality of "MFR_C" comes from two points: 1). The total amount of the heat released from the burning of samples is actually highly connected to the carbon content in composites, since it is the natural property that the burning process is the oxidation processes of carbon and hydrogen, which are abundant in organic materials. The existence of carbon influences the quantity of fuels in the burning scene, and subsequently gives impact on the final amount of heat. 2). The carbon content of the chemicals used to modify/intercalate LDHs is also counted into this feature. i.e. "MFR_C" contains also part of the information about the modification of LDHs. Under the combined influence of the two reasons mentioned above, it is understandable that the carbon content holds the highest importance in THR(RF).

Of course, the amount of FR additives should not be overlooked. Although they are not as important as the aforementioned features, they still influence the THR of FRPCs.

Overall, the features referred to FR additives plays an important role in influencing the CCT results of FRPCs. This is consistent with the ranking of features observed in other FR systems demonstrated in former sections. The addition of FR components can significantly influence the combustion behaviours and the release of heat; however, the ignition time is more dependent on the polymers themselves. The reason for this may be analogous to a water-filled barrel leaking at its shortest stave: the polymer is more flammable compared to most FR additives due to the high content of carbon inside. Sometimes, with the loading of FR additives, especially when they are carbon-rich chemicals, the TTI of FRPCs will be shorten, which has been observed in Fig. 4-9(b) that almost 70% samples in MOF-dataset demonstrate the reduced TTI values compared to neat polymers. Similarly, since most polymers are highly flammable, the development of the combustion behaviour after ignition greatly depends on the FR additives. The type and effectiveness of those chemicals determine the strength of the FR effect working while the burning of FRPCs, as well as whether and how the impact of the combustion could be mitigated.

The SVM-models based feature importance exhibit the influence of these features from another aspect in Fig. 4-18. This figure shows not only the importance, but also tells how these features influence the target properties of FRPCs. For the TTI of polymer composites, testing under low heat flux in CCT leads to long TTI. In contrast, the feature "CCT_HeatFlux" takes very low importance in RF models. The reason lies in the fact that researchers use normally 35 or 50 kW/m^2 to conduct the CCT, which makes the feature "CCT_HeatFlux" lack of diversity, showing low influence in RF models. An equally surprising fact is the disparity in the significance of "PP_Thick", which means the thickness of CCT samples, between the RF and SVM models. From the SHAP explanation, thicker samples tend to have longer TTI. The SHAP explanation focuses on the influence of the feature on the prediction of single class of target properties. The underlying assumption is that thicker samples can transfer more heat to other parts avoiding the quick accumulation of heat in the local position. Thus, this feature tends to be more important in SVM models. The FRPCs, which use polymer matrix with long TTI, high LOI and high char formation, have addition of unmodified LDHs, and high operation temperature while the production, have prolonged TTI.

Data-driven investigation of FRPCs

Unlike the TTI, pHRR of polymer composites would decrease if the composites had high char formation in TGA, use organic modified LDHs with short interlayer distance and contain high amount of MFR. Low heat flux and thin samples increases the pHRR of polymer composites. The reduction in THR of polymer composites depends on the unmodified LDHs and low heat flux in CCT. Other features in THR(SVM) are in narrow distributions, and coloured dots overlap with each other locating both in positive or negative phases.

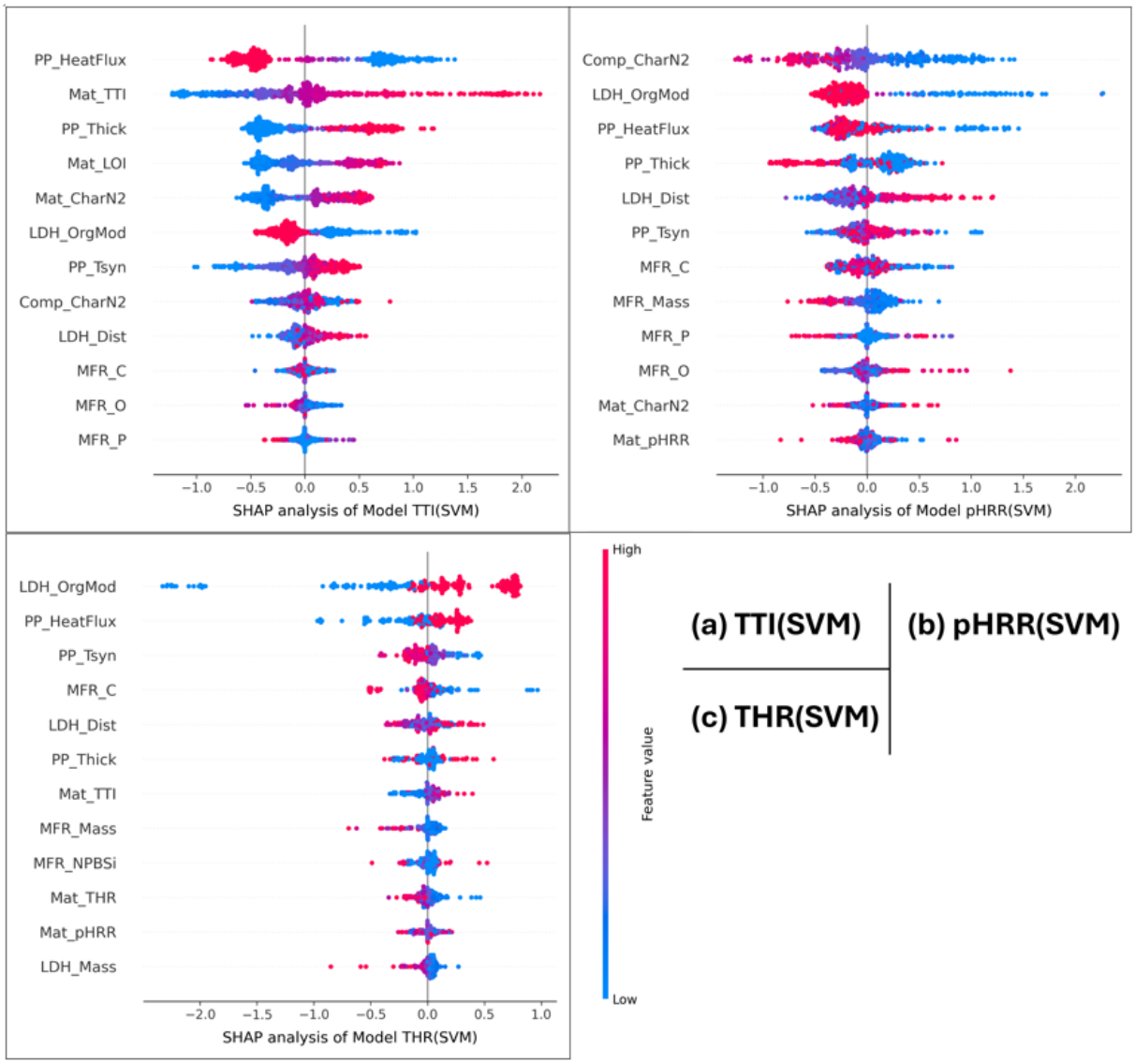

Fig. 4-18 SHAP explanation of SVM models predicting TTI, pHRR and THR in LDH-system, only the top 12 features are shown

As conclusion, the strategy to improve the CCT performance of FRPCS are different. The polymer matrix with high thermal stability and good dispersion of inorganic LDHs contribute to prolonging the TTI. The development of heat release

during the combustion scene in CCT is heavily dependent on the components of FR additives and modifications of LDHs. However, LDH-system is still complicated in FR mechanisms, especially with the addition of many other kinds of FR chemicals. Such numerous combinations of LDH-modifications and additives significantly increase the difficulty of creating a high-performing and accurate ML models with the limited dataset. Therefore, the strategies of oversampling and conversion of regression to classification are used to enhance the models' predictive accuracy at the cost of specialization and precision of target properties.

4.4. On the investigation of the integrated models

The ultimate goal of physicists is to describe all the phenomena in the universe with only a single formula. Similarly, our ultimate goal is to develop the ML models that are able to predict the TTI, pHRR and THR of all FRPCs with various additives from different FR systems. In the former three FR systems, MH-, MOF- and LDH-systems, there is actually the more FR additives inside. MH, MOF or LDH are typically not used individually but combined with other flame retardants. Mostly, these kinds of FR additives are chemical compounds consisting of various FR elements, and some could be the mixtures of these substances. Additionally, since the FR mechanisms of these flame retardants are generally referring to the participation of certain elements in various chemical reactions during the combustion behaviour of FRPCs, their features in our datasets are normally represented by their elemental contents in the compounds/mixtures. Phosphorous-containing chemicals (like red phosphorous and simple phosphates) or IFRs play an important role in these FR additives. Besides, there are flame retardants including organic silicones, (reduced) graphene oxides, nano-sized additives and boron-containing chemicals.

It is very challenging to build ML models for every FR systems due to the requirement of creating separate datasets for each of them, which are often characterized by disorganized and overlapping data with limited volume. As a result, we have only selected three above-mentioned representative and extensively studied FR systems as our milestones. Through the study and research on these systems with increasing complexity, we have laid a solid foundation for the further in-depth exploration of the possibility in data-driven supported materials development.

4.4.1. The completion of final dataset

The complete dataset for this ultimate goal comprises 828 formulations of FRPCs and almost 50 features to describe all aspects of the polymer composites. As mentioned above, the features in all three datasets (MH, MOF and LDH) consist of 4 main parts: polymer matrix, functional parts that represent the loading of MH, MOF or LDH, other FR additives marked as synergists or MFRs and the process parameters concerning the production and characterization. The difficulty in the construction of the final dataset lie in the combination of the features of these functional additives. On one side, MHs, MOFs or LDHs have their own features that influence strongly the end-performance of FRPCs. These information must be retained in the final dataset in order to build the ML models with high predictive accuracy. These features, at least most of them, are totally different to each other and cannot be consolidated into one column. On the other side, simply placing all these features into the final dataset would result in a significant increase in the number of features. An expansion in the dimension of features in the dataset significantly increases the likelihood of overfitting problem and simultaneously magnifies the requirement for the quantity of samples. However, our datasets are retrieved personally from public literature, rather than from systematic, public, and authoritative databases. Increasing the data volume is not a feasible option. Additionally, the dataset would contain a large number of missing values after such simple combination: for example, samples containing MH lack the data for MOF and LDH, and vice versa. This substantial number of missing data would inevitably have the negative impact on the optimisation of the hyperparameters and predictive performance of ML models.

The final feature groups, including the aspects of material components and processing parameters, in this dataset are the polymer matrix, main flame retardant, other parameters in processing and functional additives (short as FuA in dataset to mark the features in this group). There are six features in this "FuA-group" which contain the information about the mass, particle size (interlayer distance in case of LDHs), group of metal in periodic table, type of the additive, decomposition enthalpy of MH-type additives and organic modification of these additives. After the integration of all FR-systems in one single dataset, there are no direct relationships observed between the influencing features and target properties (pHRR, TTI, THR and LOI). Seen from the Spearman's correlation heat map in Fig. 4-19, the char formation of polymer composites in TGA, total mass

fraction of FR additives and the properties of neat polymers have certain influence on these target features. Other features with relatively deep relationships concentrate in the polymer-related features and FuA-features. This is actually attributed to the fact that all these features come from a single type of polymer or additive. That is to say, if the polymer is EVA in this formulation, all the other values in this feature group "Polymer_Matrix" are fixed; if the "FuA_Type" equals to MDH, then the other five features in "FuA-group" have also fixed values. Such situation leads to the occurrence of high Spearman's correlations between the related features.

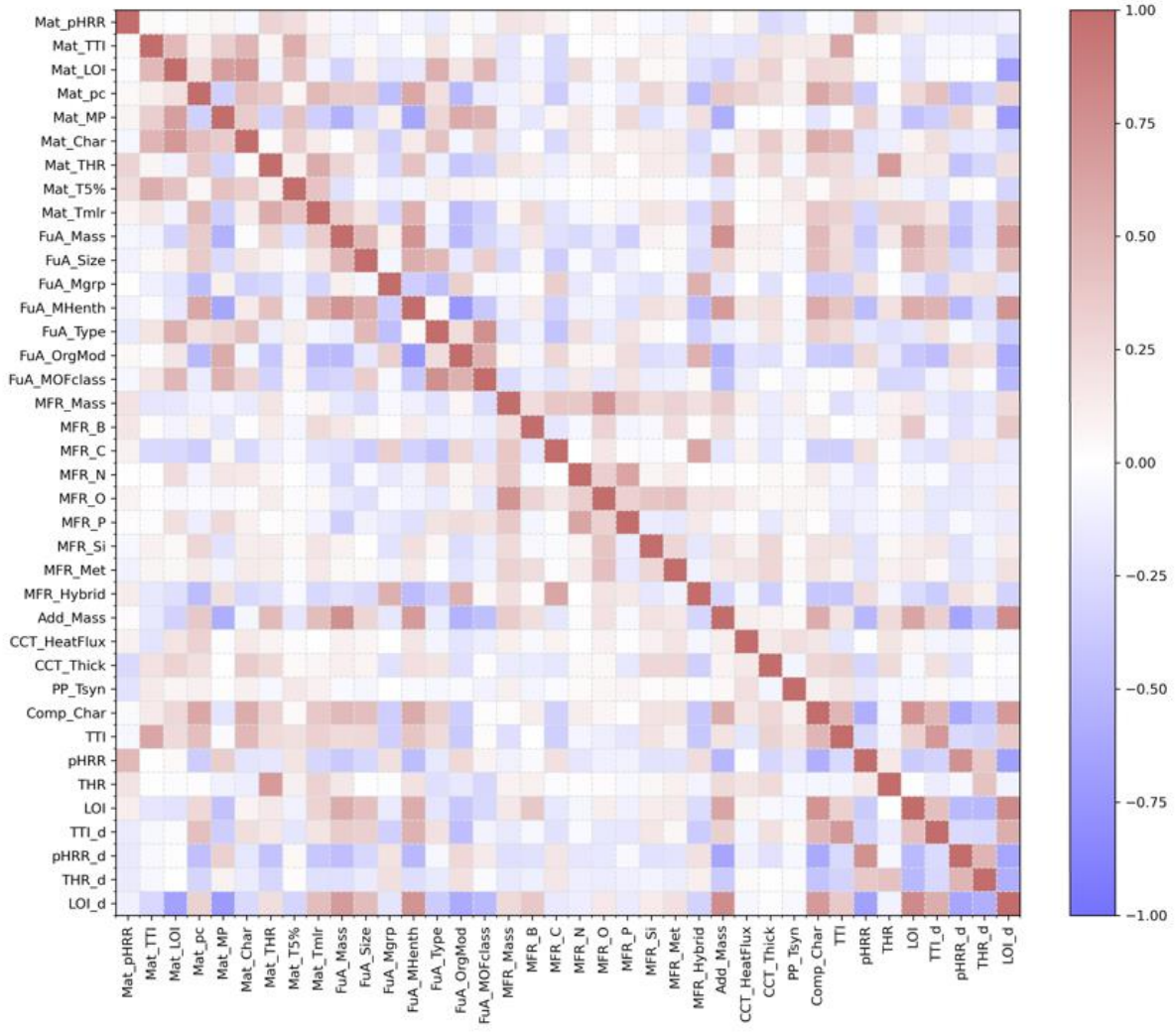

Fig. 4-19 Spearman's correlation coefficients heat map of all features

4.4.2. Model performance of complicated, integrated FR-system

The entire dataset consists of 828 rows and 33 columns, in which the to be predicted targets are categorical values of pHRR, TTI, THR and LOI. These values

have been firstly divided by the corresponding values of neat polymers and then transformed into separate classes. The regression models built based on these datasets have completely unusable results, so we applied the classification models as usual. However, the predictive performance of these classification models, including the linear combinations, are still not satisfied. After several iterations and optimisations, the rapid evaluation of ML models based on the determination coefficients R2 gives out the results of low predictive accuracy and strong overfitting problems in most models.

After expanding the classification boundaries, in other words, reducing the number of categories, the predictive accuracy has been improved to some extent, but still the models' performances remain unacceptable. The decrease in number of classes, such as reducing the original 7-classes classification of TTI-model to 4 classes, without changing the data itself, could lower the difficulty of making predictions for these fewer categories. More specifically, a TTI change of 0.5-0.6 would be one category, while 0.6-0.7 would be another in the original dataset. After reducing the number of categories, all composites' formulations with the TTI-changes between 0.5-0.7 have become a single category. This effectively simplifies the predicting but also clearly increases the inaccuracy of the predicted values. The larger the category range is, the more precise the model makes the prediction. Obviously, when there is only one category, the prediction accuracy would reach 100%; however, such a model is meaningless to our research. Moreover, when a polymer's TTI-change ranges from 0.5 to 0.8, it indicates that the TTI of polymer composites decreases by 20% to 50% compared to the neat polymer, which is not a proposed result. Such predictions significantly diverge from the required "true values" of the formulation, providing only limited value and guidance to the investigation of new materials. Furthermore, even if we have increased the class ranges from 0.1 to 0.3, the R2 values of these models only show slight improvements in Fig. 4-20.

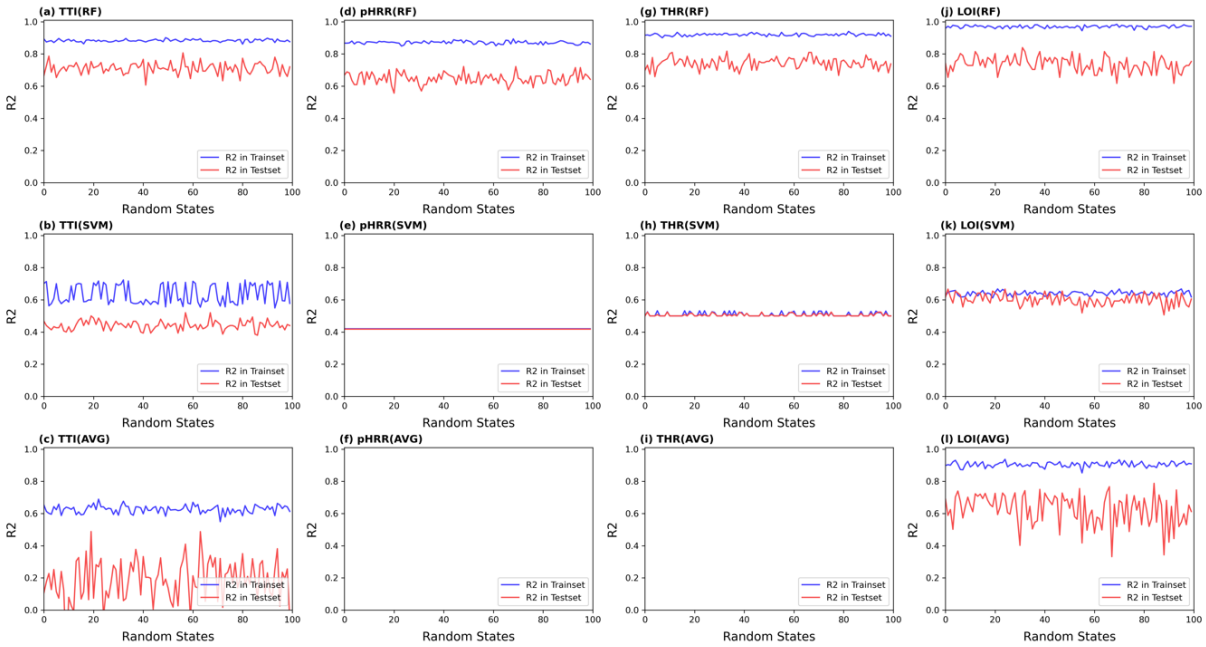

Fig. 4-20 R2 of all classification models in train- (blue) and testsets (red)

In the top row of Fig. 4-20 are four RF models predicting TTI, pHRR, THR and LOI, respectively. Although their R2 values of training sets locate above 0.8, even close to 1.0 in LOI(RF)-model, the testsets-R2 values can hardly reach 0.8. The performance of pHRR(RF) models is the lowest, with R2 equals to 0.65 in test sets, approximately. SVR models have even worse performances. The results of linear combination, i. e. the AVG-models, are similarly not usable.

Given that the RF models are barely considerable, we have conducted the feature importance analysis shown in Fig. 4-21. In all RF models, the mass fraction of functional additives takes the first place in the ranking. The difference is that this feature has much higher importance (≈ 0.20) than other features in the RF models predicting pHRR (b) and LOI (d). This feature contains the mass fraction of MHs, MOFs and LDHs in the polymer composites, in which the MH-mass varies basically from 10 to 60 wt-%. Compared to MHs, MOFs and LDHs have the typical weight percent of below 10 wt-%. Meanwhile, MHs have high influence on the pHRR of polymer composites, and also affects the LOI very much. This very high feature importance of these two models comes from this reason. As usual, the features referring to the polymer matrix have significant impact on the TTI of polymer composites, the product of thermal conductivity and density of neat polymers “Mat_pc”, melting point and char formation in TGA follows “FuA_Mass” in TTI(RF). The “Mat_pc” has direct influence on the accumulation of heat in the sample surface under cone irradiation, deciding how long it takes to heat the

locality up to certain decomposition temperatures. The influence of main flame retardants is illustrated by the yellow bars in the middle part of the ranking, starting from the loading amount of MFR with FI of 0.044. This is similar to the FI of models of individual FR-system. The ranking of feature importance in THR(RF) model has the same tendency. Besides the high influence of "FuA_Mass" caused by the strong impact of MH-addition, the significant factors controlling the THR of polymer composites come mainly from the aspect of polymer matrix. Unlike the TTI and THR, the properties of FR additives have much stronger influence on pHRR and LOI of polymer composites.

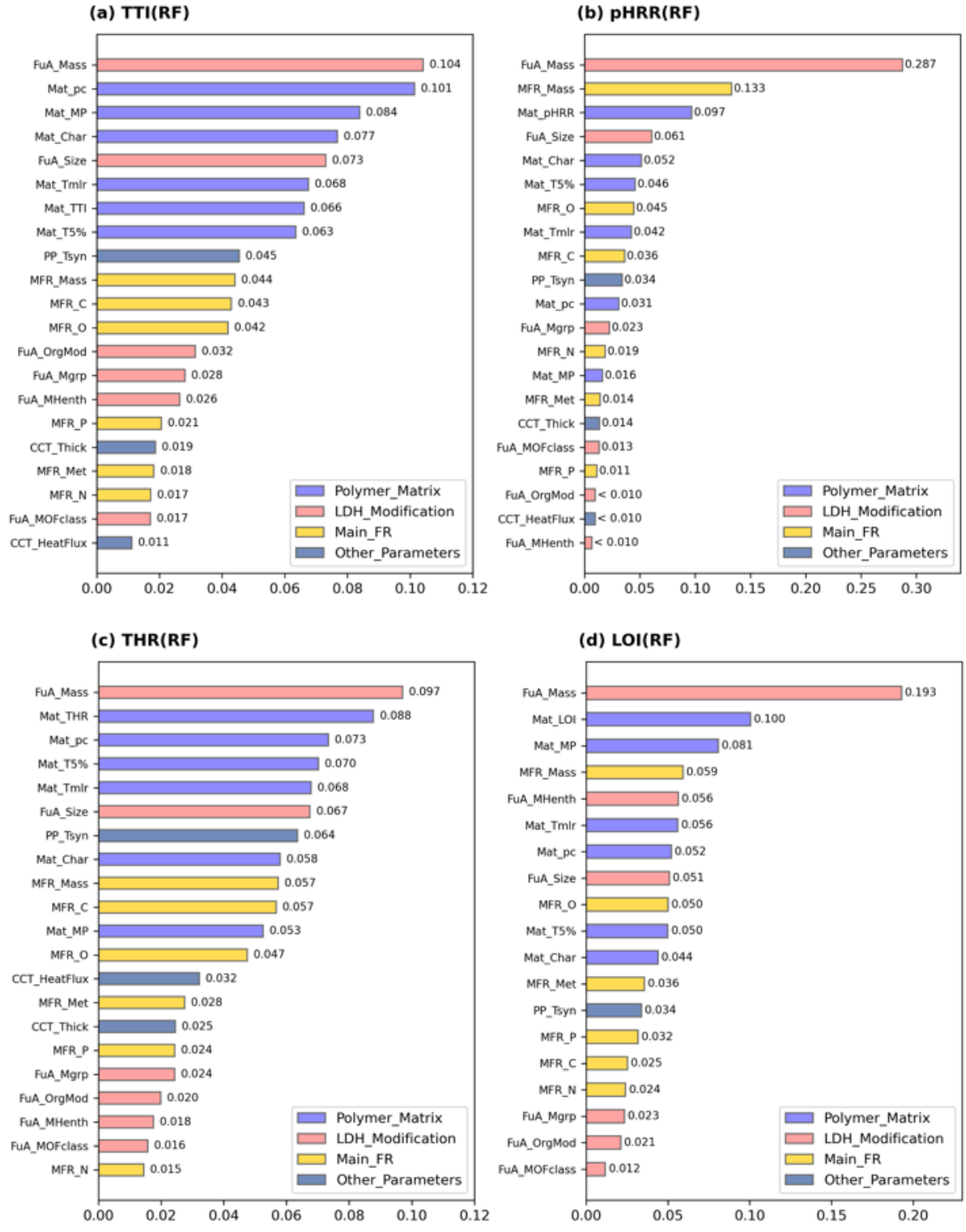

Fig. 4-21 Feature importance of RF models predicting TTI, pHRR, THR and LOI

Although the predictive accuracy of these ML models built on the integrated dataset has not met the requirements (the R2 values close to 0.8 in RF models indicates that they already have a certain degree of usability), we can clearly see the potential for achieving such goal. These models are used to predict the CCT

performance of FRPCs, which may include thousands of possible formulations: the dataset already covers 10 types of polymer matrices, at least 10 types of functional additives (i. e. MHs, MOFs, and LDHs), and more than 20 types of other flame retardants. Considering the different sample preparation methods and parameters, the entire FR system is extremely deep and complex to build the data-based models. From previous step-by-step chapters, we have understood that the simpler the objective is, the easier it is to build the corresponding model and the lower the data volume is required. Therefore, compared to the MOF- and LDH-systems, the models for the MH-system have higher performance. When we integrate these three FR systems into one (including another widely used but not listed IFR-system, which data have been totally inserted into the above-mentioned datasets) for ML modelling, the complexity of the entire system has increased greatly that can be the product of separate FR systems.

In order to improve the predictive performance of the models, the datasets used for supervised learning needs to meet certain requirements. Firstly, the quantity of data must be sufficient according to the complexity of objective. Just like humans, learning to do basic mathematical operations using the Arabic numerals 0–9 differs in difficulty from performing calculus or probability calculations, and also requires different amounts of learning materials. This is the same to the machines, for which the data requirement increases proportionally with the complexity of the problem. As mentioned at the beginning, ML is a data-driven approach to explore the intrinsic relationships between materials-processes-properties. The data is the foundation for building robust models. All the datasets in this study are derived from public literature and experimental results conducted by our research group. In total, we have gathered 828 rows of usable data for modelling. However, it has become clear that, relative to the objective we aim to investigate, the amount of data is still insufficient. We had to reduce the precision of our predicted values (classifying the change of TTI/pHRR/THR into categories of 20-50%, 50-80% or over 80%) in order to improve the model's prediction accuracy. Normally, the measuring errors in CCT are estimated to be around 10%. A prediction in the range of 30% is somehow meaningless. On the one hand, the results reported in by researchers are typically those FRPCs with improved performance, which formulations are usually optimized from existing ones or involve the substitution of one FR additive with another chemical of similar structure or property. The data retrieved from publications has indicated that adding the “flame retardant”, regardless of what

the “flame retardant” is, generally leads to a reduction in the polymer's heat release in CCT. However, in reality, there must be some formulations that are ineffective or have only little FR effect, or even degrade the fire safety performance of polymer composites. It is difficult for us to obtain information about these formulations that are useless for the researchers. Nonetheless, these formulations, which have the equal importance as the effective ones, contribute to making more accurate predictions, uncovering the inherent relationships between the PSPP links.

4.5. ML framework predicting HRR Curve

4.5.1. Time series of HRR-development

The dataset for the prediction of HRR curves is the MH-dataset, which have extra information about the development of HRR in CCT for each formulations. 9 RFC models are built to reveal the change of HRR against time. Based on the transition phase, HRR curves are divided into valley-, stair- and peak-transition as shown in **Fig. 4-22**(b). This transition phase indicates different combustion behaviours of the samples in CCT. Through the release of heat in this stage, we are able to get insight into the possible chemical or physical processes occurred during the combustion process. The formation of physical barrier, its stability and strength are also demonstrated by the change of HRR. A formulation of effective and long-term FR function should suppress the HRR in the whole testing. The arise of second peak in HRR, and usually the global maximum of HRR in the combustion, is attributed to the breakdown of the desired FR effects.

Due to the significance of the transition phases, the simplification of HRR have retained such trends in this work. In the whole dataset, samples with valley-shaped HRR curve have the largest amount of 80. The effective loading amount of MH in polymer composites contributes to lowering the HRR in the transition phase, which is the majority of records in the dataset. The occurrence of the second peak of HRR is attributed to an unsteady physical barrier formed by metal oxides that is not able to overcome the propagation of fire. Stair-transition indicates a dynamic balance between the development and suppression of combustion. In the dataset, the amounts of samples with stair- and peak-transitions are 28 and 22, respectively.

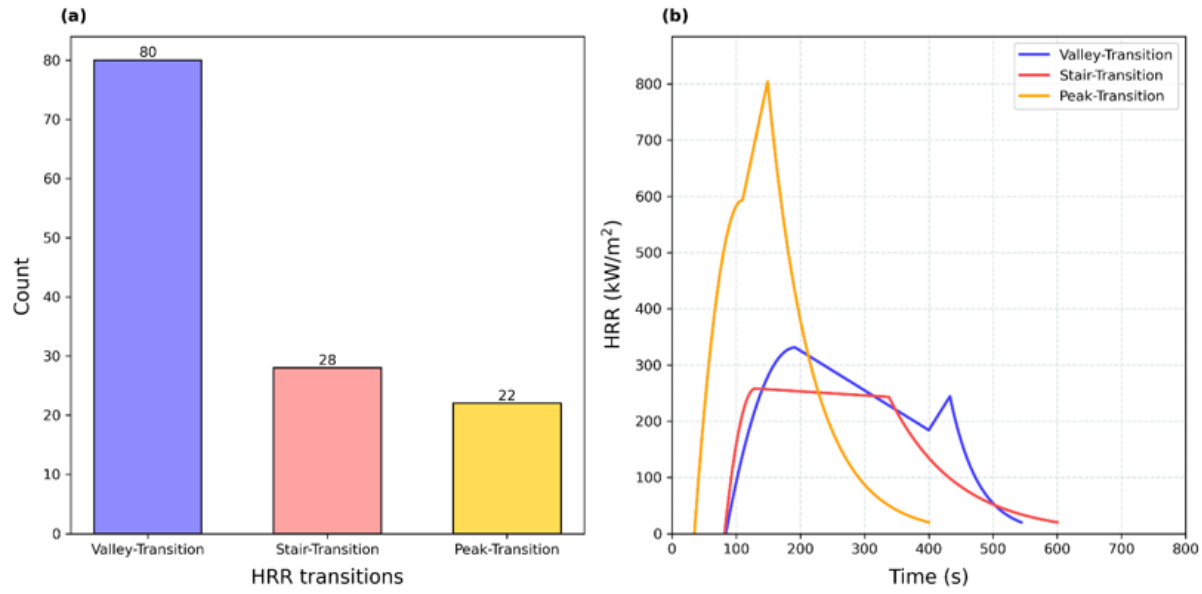

Fig. 4-22 Types of HRR curves in collected dataset: (a) amount distribution; (b) examples of 3 types

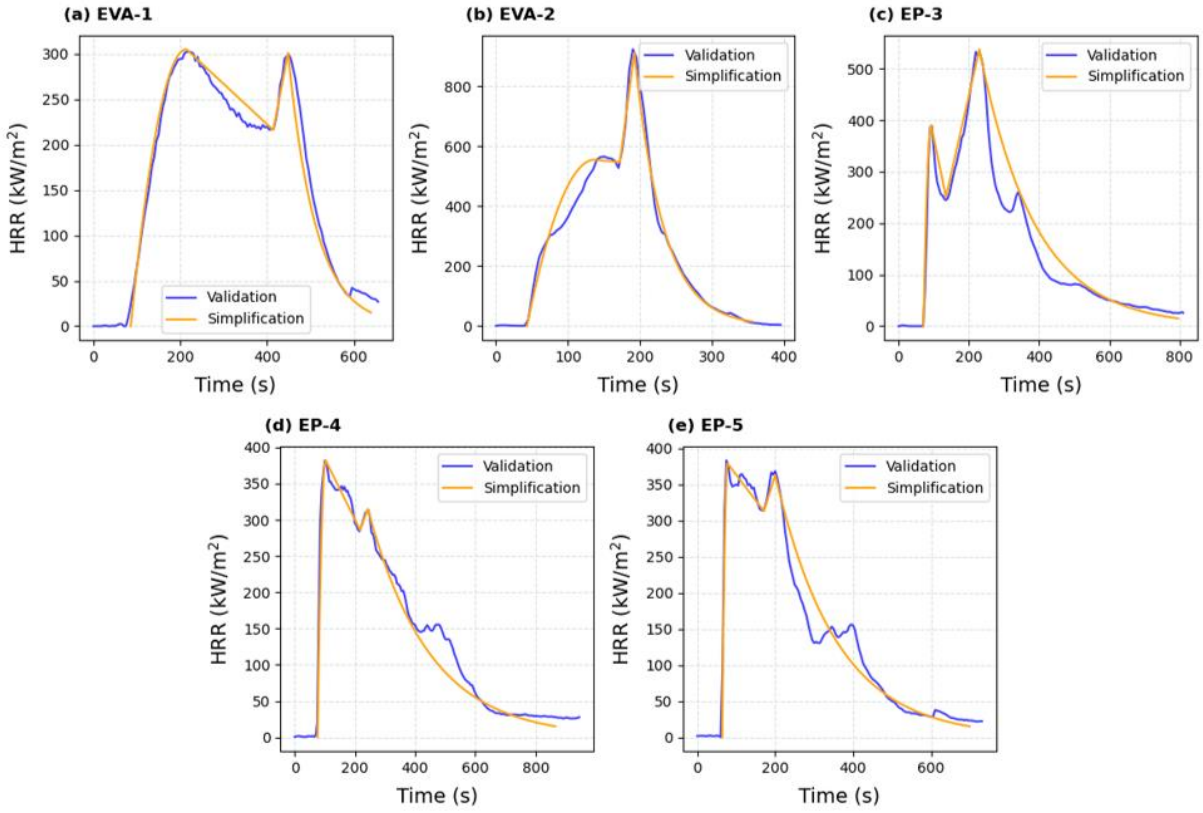

Fig. 4-23 Comparing the simplifications and measurements of polymer composites.

The **Fig. 4-23** is the comparison between simplifications and real measurements of HRR of 5 experimental samples for validation. Blue curves stand for the measured

HRR and yellow for simplified curves. The simplifications have excellent consistency with measured ones. Although there are fluctuations ignored, evident peaks and HRR transitions over time are well reserved. The measurement of HRR based on oxygen consumption is highly susceptible to facility adjustment, surrounding conditions and researcher operations. There are no two identical combustion processes in the testing. As a result, repeated experiments must be conducted on samples in the same batch to avoid abnormal results. The simplification method here can significantly reduce the difficulty in modelling in a way that loses as little information as possible, assuming that there are no critical, objective influences caused by the environment. More attention is then paid to the developing trends of HRR of the combustion processes in the cone calorimeter test.

4.5.2. ML framework of chained models

Three commonly used statistical model indices (R2, MAE and RMSE) are calculated for all 9 models in **Table 4-3.** In test set, predicting "*curve_type"* has the highest R2 of 0.89. Other models predicting the *t* and *hrr* coordinates also exhibit high R2 varied between 0.83 to 0.87. Compared to the multi-class ranges of all target features, their mean errors are very small. MAEs for all models are equal to approximately 0.2. Although the RMSE is slightly higher in models aimed to predict *hrr* and later anchor points (trans-, decay- and after-point), it still remains at a low level below 1.

Table 4-3 Model indices in training and test sets, including categories of all target features.

Target feature	Categories	R2		MAE		RMSE	
		training set	test set	training set	test set	training set	test set
curve_type	0 - 2	0.99	0.89	0.01	0.17	0.07	0.53
t_ignit	1 - 12	1.0	0.86	0	0.23	0	0.66
t_devlp	3 - 13	1.0	0.84	0	0.19	0	0.5
t_trans	7 - 16	1.0	0.85	0	0.24	0	0.68
t_decay	7 - 19	1.0	0.83	0	0.26	0	0.65
t_after	11 - 19	1.0	0.84	0	0.27	0	0.86

hrr_devlp	1 - 7	1.0	0.83	0	0.2	0	0.49
hrr_trans	1 - 8	0.98	0.83	0.02	0.28	0.14	0.82
hrr_decay	1 - 9	1.0	0.87	0	0.23	0	0.81

Besides the above indices, the ROC metric using the micro-averaged one-vs-rest technique is calculated and plotted in this multi-category classification. In simple terms, the ratio of correct predictions to false ones is treated as predictive performance. The closer the whole ROC curve is to the top left, the higher the predictive accuracy reaches. Simply, AUC percentages can be rough judgment of the accuracy, which are above 90% in eight classification models, except for *hrr_devlp* with 89.76%, indicating effective classification results of our ML models, shown in Fig. 4-24.

Seen from the evaluation indices shown above, the predictive accuracy of all 9 target features is relatively high. The ML framework fits our MH-loaded polymer composites very well. On one side, the FR mechanisms of such long-term applied additives are almost transparent, which makes it easier to extract proper features purposefully; on the other side, conversion of the numeric regression to categorical classification has brought an advantage in prediction.

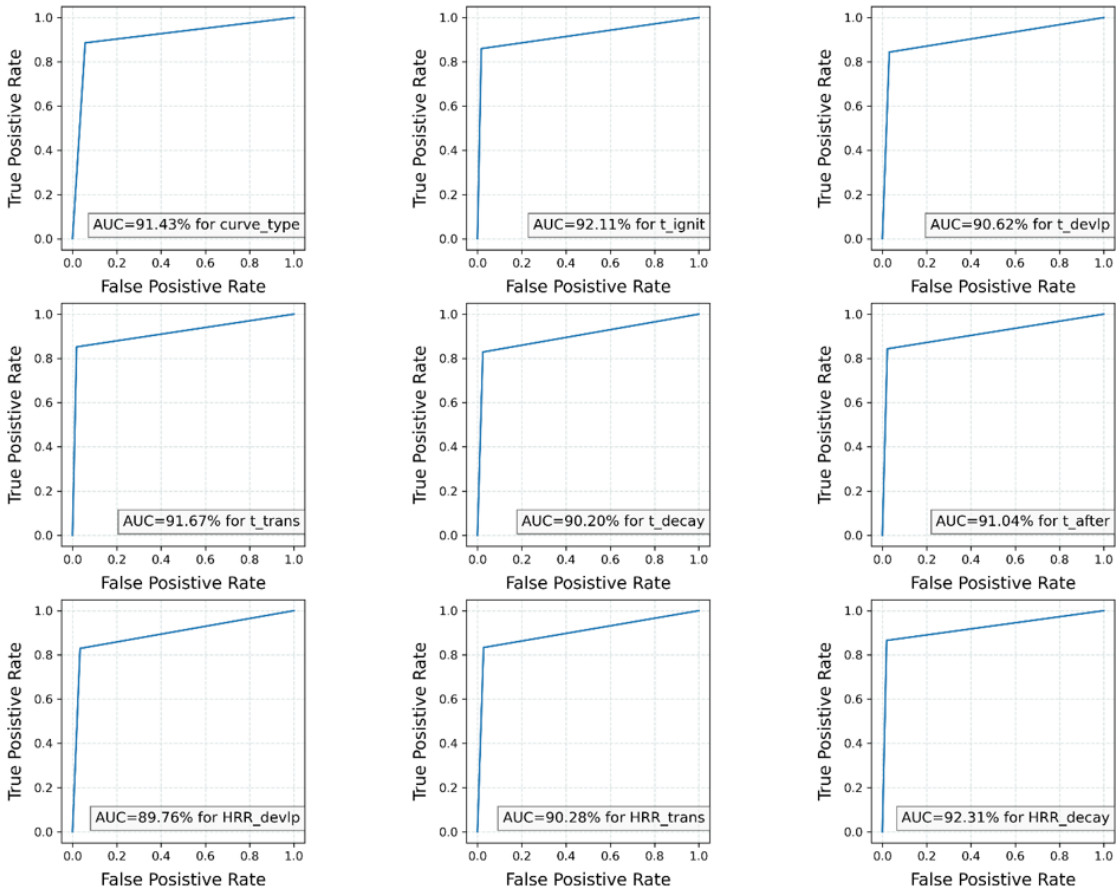

Fig. 4-24 Calculated ROC curves in predicting all target anchors (micro-averaged one-vs-rest)

4.5.3. Important features affecting the HRR-change

In our ML framework, selected features are divided into five groups concerning all aspects of sample preparation and CCT parameters. The feature groups are ranked by their Gini importance in **Fig. 4-25** for all models. The sum of the importance is 1 for all models. Higher importance means this feature group is more significant in deciding the target property. In feature selection, considering the feature importance is an essential part of the strategy.

Due to the large number of features and models built in this part, we only chose the important aspects from the ranking of FI in all models. In all 9 models, the feature group "polymer matrix" representing by the purple bars takes either first or second place. Especially in predicting *curve_type*, the sum of all polymer-related features has the importance of 0.58, indicating that the properties of neat polymer dominant in deciding the development of HRR in CCT. Loading of MH affects mostly the *hrr_devlp* with 0.32 importance. In other models, the importance of

"metal hydroxide" is also comparable to the feature group "synergist". Feature group "composites property" ranks first in models of *t_decay*, *hrr_trans* and *hrr_decay*, indicating their strong influence on the development of HRR over time. The influences of "experimental parameters" are lower than the above feature groups due to the fact that only up to 3 features are covered in this group. Although the CCT setup has a strong and complex influence, researchers intend to use similar parameters to ensure the reproducibility of experimental results. [107]

Although the influence of feature groups, but the importance of single features behaves differently. Although the "polymer matrix" takes the first place in predicting *t_ignit* and *t_devlp*, the most important features are still the mass fraction of MH and residue mass of composites after TGA. It is not surprising that the main and most important FR mechanism is the formation of the physical barrier of metal oxide in the combustion process. The features related to mass fraction and burning residue decide the quantity and quality of this protective layer. Furthermore, the importance of the synergist's amount and its oxygen content follows closely to MH loading since the synergist is intended to assist or enhance the layer structure.

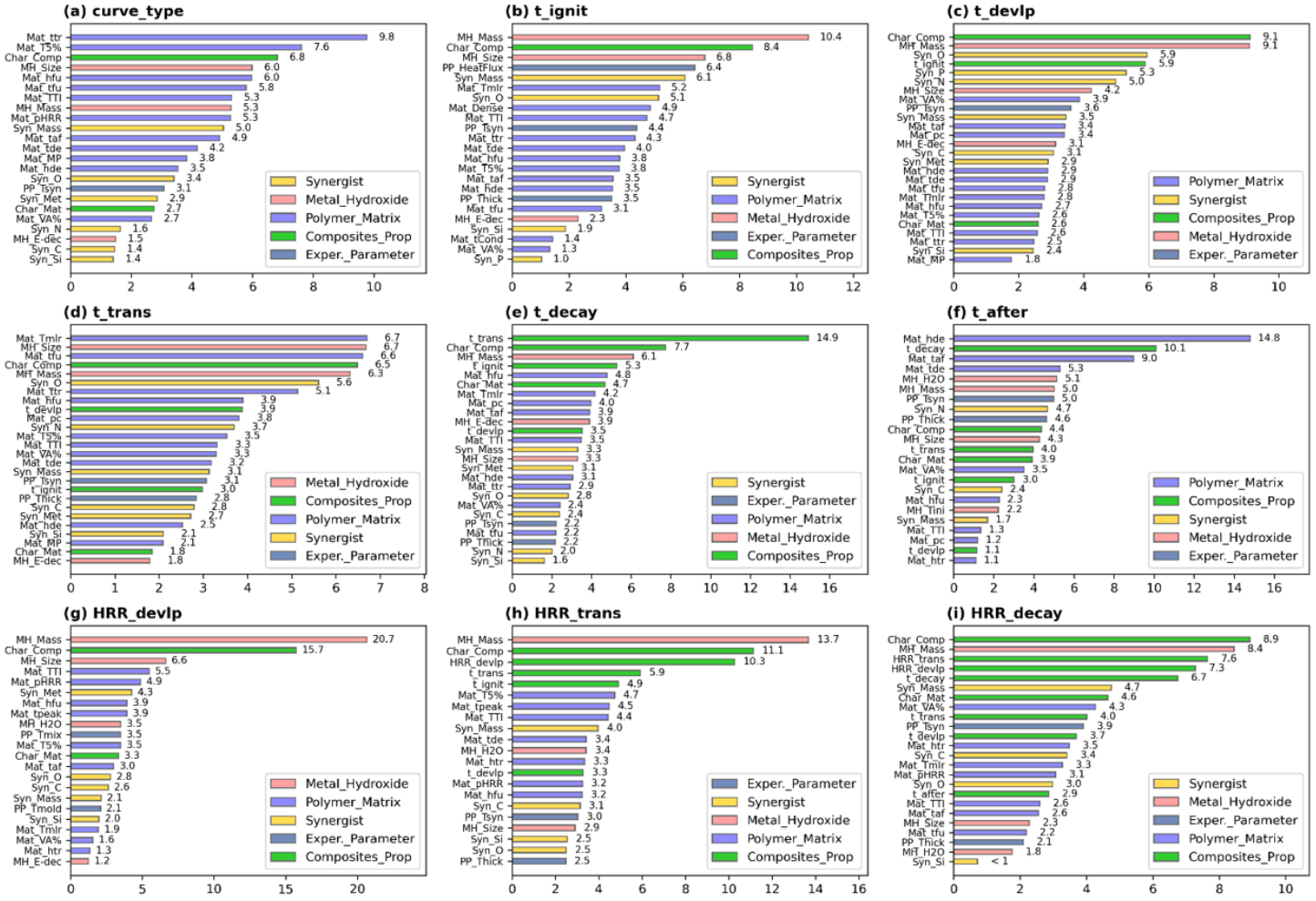

Fig. 4-25 Importance of all features, coloured legends illustrate the parent groups of each feature

4.5.4. Instantaneous prediction of HRR in the combustion phase

The ML framework is designed to predict the development of HRR in the whole CCT process. Validation samples based on different polymers and loading of MH were prepared and tested. In **Fig. 4-26**, blue lines represent the measured HRR curves of all 5 samples, whereas the red ones are the predicted HRR curves re-drawn through the five key anchor points.

In general, predicted HRR curves are in high agreement with measurements of all samples, especially for EVA-1 and EP-4. Through the predictions of developing HRR, relative characteristics like time to ignition, peak HRR, time to peak HRR and total heat release from the CCT can be obtained as measured in reality. The trends of how HRR changes over time due to the addition of flame retardants and preparation of polymer composites are accurately maintained. The EVA-1 sample with valley-transition has the highest MH loading of 53 wt.-%, which makes it extremely effective in lowering the heat release. The predicted HRR looks almost overlapped with the measured HRR. The same high accuracy in predicting is observed in the EP-4 sample containing 20 wt.-% ATH and 1 wt.-% of MOF. Through the development of HRR curves, the addition of MOF enhances the effect of flame retardancy, leading to the continuous decrease of HRR in the transition phase. This can be found from the slightly denser and stronger residues left from samples after CCT in Fig. 4-27, which is also observed in other publications using MOF as FR additives [108].

However, there are still comparable errors. The prediction of HRR curves is realized by segmentation and reassembling combustion phases, which are affected by complex physical and chemical compositions in the burning inside CCT. Theoretically, the precursory simplification of HRR curves assumes that the HRR shall have evident change (i.e., achieving local maximum or minimum, or plateau value with enough long time) in entering next combustion phases. But some measurements do not always show clear anchor points in CCT results, leading to inaccuracy in collecting data for training the models. Another error in simplification is the ignorance of small fluctuations of real curves. The testing curves in physical space are not as smooth as our re-drawn lines. These small but disharmonious changes can be responses of HRR to the sensitive testing conditions or simply measuring errors.

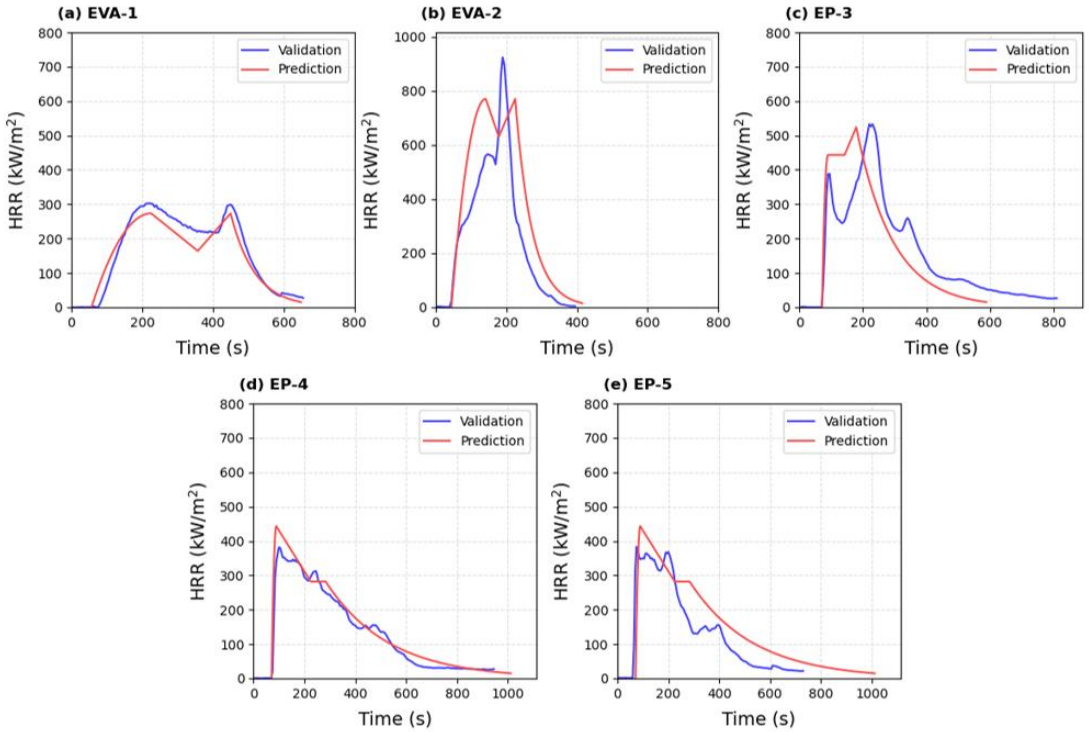

Fig. 4-26 Comparison between measured and predicted HRR curves for EVA and EP samples

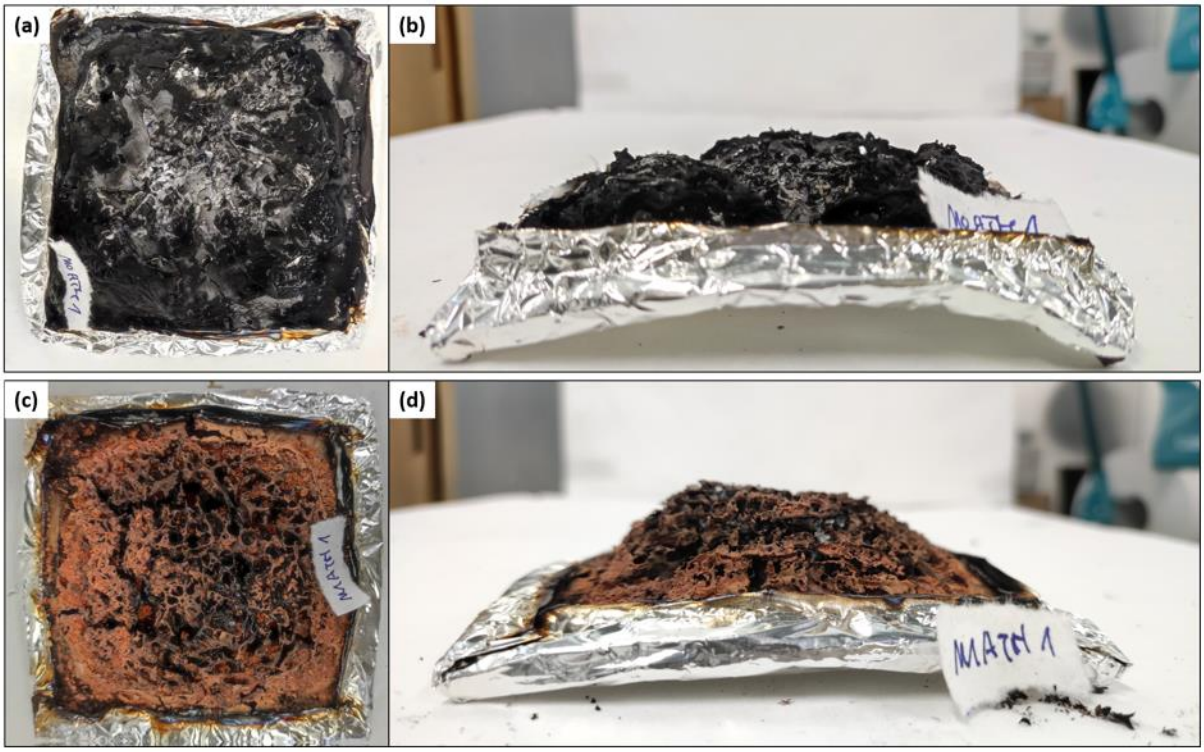

Fig. 4-27 Residues of burnt samples after CCT, (a) and (b) are the porous structure of EP based composites with 20wt-% ATH; (c) and (d) are samples with additional 1 wt-% Fe-BTC

The last disadvantage of this ML framework is the prediction of sharp peaks, which last only for a short time in HRR curves, i.e., the prediction of EVA-2. Such sharp peaks of HRR usually happen in the violent burning of small amounts of fuel or theoretically thermal thin samples like neat polymers with high flammability. On one side, our framework categorized the time characteristics with logarithmic processing, making the model un-sensitive to the change in a small-time range. On the other side, suitable FR composites are expected to have low peak HRR and suppressed HRR over time. The data collected from publications and experiments come from the efforts made in this direction, which causes inaccuracy in predicting sharp peaks similarly.

5. Conclusions

5.1. Summary of ML models

The machine learning approach based on (big-)data analysis is a promising route for materials investigation and development through the prediction of required properties. The models foreknow the properties of the formulation, distinguish the critical influence factors and indicate the direction how to optimise the formulation of materials. However, the building of ML models depends significantly on the collection and processing of data. This work faces the polymer composite with FR ability as the target object. In this work, we have successfully developed the predictive models for final properties of FRPCs, which are established in four phases: modelling for individual FR systems and final integration. The imported datasets are retrieved from either public literature or old experimental results from our group. As target properties of FRPCs are the typical characteristics of CCT, namely TTI, PHRR and THR. Based on different sub-works, more target properties like the flame-retardant index, storage modulus of DMA and limiting oxygen index, are also predicted by several models.

1. The MH-models have reached good prediction accuracy due to its simple FR mechanisms and effectiveness in high MH-loading. The R-squared values for all MH-models in training sets are close to 1 and those in test sets over 0.81 (highest R2 of 0.9 for TTI-prediction). The implementation of supervised learning algorithm of Random Forest also provides the ability of feature importance analysis. It reveals that the amount of MHs is a prime governing factor for deciding CCT properties, especially in pHRR prediction. Features related to neat polymers are also important. Furthermore, a machine-generated virtual dataset contributes to reinforcing the decision-making of proper formulation, providing suggestions about high mass fractions of MHs, high content of silicon, low addition of synergists, and low processing temperature in sample preparation.
2. In the MOF-system, RF, SVM and AVG-models are built through the collected data. Compared to MH-addition, the loading of MOF in polymer composites have more complex influences on the burning behaviour of sheet-like samples in CCT. Except for CCT results, the storage modulus at room

temperature is also involved. The models predicting all four properties have reached 0.75 in testsets, and their AUC values representing the classification accuracy are over 80%. In addition, the storage modulus of polymer composite is principally influenced by the mechanical property of neat polymer. Although MOF is added with the aim to improve the mechanical property of FRPCs, the addition of MOF has only moderate impact. From TTI(SVM) model, highly thermal stable polymer matrix with "MIL-type" MOF can prolong the TTI of polymer composite accordingly. As to pHRR and THR, the influence of other flame-retardant additives gains prominence.

3. LDH-system has the similar results of ML modelling. With the high R2 values in testsets of AVG-models predicting TTI, pHRR and THR, the classification accuracies are exhibited with confusion matrix of the misclassifications. The AUC values of the AVG-models are close to 90%. The analysis of feature importance indicates that the interlayer distance of LDHs have at least moderate influence on the CCT results, and the organic modification affect significantly the release of heat during the combustion process.
4. These ML models built for the individual FR systems have demonstrated the possibility of developing usable models to predict certain properties of polymer composites with less than 300 rows of data, without meeting the common requirements of the big data. An attempt to build the ultimate models to predict fire performance of FRPCs, which contain MH, MOF or LDH as functional additives, together with other FR chemicals, has been conducted with classifiers. The RF classifiers have shown potential accuracy in predicting the categorized properties. The R2 values of these models in testsets can reach up to 0.8 in some cases. With the increase in the size of dataset, ML models should exhibit higher performance in making prediction of CCT properties of all kinds of FRPCs.
5. Besides, we proved that not only the single property, but also the development of HRR against time is able to be predicted by integrated ML framework. The whole framework consists of key-points-simplification, chained-modelling and HRR-curve-recovery. Five key anchor points marking combustion phases are selected to represent the HRR development without losing much information. Models are built with the RF classifiers and R2 values varying from 0.83 to 0.89 in test sets indicate high accuracy

in predicting all desired target properties. Low errors below 1 level for all categories are also achieved in all models. Feature importance analysis contributes to selecting features and improving predictive performance. Although the ranking of all feature groups shows that the influence factors on HRR still come from all aspects, the latter part of HRR curves is more influenced by features related to MH loading and composites properties, while the features about neat polymer affect transition phase and time to ignition more deeply.

To conclude, this study has retrieved 828 data points from the publications in the last decade, structured with over 50 features covering the influence factors from various sources. The FR systems in this work has referred to the simple inorganic fillers, novel MOFs, organic-modified LDHs and intumescent flame retardants. The formulations of FRPCs involved in this work vary from the selection of polymer matrix, combination of various FR additives and different preparation and characterisation methods. We have conducted the feature engineering to select proper descriptors to introduce necessary information to make predictions of the results from CCT, DAM or LOI test. These features do not require highly specialized or expensive instruments to measure. Most of them are accessible from the publicly available database or literature. Although there are some descriptors not accurate enough to manifest e.g. micro-structure or morphology, the application of variety of indirect features has been used to complement this information loss.

This work has proven that it is possible to build ML models with certain accuracy to predict the fire performance of complex polymer composites, just based on the data collection by individual person. Therefore, it is evident that we are able to establish more reliable and accurate big-data models to assist the investigation and characterization of various materials. A comprehensive, extensive, and trustworthy database about the materials, founded by authoritative organizations or important groups, is the necessary condition for the advancement of materials informatics. With the development of science technology, the improvement of computer technology, the proliferation of high-performance processors, and the broadening horizons of researchers, using high-performance machines to assist the traditional experiments has become increasingly attractive. At the same time, the mathematical models, either constructed with computational technology or built

upon the big-data analysis, will definitely play an increasingly significant role in the research and development of new materials in the future.

5.2. Future plan

In the PhD work during the last four years, data-driven mathematical models have been built to predict the CCT properties of FRPCs. The predictive accuracy of the above-mentioned models have been illustrated in the contents. However, the performance of the computational models have the possibility to find more applications in other aspects and the potential to be improved for advanced usage.

In the future, there are mainly two directions following this PhD work: optimisation of the comprehensive big-data model and expansion of the application scenarios.

5.2.1. Optimisation of the "big model"

As we described before, the complexity and performance of a ML model is strongly correlated with the problem being studied. Standard FRPC is consist of the polymer matrix and functional additives. These polymers have different chemical compositions, molecular structures, and processing parameters, leading to unique physical properties in products. Meanwhile, the application of functional additives produces various chemical and physical processes in the preparation of polymer composites. Therefore, our work began with the simple FR-systems and expanded to the whole FRPCs. But the performance of the ML models for predicting the properties of any kind of FRPCs (in section 4.4) has still potential to be optimized.

1). The most effective and urgent method to enhance the big model is to add more data into the machine. As mentioned in last chapter, we have 828 records to build the final model for FRPCs with any kind of additives. However, taking into consideration that we have over 10 types of polymers, 80+ types of FR additives, 5+ preparation processes and different modification methods on the additives, these records are actually not enough. The formulations, or data points in the dataset comes from personal collections by reading public literatures. In order to obtain more data, we intend to carry out cooperation with other research groups and share part of the research data. Furthermore, we have developed a software for simple prediction of CCT results of certain FRPCs. We are able to collect the experimental details of the customers with informed consent. Besides, the

literature survey covering the FRPCs will not stop. Our goal is to increase the number of data in the dataset to over 1000.

2). Feature space optimization is necessary to achieve better performance. Unlike the pure mathematic problems, the different working mechanisms of FR additives require to provide different features for different FR-systems. In the work that has already been done, features of all FR-additives have been generalized to reduce the number of features. This leads to the disadvantage of losing key information of specific additives, deteriorating the predictive accuracy of ML models. To prevent the information loss while maintain the similar number of features, we plan to consolidate the features of single FR-systems into one feature to reduce the dimension of feature space. The disadvantage of feature dimensionality reduction (FDR) is that you can hardly find out the influence of separate feature on the target properties.

3). Using different modelling strategy is worthy trying. Besides the RF and SVM models, the deep-learning models have different performance on complex problems. As an example, the algorithm multi-layer perceptron (MLP) consisting of different activation layers between input and output, simulating the human brain can provide more insights in ML modelling from other aspects. Although we have tried to build MLP models with the whole dataset and the results are not optimistic, the attempt to build deep-learning models after increasing the size of dataset and feature engineering is still meaningful.

5.2.2. Expansion of application scenarios

Our research focus is the characterization of FRPCs in CCT. Other properties of polymer composites can be predicted likewise. In the models of MOF-system, we have conducted the prediction of mechanical properties of the composites and the model performance has reached good results.

Besides the CCT, there are other commonly used methods to evaluate the fire performance of FRPCs like LOI tests and UL-94 test. The former characteristic has been involved in our previous contents. In the next period, the construction of ML model to predict the LOI values of various FRPCs (polymer matrix with any kinds and numbers of FR additives) is ongoing. A dataset consisting of 790 data points that were revealed from the same literatures has been put into analysis. Results shows that the selection of FR additives have significant influence on LOI

values of FRPCs, especially the inorganic fillers (MHs). Early model to predict the LOI indicates that the existing dataset does not meet the requirements for better predictive performance: the data related to FRPCs in MH-system dominants in the supervised learning process. Thus, feature engineering is necessary to be conducted before further modelling. This research can be transferred to build predictive models for UL-94 results in the same manner.

Another aspect of the application is the prediction of mechanical properties, which are the important parameters deciding how the products can be used in industry or daily life. In this part, the work is consisting of four steps that starts with the data collection too. The following and most important step is the selection of features that exhibit the influence factors from the aspects of materials and processing. Unlike the FR effect, the development of mechanical performance has relationship with the microstructural changes, molecular configurations, physical dispersion and possible defect distribution. These information should be contained by the input features. The subsequent modelling and evaluation steps will utilize similar methods mentioned in our work. With the integrated models covering all aspects of FRPCs, it is possible to customize the properties of polymer-based products for different application, achieve the accurate regulation of the formulations.

Annexes

All the data for ML modelling are collected from public literature. There are in total 150 publications used in this work. Below is the list of all involved papers.

MDH-dataset: [109–133]

MOF-dataset: [50,134–191]

LDH-dataset: [49,50,192–227]

References

[1] J. Jordan, K.I. Jacob, R. Tannenbaum, M.A. Sharaf, I. Jasiuk, Experimental trends in polymer nanocomposites—a review, Materials Science and Engineering: A 393 (2005) 1–11. https://doi.org/10.1016/j.msea.2004.09.044.

[2] F. Hussain, M. Hojjati, M. Okamoto, R.E. Gorga, Review article: Polymer-matrix Nanocomposites, Processing, Manufacturing, and Application: An Overview, Journal of Composite Materials 40 (2006) 1511–1575. https://doi.org/10.1177/0021998306067321.

[3] F. Laoutid, L. Bonnaud, M. Alexandre, J.-M. Lopez-Cuesta, P. Dubois, New prospects in flame retardant polymer materials: From fundamentals to nanocomposites, Materials Science and Engineering: R: Reports 63 (2009) 100–125. https://doi.org/10.1016/j.mser.2008.09.002.

[4] X.-Y. Zhao, H.-J. Liu, Review of polymer materials with low dielectric constant, Polymer International 59 (2010) 597–606. https://doi.org/10.1002/pi.2809.

[5] J. Chen, Y. Zhu, Z. Guo, A.G. Nasibulin, Recent Progress on Thermo-electrical Properties of Conductive Polymer Composites and Their Application in Temperature Sensors, Eng. Sci. (2020). https://doi.org/10.30919/es8d1129.

[6] MITSUBISHI HEAVY INDUSTRIES, LTD., Development of Smart Polymer Materials and its Various Applications,Mitsubishi Heavy Industries Technical Review Vol.41 No.1(2004).

[7] X. Zhao, L. Lv, B. Pan, W. Zhang, S. Zhang, Q. Zhang, Polymer-supported nanocomposites for environmental application: A review, Chemical Engineering Journal 170 (2011) 381–394. https://doi.org/10.1016/j.cej.2011.02.071.

[8] S.C. Rasmussen, From Parkesine to Celluloid: The Birth of Organic Plastics, Angew. Chem. Int. Ed Engl. 60 (2021) 8012–8016. https://doi.org/10.1002/anie.202015095.

[9] Center of Fire Statistics, World fire statistics, Center of Fire Statistics, 2022.

[10] E.E. Mbamalu, U.E. Chioma, A. Epere, Applications of fire retardant polymer composites for improved safety in the industry: a review, Proc.Indian Natl. Sci. Acad. (2024). https://doi.org/10.1007/s43538-024-00333-7.

[11] Y. Kim, S. Lee, H. Yoon, Fire-Safe Polymer Composites: Flame-Retardant Effect of Nanofillers, Polymers (Basel) 13 (2021). https://doi.org/10.3390/polym13040540.

[12] J. Rychlý, K. Veselý, E. Gál, M. Kummer, J. Jančář, L. Rychlá, Use of thermal methods in the characterization of the high-temperature decomposition and ignition of polyolefins and EVA copolymers filled with Mg(OH)2, Al(OH)3 and CaCO3, Polymer Degradation and Stability 30 (1990) 57–72. https://doi.org/10.1016/0141-3910(90)90117-P.

[13] P. R. Hornsby, Colin L. Watson, A Study of the Mechanism of Flame Retardance and Smoke Suppression in Polymer Filled with Magnesium Hydroxide, Polymer Degradation and Stability 30 (1990) 73–87.

[14] R. N. Rothon, P. R. Hornsby, Flame retardant effects of magnesium hydroxide, Polymer Degradation and Stability 54 (1996) 383–385.

[15] P.R. Hornsby, J. Wang, R. Rothon, G. Jackson, G. Wilkinson, K. Cossick, Thermal decomposition behaviour of polyamide fire-retardant compositions containing magnesium hydroxide filler, Polymer Degradation and Stability 51 (1996) 235–249. https://doi.org/10.1016/0141-3910(95)00181-6.

[16] H. Chai, Q. Duan, L. Jiang, J. Sun, Effect of inorganic additive flame retardant on fire hazard of polyurethane exterior insulation material, J Therm Anal Calorim 135 (2019) 2857–2868. https://doi.org/10.1007/s10973-018-7797-3.

[17] L. Wang, X. Wu, C. Wu, J. Yu, G. Wang, P. Jiang, Study on the flame retardancy of EVM/magnesium hydroxide composites optimized with a flame retardant containing phosphorus and silicon, J. Appl. Polym. Sci. 121 (2011) 68–77. https://doi.org/10.1002/app.33226.

[18] L. Chen, Y.-Z. Wang, A review on flame retardant technology in China. Part I: development of flame retardants, Polymers for Advanced Techs 21 (2010) 1–26. https://doi.org/10.1002/pat.1550.

[19] H. Chai, Q. Duan, L. Jiang, J. Sun, Effect of inorganic additive flame retardant on fire hazard of polyurethane exterior insulation material, J Therm Anal Calorim 135 (2019) 2857–2868. https://doi.org/10.1007/s10973-018-7797-3.

[20] Y.-T. Pan, Z. Zhang, R. Yang, The rise of MOFs and their derivatives for flame retardant polymeric materials: A critical review, Composites Part B: Engineering 199 (2020) 108265. https://doi.org/10.1016/j.compositesb.2020.108265.

[21] F. Seidi, M. Jouyandeh, M. Taghizadeh, A. Taghizadeh, H. Vahabi, S. Habibzadeh, K. Formela, M.R. Saeb, Metal-Organic Framework (MOF)/Epoxy Coatings: A Review, Materials (Basel) 13 (2020). https://doi.org/10.3390/ma13122881.

[22] V. Unnikrishnan, O. Zabihi, M. Ahmadi, Q. Li, P. Blanchard, A. Kiziltas, M. Naebe, Metal–organic framework structure–property relationships for high-performance multifunctional polymer nanocomposite applications, J. Mater. Chem. A 9 (2021) 4348–4378. https://doi.org/10.1039/D0TA11255K.

[23] Q. Kong, T. Wu, J. Zhang, D.-Y. Wang, Simultaneously improving flame retardancy and dynamic mechanical properties of epoxy resin nanocomposites through layered copper phenylphosphate, Composites Science and Technology 154 (2018) 136–144. https://doi.org/10.1016/j.compscitech.2017.10.013.

[24] Q. Kong, Y. Sun, C. Zhang, H. Guan, J. Zhang, D.-Y. Wang, F. Zhang, Ultrathin iron phenyl phosphonate nanosheets with appropriate thermal stability for improving fire safety in epoxy, Composites Science and Technology 182 (2019) 107748. https://doi.org/10.1016/j.compscitech.2019.107748.

[25] D.-Y. Wang, X.-X. Cai, M.-H. Qu, Y. Liu, J.-S. Wang, Y.-Z. Wang, Preparation and flammability of a novel intumescent flame-retardant poly(ethylene-co-vinyl acetate)

system, Polymer Degradation and Stability 93 (2008) 2186–2192. https://doi.org/10.1016/j.polymdegradstab.2008.07.032.

[26] D.-Y. Wang, Y. Liu, X.-G. Ge, Y.-Z. Wang, A. Stec, B. Biswas, T.R. Hull, D. Price, Effect of metal chelates on the ignition and early flaming behaviour of intumescent fire-retarded polyethylene systems, Polymer Degradation and Stability 93 (2008) 1024–1030. https://doi.org/10.1016/j.polymdegradstab.2007.12.011.

[27] Y. Zhang, X. Li, Z. Fang, T.R. Hull, A. Kelarakis, A.A. Stec, Mechanism of enhancement of intumescent fire retardancy by metal acetates in polypropylene, Polymer Degradation and Stability 136 (2017) 139–145. https://doi.org/10.1016/j.polymdegradstab.2016.12.018.

[28] R. Sonnier, L. Ferry, C. Longuet, F. Laoutid, B. Friederich, A. Laachachi, J.-M. Lopez - Cuesta, Combining cone calorimeter and PCFC to determine the mode of action of flame - retardant additives, Polymers for Advanced Techs 22 (2011) 1091-1099. https://doi.org/10.1002/pat.1989.

[29] J. Reuter, L. Greiner, P. Kukla, M. Döring, Efficient flame retardant interplay of unsaturated polyester resin formulations based on ammonium polyphosphate, Polymer Degradation and Stability 178 (2020) 109134. https://doi.org/10.1016/j.polymdegradstab.2020.109134.

[30] G.B. Olson, Computational Design of Hierarchically Structured Materials, Science 277 (1997) 1237–1242. https://doi.org/10.1126/science.277.5330.1237.

[31] SEBASTIEN CANDEL, COMBUSTION DYNAMICS AND CONTROL: PROGRESS AND CHALLENGES, Proceedings of the Combustion Institute 29 (2002) 1–28.

[32] Andrea Dussoa, Stefano Grimaz, Ernesto Salzano, Rapid Estimation of the Heat Release Rate of Combustible Items, CHEMICAL ENGINEERING 53 (2016). https://doi.org/10.3303/CET1653005.

[33] J. Marti, J. de La Vega, D.-Y. Wang, E. Oñate, Numerical Simulation of Flame Retardant Polymers Using a Combined Eulerian–Lagrangian Finite Element Formulation, Applied Sciences 11 (2021) 5952. https://doi.org/10.3390/app11135952.

[34] H.T. Nguyen, K.T.Q. Nguyen, T.C. Le, G. Zhang, Review on the Use of Artificial Intelligence to Predict Fire Performance of Construction Materials and Their Flame Retardancy, Molecules 26 (2021). https://doi.org/10.3390/molecules26041022.

[35] K.T. Butler, D.W. Davies, H. Cartwright, O. Isayev, A. Walsh, Machine learning for molecular and materials science, Nature 559 (2018) 547–555. https://doi.org/10.1038/s41586-018-0337-2.

[36] LEO BREIMAN, Random Forests, Machine Learning 45 (2001) 5–32.

[37] Q. Ren, H. Cheng, H. Han (Eds.), Research on machine learning framework based on random forest algorithm.

[38] Mark R. Segal, Machine Learning Benchmarks and Random Forest Regression, 2003.

[39] M.A. Chandra, S.S. Bedi, Survey on SVM and their application in image classification, Int. j. inf. tecnol. 13 (2021) 1–11. https://doi.org/10.1007/s41870-017-0080-1.

[40] S. Huang, N. Cai, P.P. Pacheco, S. Narrandes, Y. Wang, W. Xu, Applications of Support Vector Machine (SVM) Learning in Cancer Genomics, Cancer Genomics Proteomics 15 (2018) 41–51. https://doi.org/10.21873/cgp.20063.

[41] Directorate-General for Environment, Regulatory strategy for flame retardants, European Chemicals Agency, 2023.

[42] E.N. Kalali, S. de Juan, X. Wang, S. Nie, R. Wang, D.-Y. Wang, Comparative study on synergistic effect of LDH and zirconium phosphate with aluminum trihydroxide on flame retardancy of EVA composites, J Therm Anal Calorim 121 (2015) 619–626. https://doi.org/10.1007/s10973-015-4598-9.

[43] D.-X. Ma, Y. Yang, G.-Z. Yin, A. Vázquez-López, Y. Jiang, N. Wang, D.-Y. Wang, ZIF-67 In Situ Grown on Attapulgite: A Flame Retardant Synergist for Ethylene Vinyl Acetate/Magnesium Hydroxide Composites, Polymers (Basel) 14 (2022). https://doi.org/10.3390/polym14204408.

[44] D. Basu, A. Das, K.W. Stöckelhuber, U. Wagenknecht, G. Heinrich, Advances in layered double hydroxide (LDH)-based elastomer composites, Progress in Polymer Science 39 (2014) 594–626. https://doi.org/10.1016/j.progpolymsci.2013.07.011.

[45] G. Heideman, Reduced zinc oxide levels in sulphur vulcanisation of rubber compounds: mechanistic aspects of the role of activators and multifunctional additives. Ph.D. Thesis, 2004.

[46] L. Dong, C. Ge, P. Qin, Y. Chen, Q. Xu, Immobilization and catalytic properties of candida lipolytic lipase on surface of organic intercalated and modified MgAl-LDHs, Solid State Sciences 31 (2014) 8–15. https://doi.org/10.1016/j.solidstatesciences.2014.02.006.

[47] Z.D. Han, X.K. Zhang, Y. Wang, Z.Q. Jiang, P. Wang, Characterization of Layered Double Hydroxide Modified with Sodium Dodecyl Sulfate and its Dispersion in Polyethylene, KEM 591 (2013) 138–141. https://doi.org/10.4028/www.scientific.net/KEM.591.138.

[48] S. Naseem, S.P. Lonkar, A. Leuteritz (Eds.), Study of modified LDHs as UV protecting materials for polypropylene (PP), 2019.

[49] Z.-B. Shao, J. Cui, X.-B. Lin, X.-L. Li, R.-K. Jian, D.-Y. Wang, In-situ coprecipitation formed Fe/Zn-layered double hydroxide/ammonium polyphosphate hybrid material for flame retardant epoxy resin via synergistic catalytic charring, Composites Part A: Applied Science and Manufacturing 155 (2022) 106841. https://doi.org/10.1016/j.compositesa.2022.106841.

[50] K. Song, X. Li, Y.-T. Pan, B. Hou, Z.U. Rehman, J. He, R. Yang, The influence on flame retardant epoxy composites by a bird's nest-like structure of Co-based isomers

evolved from zeolitic imidazolate framework-67, Polymer Degradation and Stability 211 (2023) 110318. https://doi.org/10.1016/j.polymdegradstab.2023.110318.

[51] MICHAEL PAZZANI, DANIEL BILLSUS, Learning and Revising User Profiles: The Identification of Interesting Web Sites, Machine Learning 27 (1997) 313–331.

[52] X. Ke, Y. Duan, Coupling machine learning with thermodynamic modelling to develop a composition-property model for alkali-activated materials, Composites Part B: Engineering 216 (2021) 108801. https://doi.org/10.1016/j.compositesb.2021.108801.

[53] D. Banerjee, C.M. Simon, A.M. Plonka, R.K. Motkuri, J. Liu, X. Chen, B. Smit, J.B. Parise, M. Haranczyk, P.K. Thallapally, Metal-organic framework with optimally selective xenon adsorption and separation, Nat. Commun. 7 (2016) ncomms11831. https://doi.org/10.1038/ncomms11831.

[54] Abdullateef M. Al-Khaleefi, Mohammad J. Terro, Alex P. Alex, Yong Wang, Prediction of fire resistance of concrete filled tubular steel columns using neural networks, Fire Safety Journal 37 (2002) 339–352.

[55] A. Basuchoudhary, J.T. Bang, 2018. Predicting Terrorism with Machine Learning: Lessons from "Predicting Terrorism: A Machine Learning Approach". Peace Economics, Peace Science and Public Policy 24, 20180040. https://doi.org/10.1515/peps-2018-0040.

[56] Q. Rong, H. Wei, X. Huang, H. Bao, Predicting the effective thermal conductivity of composites from cross sections images using deep learning methods, Composites Science and Technology 184 (2019) 107861. https://doi.org/10.1016/j.compscitech.2019.107861.

[57] S.M. Moosavi, A. Chidambaram, L. Talirz, M. Haranczyk, K.C. Stylianou, B. Smit, Capturing chemical intuition in synthesis of metal-organic frameworks, Nat. Commun. 10 (2019) 539. https://doi.org/10.1038/s41467-019-08483-9.

[58] T. Sabiston, K. Inal, P. Lee-Sullivan, Application of Artificial Neural Networks to predict fibre orientation in long fibre compression moulded composite materials, Composites Science and Technology 190 (2020) 108034. https://doi.org/10.1016/j.compscitech.2020.108034.

[59] X. Wang, L. Wang, F. Li, Y. Teng, C. Ji, H. Wu, Toxicity pathways of lipid metabolic disorders induced by typical replacement flame retardants via data-driven analysis, in silico and in vitro approaches, Chemosphere 287 (2022) 132419. https://doi.org/10.1016/j.chemosphere.2021.132419.

[60] J. Mendikute, J. Plazaola, M. Baskaran, E. Zugasti, L. Aretxabaleta, J. Aurrekoetxea, Impregnation quality diagnosis in Resin Transfer Moulding by machine learning, Composites Part B: Engineering 221 (2021) 108973. https://doi.org/10.1016/j.compositesb.2021.108973.

[61] Timothy Erps, Michael Foshey, Mina Konaković Luković, Wan Shou, Hanns Hagen Goetzke, Herve Dietsch, Klaus Stoll, Bernhard von Vacano, Wojciech Matusik,

Accelerated Discovery of 3D Printing Materials Using Data-Driven Multi-Objective Optimization, Accelerated Discovery of 3D Printing Materials (2021).

[62] K.D. Humfeld, D. Gu, G.A. Butler, K. Nelson, N. Zobeiry, A machine learning framework for real-time inverse modeling and multi-objective process optimization of composites for active manufacturing control, Composites Part B: Engineering 223 (2021) 109150. https://doi.org/10.1016/j.compositesb.2021.109150.

[63] Lydia Kang, Tian Wei, Zhang Ho, An integrated recommender system and machine learning-assisted approach to predict epoxy-silica composites' mechanical behavaviors, International Research Journal of Engineering and Technology 08 (2021) 684–691.

[64] A. Alimadadi, S. Aryal, I. Manandhar, P.B. Munroe, B. Joe, X. Cheng, Artificial intelligence and machine learning to fight COVID-19, Physiol. Genomics 52 (2020) 200–202. https://doi.org/10.1152/physiolgenomics.00029.2020.

[65] D.-A. Mendels, L. Dortet, C. Emeraud, S. Oueslati, D. Girlich, J.-B. Ronat, S. Bernabeu, S. Bahi, G.J.H. Atkinson, T. Naas, Using artificial intelligence to improve COVID-19 rapid diagnostic test result interpretation, Proc. Natl. Acad. Sci. U. S. A. 118 (2021). https://doi.org/10.1073/pnas.2019893118.

[66] D. Driggs, I. Selby, M. Roberts, E. Gkrania-Klotsas, J.H.F. Rudd, G. Yang, J. Babar, E. Sala, C.-B. Schönlieb, Machine Learning for COVID-19 Diagnosis and Prognostication: Lessons for Amplifying the Signal While Reducing the Noise, Radiol. Artif. Intell. 3 (2021) e210011. https://doi.org/10.1148/ryai.2021210011.

[67] R. Fusco, R. Grassi, V. Granata, S.V. Setola, F. Grassi, D. Cozzi, B. Pecori, F. Izzo, A. Petrillo, Artificial Intelligence and COVID-19 Using Chest CT Scan and Chest X-ray Images: Machine Learning and Deep Learning Approaches for Diagnosis and Treatment, J. Pers. Med. 11 (2021). https://doi.org/10.3390/jpm11100993.

[68] F. Chen, J. Wang, Z. Guo, F. Jiang, R. Ouyang, P. Ding, Machine Learning and Structural Design to Optimize the Flame Retardancy of Polymer Nanocomposites with Graphene Oxide Hydrogen Bonded Zinc Hydroxystannate, ACS Appl. Mater. Interfaces 13 (2021) 53425–53438. https://doi.org/10.1021/acsami.1c12767.

[69] H. Fang, S.M. Lo, Y. Zhang, Y. Shen, Development of a machine-learning approach for identifying the stages of fire development in residential room fires, Fire Safety Journal 126 (2021) 103469. https://doi.org/10.1016/j.firesaf.2021.103469.

[70] M.Z. Naser, Fire resistance evaluation through artificial intelligence - A case for timber structures, Fire Safety Journal 105 (2019) 1–18. https://doi.org/10.1016/j.firesaf.2019.02.002.

[71] Z. Wang, T. Zhang, X. Huang, Predicting real-time fire heat release rate by flame images and deep learning, Proceedings of the Combustion Institute 39 (2023) 4115–4123. https://doi.org/10.1016/j.proci.2022.07.062.

[72] Vytenis Babrauskas, Development of the cone calorimeter-A bench-scale heat release rate apparatus based on oxygen consumption, Fire and Materials 8 (1984) 81–95.

[73] Clayton Huggett, Estimation of rate of heat release by means of oxygen consumption measurements, Fire and Materials 4 (1980) 61–65.

[74] M.J. Hurley, D. Gottuk, J.R. Hall, K. Harada, E. Kuligowski, M. Puchovsky, J. Torero, J.M. Watts, C. Wieczorek (Eds.), SFPE Handbook of Fire Protection Engineering, Springer New York, New York, NY, 2016.

[75] B. Schartel, K. Kebelmann (Eds.), Fire Testing for the Development of Flame Retardant Polymeric Materials.

[76] M. Werrel, J.H. Deubel, S. Krüger, A. Hofmann, U. Krause, The calculation of the heat release rate by oxygen consumption in a controlled-atmosphere cone calorimeter, Fire Mater. 38 (2014) 204–226. https://doi.org/10.1002/fam.2175.

[77] V. Kodur, P. Kumar, M.M. Rafi, Fire hazard in buildings: review, assessment and strategies for improving fire safety, PRR 4 (2019) 1–23. https://doi.org/10.1108/PRR-12-2018-0033.

[78] M. Chen, Review on Heat Release Reduction of Flexible Polyurethane Foam, Journal of Xihua University (Natural Science Edition) 39 (2020) 57–66.

[79] B. Schartel, T.R. Hull, Development of fire-retarded materials—Interpretation of cone calorimeter data, Fire Mater. 31 (2007) 327–354. https://doi.org/10.1002/fam.949.

[80] National Fire Protection Association, Standard for Smoke Management System in Malls, Atria, and Large Spaces: NFPA 92B, 2005.

[81] B. Schartel, K. Kebelmann, Fire Testing for the Development of Flame Retardant Polymeric Materials, in: Y. Hu, X. Wang (Eds.), Flame Retardant Polymeric Materials, CRC Press, Boca Raton CRC Press, [2020] | Series: Series in materials science and engineering, 2019, pp. 35–55.

[82] Richard C. Rothermel, A mathematical model for predicting fire spread in wildland fuels, Res. Pap. INT-firstfifteenth, 1972.

[83] W.-H. Park, K.-B. Yoon, Optimization of pyrolysis properties using TGA and cone calorimeter test, J. Therm. Sci. 22 (2013) 168–173. https://doi.org/10.1007/s11630-013-0608-z.

[84] Clayton Huggett, Estimation of rate of heat release by means of oxygen consumption measurements, Fire and Materials 4 (1980) 61–65.

[85] Patrick A. Enright, Charles M. Fleischmann, Uncertainty of Heat Release Rate Calculation of the ISO5660-1 Cone Calorimeter Standard Test Method, Fire Technology 35 (1999) 153–169.

[86] L. Zhao, N.A. Dembsey, Measurement uncertainty analysis for calorimetry apparatuses, Fire Mater. 32 (2008) 1–26. https://doi.org/10.1002/fam.947.

[87] Fabian Pedregosa, Gaël Varoquaux, Alexandre Gramfort, Vincent Michel, Bertrand Thirion, Olivier Grisel, Mathieu Blondel, Peter Prettenhofer, Ron Weiss, Vincent Dubourg, Jake Vanderplas, Alexandre Passos, David Cournapeau, Matthieu Brucher, Matthieu Perrot, Édouard Duchesnay, Scikit-learn: Machine Learning in Python, Journal of Machine Learning Research 12 (2011) 2825–2830.

[88] K.P. Sinaga, M.-S. Yang, Unsupervised K-Means Clustering Algorithm, IEEE Access 8 (2020) 80716–80727. https://doi.org/10.1109/ACCESS.2020.2988796.

[89] A. Fatima, N. Nazir, M.G. Khan, Data Cleaning In Data Warehouse: A Survey of Data Pre-processing Techniques and Tools, IJITCS 9 (2017) 50–61. https://doi.org/10.5815/ijitcs.2017.03.06.

[90] Johan Lindholm, Anders Brink, Mikko Hupa (Eds.), Cone calorimeter - a tool for measuring heat release rate, 2008.

[91] Patrick A. Enright, Charles M. Fleischman, Uncertainty of Heat Release Rate Calculation of the ISO5660-1 Cone Calorimeter Standard Test Method, Fire Technology 35 (1999) 153–169. https://doi.org/10.1023/A:1015416005888.

[92] L. Zhao, N.A. Dembsey, Measurement uncertainty analysis for calorimetry apparatuses, Fire Mater. 32 (2008) 1–26. https://doi.org/10.1002/fam.947.

[93] Clayton Huggett, Estimation of rate of heat release by means of oxygen consumption measurements, Fire and Materials 4 (1980) 61–65.

[94] J. Zhang, X. Wang, F. Zhang, A. Richard Horrocks, Estimation of heat release rate for polymer–filler composites by cone calorimetry, Polymer Testing 23 (2004) 225–230. https://doi.org/10.1016/S0142-9418(03)00098-9.

[95] G. Camino, M.B. A. Maffezzoli, M. De Lazzaro, M. Zammarano, Effect of hydroxide and hydroxycarbonate structure on fire retardant effectiveness and mechanical properties in ethylene-vinyl acetate copolymer, Polymer Degradation and Stability 74 (2001) 457–464. https://doi.org/10.1016/S0141-3910(01)00167-7.

[96] G. Lo Dico, Á.P. Nuñez, V. Carcelén, M. Haranczyk, Machine-learning-accelerated multimodal characterization and multiobjective design optimization of natural porous materials, Chem. Sci. 12 (2021) 9309–9317. https://doi.org/10.1039/d1sc00816a.

[97] P.R. Hornsby, The application of magnesium hydroxide as a fire retardant and smoke-suppressing additive for polymers, Fire Mater. 18 (1994) 269–276.

[98] M. Fu, B. Qu, Synergistic flame retardant mechanism of fumed silica in ethylene-vinyl acetate/magnesium hydroxide blends, Polymer Degradation and Stability 85 (2004) 633–639. https://doi.org/10.1016/j.polymdegradstab.2004.03.002.

[99] J. Xiao, J. Hobson, A. Ghosh, M. Haranczyk, D.-Y. Wang, Flame retardant properties of metal hydroxide-based polymer composites: A machine learning approach, Composites Communications 40 (2023) 101593. https://doi.org/10.1016/j.coco.2023.101593.

[100] W. Chen, Y. Jiang, R. Qiu, W. Xu, Y. Hou, Investigation of UiO-66 as Flame Retardant and Its Application in Improving Fire Safety of Polystyrene, Macromol. Res. 28 (2020) 42–50. https://doi.org/10.1007/s13233-019-7165-6.

[101] X. Chen, X. Chen, S. Li, C. Jiao, Copper metal - organic framework toward flame - retardant enhancement of thermoplastic polyurethane elastomer composites based on ammonium polyphosphate, Polymers for Advanced Techs 32 (2021) 2829-2842. https://doi.org/10.1002/pat.5260.

[102] R. Duan, H. Wu, J. Li, Z. Zhou, W. Meng, L. Liu, H. Qu, J. Xu, Phosphor nitrile functionalized UiO-66-NH2/graphene hybrid flame retardants for fire safety of epoxy, Colloids and Surfaces A: Physicochemical and Engineering Aspects 635 (2022) 128093. https://doi.org/10.1016/j.colsurfa.2021.128093.

[103] Y. Zheng, Y. Lu, K. Zhou, A novel exploration of metal–organic frameworks in flame-retardant epoxy composites, J Therm Anal Calorim 138 (2019) 905–914. https://doi.org/10.1007/s10973-019-08267-9.

[104] X. Fan, F. Xin, W. Zhang, H. Liu, Effect of phosphorus-containing modified UiO-66-NH2 on flame retardant and mechanical properties of unsaturated polyester, Reactive and Functional Polymers 174 (2022) 105260. https://doi.org/10.1016/j.reactfunctpolym.2022.105260.

[105] Y.-T. Pan, L. Zhang, X. Zhao, D.-Y. Wang, Interfacial engineering of renewable metal organic framework derived honeycomb-like nanoporous aluminum hydroxide with tunable porosity, Chem. Sci. 8 (2017) 3399–3409. https://doi.org/10.1039/c6sc05695d.

[106] Y. Hou, S. Qiu, Z. Xu, F. Chu, C. Liao, Z. Gui, L. Song, Y. Hu, W. Hu, Which part of metal-organic frameworks affects polymers' heat release, smoke emission and CO production behaviors more significantly, metallic component or organic ligand?, Composites Part B: Engineering 223 (2021) 109131. https://doi.org/10.1016/j.compositesb.2021.109131.

[107] B. Schartel, M. Bartholmai, U. Knoll, Some comments on the use of cone calorimeter data, Polymer Degradation and Stability 88 (2005) 540–547. https://doi.org/10.1016/j.polymdegradstab.2004.12.016.

[108] J. Zhang, Z. Li, L. Zhang, J. García Molleja, D.-Y. Wang, Bimetallic metal-organic frameworks and graphene oxide nano-hybrids for enhanced fire retardant epoxy composites: A novel carbonization mechanism, Carbon 153 (2019) 407–416. https://doi.org/10.1016/j.carbon.2019.07.003.

[109] Fabien Carpentier, Serge Bourbigot, Michel Le Bras, ReneÂ Delobel, Michel Foulon, Charring of ®re retarded ethylene vinyl acetate copolymer Ð magnesium hydroxide/zinc borate formulations, Polymer Degradation and Stability 69 (2000) 83–92.

[110] Serge Bourbigot, Michel Le Bras Robert Leeuwendal, Kelvin K. Shen, David Schubert, Recent advances in the use of zinc borates in ¯ame retardancy of EVA, Polymer Degradation and Stability 64 (1999) 419–425.

[111] H. Balakrishnan, A. Hassan, N.A. Isitman, C. Kaynak, On the use of magnesium hydroxide towards halogen-free flame-retarded polyamide-6/polypropylene blends, Polymer Degradation and Stability 97 (2012) 1447–1457. https://doi.org/10.1016/j.polymdegradstab.2012.05.011.

[112] G. Beyer, Flame retardant properties of EVA - nanocomposites and improvements by combination of nanofillers with aluminium trihydrate, Fire and Materials 25 (2001) 193-197. https://doi.org/10.1002/fam.776.

[113] Q. Bi, D. Yao, G.-Z. Yin, J. You, X.-Q. Liu, N. Wang, D.-Y. Wang, Surface engineering of magnesium hydroxide via bioinspired iron-loaded polydopamine as green and efficient strategy to epoxy composites with improved flame retardancy and reduced smoke release, Reactive and Functional Polymers 155 (2020) 104690. https://doi.org/10.1016/j.reactfunctpolym.2020.104690.

[114] S. Bourbigot, S. Duquesne, Z. Sébih, S. Ségura, R. Delobel, Synergistic Aspects of the Combination of Magnesium Hydroxide and Ammonium Polyphosphate in Flame Retardancy of Ethylene-Vinyl Acetate Copolymer, in: C.A. Wilkie, G.L. Nelson (Eds.), Fire and Polymers IV, American Chemical Society, Washington, DC, 2005, pp. 200–212.

[115] S. Elbasuney, Novel multi-component flame retardant system based on nanoscopic aluminium-trihydroxide (ATH), Powder Technology 305 (2017) 538–545. https://doi.org/10.1016/j.powtec.2016.10.038.

[116] K.-C. Cheng, C.-B. Yu, W. Guo, S.-F. Wang, T.-H. Chuang, Y.-H. Lin, Thermal properties and flammability of polylactide nanocomposites with aluminum trihydrate and organoclay, Carbohydrate Polymers 87 (2012) 1119–1123. https://doi.org/10.1016/j.carbpol.2011.08.065.

[117] M. Fu, B. Qu, Synergistic flame retardant mechanism of fumed silica in ethylene-vinyl acetate/magnesium hydroxide blends, Polymer Degradation and Stability 85 (2004) 633–639. https://doi.org/10.1016/j.polymdegradstab.2004.03.002.

[118] L. Haurie, A.I. Fernández, J.I. Velasco, J.M. Chimenos, J.-M. Lopez Cuesta, F. Espiell, Synthetic hydromagnesite as flame retardant. Evaluation of the flame behaviour in a polyethylene matrix, Polymer Degradation and Stability 91 (2006) 989–994. https://doi.org/10.1016/j.polymdegradstab.2005.08.009.

[119] W. He, H. Zhu, Y. Xiang, L. Long, S. Qin, J. Yu, Enhancement of flame retardancy and mechanical properties of polyamide 6 by incorporating an aluminum salt of diisobutylphosphinic combined with organoclay, Polymer Degradation and Stability 144 (2017) 442–453. https://doi.org/10.1016/j.polymdegradstab.2017.09.003.

[120] H. Huang, M. Tian, L. Liu, W. Liang, L. Zhang, Effect of particle size on flame retardancy of Mg(OH) 2 - filled ethylene vinyl acetate copolymer composites, J of Applied Polymer Sci 100 (2006) 4461-4469. https://doi.org/10.1002/app.22677.

[121] F. Laoutid, L. Ferry, E. Leroy, J.M. Lopez Cuesta, Intumescent mineral fire retardant systems in ethylene–vinyl acetate copolymer: Effect of silica particles on char cohesion, Polymer Degradation and Stability 91 (2006) 2140–2145. https://doi.org/10.1016/j.polymdegradstab.2006.01.010.

[122] F. Laoutid, P. Gaudon, J.-M. Taulemesse, J.M. Lopez Cuesta, J.I. Velasco, A. Piechaczyk, Study of hydromagnesite and magnesium hydroxide based fire retardant systems for ethylene–vinyl acetate containing organo-modified montmorillonite, Polymer Degradation and Stability 91 (2006) 3074–3082. https://doi.org/10.1016/j.polymdegradstab.2006.08.011.

[123] F. Laoutid, M. Lorgouilloux, D. Lesueur, L. Bonnaud, P. Dubois, Calcium-based hydrated minerals: Promising halogen-free flame retardant and fire resistant additives for polyethylene and ethylene vinyl acetate copolymers, Polymer Degradation and Stability 98 (2013) 1617–1625. https://doi.org/10.1016/j.polymdegradstab.2013.06.020.

[124] J. Lenża, K. Merkel, H. Rydarowski, Comparison of the effect of montmorillonite, magnesium hydroxide and a mixture of both on the flammability properties and mechanism of char formation of HDPE composites, Polymer Degradation and Stability 97 (2012) 2581–2593. https://doi.org/10.1016/j.polymdegradstab.2012.07.010.

[125] L. Song, Y. Hu, Z. Lin, S. Xuan, S. Wang, Z. Chen, W. Fan, Preparation and properties of halogen-free flame-retarded polyamide 6/organoclay nanocomposite, Polymer Degradation and Stability 86 (2004) 535–540. https://doi.org/10.1016/j.polymdegradstab.2004.06.007.

[126] R. Suihkonen, K. Nevalainen, O. Orell, M. Honkanen, L. Tang, H. Zhang, Z. Zhang, J. Vuorinen, Performance of epoxy filled with nano- and micro-sized Magnesium hydroxide, J Mater Sci 47 (2012) 1480–1488. https://doi.org/10.1007/s10853-011-5933-6.

[127] H. Wang, X. Shi, S. Zhao, Effects of Magnesium Hydroxide on the Flame Retardancy of Ethylene-Vinyl Acetate Copolymers/Nitrile Rubber Blends, Journal of Macromolecular Science, Part B 53 (2014) 769–780. https://doi.org/10.1080/00222348.2013.861301.

[128] L. Wang, X. Wu, C. Wu, J. Yu, G. Wang, P. Jiang, Study on the flame retardancy of EVM/magnesium hydroxide composites optimized with a flame retardant containing phosphorus and silicon, J of Applied Polymer Sci 121 (2011) 68–77. https://doi.org/10.1002/app.33226.

[129] C.A. Wilkie, G.L. Nelson (Eds.), Fire and Polymers IV, American Chemical Society, Washington, DC, 2005.

[130] Y. Yang, M. Niu, J. Li, B. Xue, J. Dai, Preparation of carbon microspheres coated magnesium hydroxide and its application in polyethylene terephthalate as flame retardant, Polymer Degradation and Stability 134 (2016) 1–9. https://doi.org/10.1016/j.polymdegradstab.2016.09.019.

[131] Y.-Y. Yen, H.-T. Wang, W.-J. Guo, Synergistic flame retardant effect of metal hydroxide and nanoclay in EVA composites, Polymer Degradation and Stability 97 (2012) 863–869. https://doi.org/10.1016/j.polymdegradstab.2012.03.043.

[132] S. Zhang, X. Bu, X. Gu, J. Sun, H. Li, W. Tang, Improving the mechanical properties and flame retardancy of ethylene - vinyl acetate copolymer by introducing bis [3 - (triethoxysilyl) propyl] tetrasulfide modified magnesium hydroxide, Surface & Interface Analysis 49 (2017) 607–614. https://doi.org/10.1002/sia.6199.

[133] R. Zhou, Z. Ming, J. He, Y. Ding, J. Jiang, Effect of Magnesium Hydroxide and Aluminum Hydroxide on the Thermal Stability, Latent Heat and Flammability Properties of Paraffin/HDPE Phase Change Blends, Polymers (Basel) 12 (2020). https://doi.org/10.3390/polym12010180.

[134] W. Chen, Y. Jiang, R. Qiu, W. Xu, Y. Hou, Investigation of UiO-66 as Flame Retardant and Its Application in Improving Fire Safety of Polystyrene, Macromol. Res. 28 (2020) 42–50. https://doi.org/10.1007/s13233-019-7165-6.

[135] X. Chen, X. Chen, S. Li, C. Jiao, Copper metal - organic framework toward flame - retardant enhancement of thermoplastic polyurethane elastomer composites based on ammonium polyphosphate, Polymers for Advanced Techs 32 (2021) 2829-2842. https://doi.org/10.1002/pat.5260.

[136] R. Duan, H. Wu, J. Li, Z. Zhou, W. Meng, L. Liu, H. Qu, J. Xu, Phosphor nitrile functionalized UiO-66-NH2/graphene hybrid flame retardants for fire safety of epoxy, Colloids and Surfaces A: Physicochemical and Engineering Aspects 635 (2022) 128093. https://doi.org/10.1016/j.colsurfa.2021.128093.

[137] X. Fan, F. Xin, W. Zhang, H. Liu, Effect of phosphorus-containing modified UiO-66-NH2 on flame retardant and mechanical properties of unsaturated polyester, Reactive and Functional Polymers 174 (2022) 105260. https://doi.org/10.1016/j.reactfunctpolym.2022.105260.

[138] H. Guo, Y. Wang, C. Li, K. Zhou, Construction of sandwich-structured CoAl-layered double hydroxide@zeolitic imidazolate framework-67 (CoAl-LDH@ZIF-67) hybrids: towards enhancing the fire safety of epoxy resins, RSC Adv. 8 (2018) 36114–36122. https://doi.org/10.1039/c8ra06355a.

[139] W. Guo, S. Nie, E.N. Kalali, X. Wang, W. Wang, W. Cai, L. Song, Y. Hu, Construction of SiO2@UiO-66 core–shell microarchitectures through covalent linkage as flame retardant and smoke suppressant for epoxy resins, Composites

Part B: Engineering 176 (2019) 107261. https://doi.org/10.1016/j.compositesb.2019.107261.

[140] Y. Hou, W. Hu, Z. Gui, Y. Hu, A novel Co(Ⅱ)-based metal-organic framework with phosphorus-containing structure: Build for enhancing fire safety of epoxy, Composites Science and Technology 152 (2017) 231-242. https://doi.org/10.1016/j.compscitech.2017.08.032.

[141] Y. Hou, W. Hu, Z. Gui, Y. Hu, Preparation of Metal–Organic Frameworks and Their Application as Flame Retardants for Polystyrene, Ind. Eng. Chem. Res. 56 (2017) 2036–2045. https://doi.org/10.1021/acs.iecr.6b04920.

[142] Y. Hou, L. Liu, S. Qiu, X. Zhou, Z. Gui, Y. Hu, DOPO-Modified Two-Dimensional Co-Based Metal-Organic Framework: Preparation and Application for Enhancing Fire Safety of Poly(lactic acid), ACS Appl. Mater. Interfaces 10 (2018) 8274–8286. https://doi.org/10.1021/acsami.7b19395.

[143] Y. Hou, S. Qiu, Z. Xu, F. Chu, C. Liao, Z. Gui, L. Song, Y. Hu, W. Hu, Which part of metal-organic frameworks affects polymers' heat release, smoke emission and CO production behaviors more significantly, metallic component or organic ligand?, Composites Part B: Engineering 223 (2021) 109131. https://doi.org/10.1016/j.compositesb.2021.109131.

[144] J. Huang, W. Guo, X. Wang, H. Niu, L. Song, Y. Hu, Combination of cardanol-derived flame retardant with SiO2@MOF particles for simultaneously enhancing the toughness, anti-flammability and smoke suppression of epoxy thermosets, Composites Communications 27 (2021) 100904. https://doi.org/10.1016/j.coco.2021.100904.

[145] R. Huang, X. Guo, S. Ma, J. Xie, J. Xu, J. Ma, Novel Phosphorus-Nitrogen-Containing Ionic Liquid Modified Metal-Organic Framework as an Effective Flame Retardant for Epoxy Resin, Polymers (Basel) 12 (2020). https://doi.org/10.3390/polym12010108.

[146] A. Kathuria, M.G. Abiad, R. Auras, Toughening of poly(l-lactic acid) with Cu3BTC2 metal organic framework crystals, Polymer 54 (2013) 6979–6986. https://doi.org/10.1016/j.polymer.2013.11.005.

[147] A. Li, W. Xu, R. Chen, Y. Liu, W. Li, Fabrication of zeolitic imidazolate frameworks on layered double hydroxide nanosheets to improve the fire safety of epoxy resin, Composites Part A: Applied Science and Manufacturing 112 (2018) 558–571. https://doi.org/10.1016/j.compositesa.2018.07.001.

[148] X. Li, F. Zhang, M. Zhang, X. Zhou, H. Zhang, Comparative Study on the Flame Retardancy and Retarding Mechanism of Rare Earth (La, Ce, and Y)-Based Organic Frameworks on Epoxy Resin, ACS Omega 6 (2021) 35548–35558. https://doi.org/10.1021/acsomega.1c05088.

[149] Y. Li, X. Li, Y.-T. Pan, X. Xu, Y. Song, R. Yang, Mitigation the release of toxic PH3 and the fire hazard of PA6/AHP composite by MOFs, J. Hazard. Mater. 395 (2020) 122604. https://doi.org/10.1016/j.jhazmat.2020.122604.

[150] X. Liu, P. Guo, B. Zhang, J. Mu, A novel ternary inorganic–organic hybrid flame retardant containing biomass and MOFs for high-performance rigid polyurethane foam, Colloids and Surfaces A: Physicochemical and Engineering Aspects 671 (2023) 131625. https://doi.org/10.1016/j.colsurfa.2023.131625.

[151] X. Lu, A.F. Lee, X. Gu, Improving the flame retardancy of sustainable lignin-based epoxy resins using phosphorus/nitrogen treated cobalt metal-organic frameworks, Materials Today Chemistry 26 (2022) 101184. https://doi.org/10.1016/j.mtchem.2022.101184.

[152] Lu Zhang, Siqi Chen, Ye-Tang Pan, Shuidong Zhang, Shibin Nie, Ping Wei, Xiuqin Zhang, Rui Wang, and De-Yi Wang, Nickel Metal-Organic Framework derived Hierarchically Mesoporous Nickel Phosphate towards Smoke Suppression and Mechanical Enhancement of Intumescent Flame Retardant Wood Fiber/Poly(lactic acid) Composites.

[153] X. Lv, W. Zeng, Z. Yang, Y. Yang, Y. Wang, Z. Lei, J. Liu, D. Chen, Fabrication of ZIF - 8@Polyphosphazene core - shell structure and its efficient synergism with ammonium polyphosphate in flame - retarding epoxy resin, Polymers for Advanced Techs 31 (2020) 997–1006. https://doi.org/10.1002/pat.4834.

[154] T. Ma, W. Wang, R. Wang, Thermal Degradation and Carbonization Mechanism of Fe-Based Metal-Organic Frameworks onto Flame-Retardant Polyethylene Terephthalate, Polymers (Basel) 15 (2023). https://doi.org/10.3390/polym15010224.

[155] E.M. Mahdi, J.-C. Tan, Dynamic molecular interactions between polyurethane and ZIF-8 in a polymer-MOF nanocomposite: Microstructural, thermo-mechanical and viscoelastic effects, Polymer 97 (2016) 31–43. https://doi.org/10.1016/j.polymer.2016.05.012.

[156] W. Meng, H. Wu, X. Bi, Z. Huo, J. Wu, Y. Jiao, J. Xu, M. Wang, H. Qu, Synthesis of ZIF-8 with encapsulated hexachlorocyclotriphosphazene and its quenching mechanism for flame-retardant epoxy resin, Microporous and Mesoporous Materials 314 (2021) 110885. https://doi.org/10.1016/j.micromeso.2021.110885.

[157] H. Nabipour, X. Wang, L. Song, Y. Hu, Organic-inorganic hybridization of isoreticular metal-organic framework-3 with melamine for efficiently reducing the fire risk of epoxy resin, Composites Part B: Engineering 211 (2021) 108606. https://doi.org/10.1016/j.compositesb.2021.108606.

[158] X.-L. Qi, D.-D. Zhou, J. Zhang, S. Hu, M. Haranczyk, D.-Y. Wang, Simultaneous Improvement of Mechanical and Fire-Safety Properties of Polymer Composites with Phosphonate-Loaded MOF Additives, ACS Appl. Mater. Interfaces 11 (2019) 20325–20332. https://doi.org/10.1021/acsami.9b02357.

[159] Z. Qian, B. Zou, Y. Xiao, S. Qiu, Z. Xu, Y. Yang, G. Jiang, Z. Zhang, L. Song, Y. Hu, Targeted modification of black phosphorus by MIL-53(Al) inspired by "Cannikin's Law" to achieve high thermal stability of flame retardant polycarbonate at ultra-low additions, Composites Part B: Engineering 238 (2022) 109943. https://doi.org/10.1016/j.compositesb.2022.109943.

[160] S. Qiu, Y. Zhou, X. Zhou, T. Zhang, C. Wang, R.K.K. Yuen, W. Hu, Y. Hu, Air-Stable Polyphosphazene-Functionalized Few-Layer Black Phosphorene for Flame Retardancy of Epoxy Resins, Small 15 (2019) e1805175. https://doi.org/10.1002/smll.201805175.

[161] T. Sai, S. Ran, Z. Guo, Z. Fang, A Zr-based metal organic frameworks towards improving fire safety and thermal stability of polycarbonate, Composites Part B: Engineering 176 (2019) 107198. https://doi.org/10.1016/j.compositesb.2019.107198.

[162] L. Sang, Y. Cheng, R. Yang, J. Li, Q. Kong, J. Zhang, Polyphosphazene-wrapped Fe–MOF for improving flame retardancy and smoke suppression of epoxy resins, J Therm Anal Calorim 144 (2021) 51–59. https://doi.org/10.1007/s10973-020-09481-6.

[163] Z.-B. Shao, J. Zhang, R.-K. Jian, C.-C. Sun, X.-L. Li, D.-Y. Wang, A strategy to construct multifunctional ammonium polyphosphate for epoxy resin with simultaneously high fire safety and mechanical properties, Composites Part A: Applied Science and Manufacturing 149 (2021) 106529. https://doi.org/10.1016/j.compositesa.2021.106529.

[164] R. Shen, T.-H. Yan, R. Ma, E. Joseph, Y. Quan, H.-C. Zhou, Q. Wang, Flammability and Thermal Kinetic Analysis of UiO-66-Based PMMA Polymer Composites, Polymers (Basel) 13 (2021). https://doi.org/10.3390/polym13234113.

[165] K. Song, B. Hou, Z. Ur Rehman, Y.-T. Pan, J. He, D.-Y. Wang, R. Yang, "Sloughing" of metal-organic framework retaining nanodots via step-by-step carving and its flame-retardant effect in epoxy resin, Chemical Engineering Journal 448 (2022) 137666. https://doi.org/10.1016/j.cej.2022.137666.

[166] K. Song, Y. Wang, F. Ruan, W. Yang, Z. Fang, D. Zheng, X. Li, N. Li, M. Qiao, J. Liu, Synthesis of a Reactive Template-Induced Core-Shell PZS@ZIF-67 Composite Microspheres and Its Application in Epoxy Composites, Polymers (Basel) 13 (2021). https://doi.org/10.3390/polym13162646.

[167] V. Unnikrishnan, O. Zabihi, Q. Li, M. Ahmadi, M.R.G. Ferdowsi, T. Kannangara, P. Blanchard, A. Kiziltas, P. Joseph, M. Naebe, Multifunctional PA6 composites using waste glass fiber and green metal organic framework/graphene hybrids, Polymer Composites 43 (2022) 5877–5893. https://doi.org/10.1002/pc.27002.

[168] M. Wan, C. Shi, X. Qian, Y. Qin, J. Jing, H. Che, Metal-organic Framework ZIF-67 Functionalized MXene for Enhancing the Fire Safety of Thermoplastic Polyurethanes, Nanomaterials (Basel) 12 (2022). https://doi.org/10.3390/nano12071142.

[169] H. Wang, H. Qiao, J. Guo, J. Sun, H. Li, S. Zhang, X. Gu, Preparation of cobalt-based metal organic framework and its application as synergistic flame retardant in thermoplastic polyurethane (TPU), Composites Part B: Engineering 182 (2020) 107498. https://doi.org/10.1016/j.compositesb.2019.107498.

[170] J. Wang, Y. Liu, X. Guo, H. Qu, R. Chang, J. Ma, Efficient Adsorption of Dyes Using Polyethyleneimine-Modified NH2-MIL-101(Al) and its Sustainable Application as a Flame Retardant for an Epoxy Resin, ACS Omega 5 (2020) 32286–32294. https://doi.org/10.1021/acsomega.0c04118.

[171] R. Wang, Y. Chen, Y. Liu, M. Ma, Z. Tong, X. Chen, Y. Bi, W. Huang, Z. Liao, S. Chen, X. Zhang, Q. Li, Metal - organic frameworks derived ZnO @ MOF @ PZS flame retardant for reducing fire hazards of polyurea nanocomposites, Polymers for Advanced Techs 32 (2021) 4700–4709. https://doi.org/10.1002/pat.5462.

[172] X.G. Wang, P. Qi, S.J. Zhang, S.L. Jiang, Y.C. Li, J. Sun, B. Fei, X.Y. Gu, S. Zhang, A novel flame-retardant modification strategy for UiO66-NH2 by encapsulating triethyl phosphate: preparation, characterization, and multifunctional application in poly (lactic acid), Materials Today Chemistry 30 (2023) 101550. https://doi.org/10.1016/j.mtchem.2023.101550.

[173] X. Wang, S. Wang, W. Wang, H. Li, X. Liu, X. Gu, S. Bourbigot, Z. Wang, J. Sun, S. Zhang, The flammability and mechanical properties of poly (lactic acid) composites containing Ni-MOF nanosheets with polyhydroxy groups, Composites Part B: Engineering 183 (2020) 107568. https://doi.org/10.1016/j.compositesb.2019.107568.

[174] B. Xu, W. Xu, G. Wang, L. Liu, J. Xu, Zeolitic imidazolate frameworks - 8 modified graphene as a green flame retardant for reducing the fire risk of epoxy resin, Polymers for Advanced Techs 29 (2018) 1733-1743. https://doi.org/10.1002/pat.4278.

[175] W. Xu, Z. Cheng, Di Zhong, Z. Qin, N. Zhou, W. Li, Effect of two - dimensional zeolitic imidazolate frameworks - L on flame retardant property of thermoplastic polyurethane elastomers, Polymers for Advanced Techs 32 (2021) 2072-2081. https://doi.org/10.1002/pat.5237.

[176] W. Xu, L. Fan, Z. Qin, Y. Liu, M. Li, Silica-coated metal-organic framework-β-FeOOH hybrid for improving the flame retardant and smoke suppressive properties of epoxy resin, Plastics, Rubber and Composites 50 (2021) 396–405. https://doi.org/10.1080/14658011.2021.1909232.

[177] W. Xu, G. Wang, Y. Liu, R. Chen, W. Li, Zeolitic imidazolate framework-8 was coated with silica and investigated as a flame retardant to improve the flame retardancy and smoke suppression of epoxy resin, RSC Adv. 8 (2018) 2575–2585. https://doi.org/10.1039/c7ra12816a.

[178] W. Xu, X. Wang, Y. Wu, W. Li, C. Chen, Functionalized graphene with Co-ZIF adsorbed borate ions as an effective flame retardant and smoke suppression agent for epoxy resin, J. Hazard. Mater. 363 (2019) 138–151. https://doi.org/10.1016/j.jhazmat.2018.09.086.

[179] Z. Xu, W. Xing, Y. Hou, B. Zou, L. Han, W. Hu, Y. Hu, The combustion and pyrolysis process of flame-retardant polystyrene/cobalt-based metal organic frameworks (MOF) nanocomposite, Combustion and Flame 226 (2021) 108–116. https://doi.org/10.1016/j.combustflame.2020.11.013.

[180] J. Yang, A. Zhang, Y. Chen, L. Wang, M. Li, H. Yang, Y. Hou, Surface modification of core–shell structured ZIF-67@Cobalt coordination compound to improve the fire safety of biomass aerogel insulation materials, Chemical Engineering Journal 430 (2022) 132809. https://doi.org/10.1016/j.cej.2021.132809.

[181] X. Yang, L. Zhao, F. Peng, Y. Zhu, G. Wang, Co-based metal-organic framework with phosphonate and triazole structures for enhancing fire retardancy of epoxy resin, Polymer Degradation and Stability 193 (2021) 109721. https://doi.org/10.1016/j.polymdegradstab.2021.109721.

[182] S. Yu, C. Cheng, K. Li, J. Wang, Z. Wang, H. Zhou, W. Wang, Y. Zhang, Y. Quan, Fire-safe epoxy composite realized by MXenes based nanostructure with vertically arrayed MOFs derived from interfacial assembly strategy, Chemical Engineering Journal 465 (2023) 143039. https://doi.org/10.1016/j.cej.2023.143039.

[183] X. Yang, B.L. Bonnett, G.A. Spiering, H.D. Cornell, B.J. Gibbons, R.B. Moore, E.J. Foster, A.J. Morris, Understanding the Mechanical Reinforcement of Metal-Organic Framework-Polymer Composites: The Effect of Aspect Ratio, ACS Appl. Mater. Interfaces 13 (2021) 51894–51905. https://doi.org/10.1021/acsami.1c05430.

[184] F. Zhang, X. Li, L. Yang, Y. Zhang, M. Zhang, A Mo - based metal - organic framework toward improving flame retardancy and smoke suppression of epoxy resin, Polymers for Advanced Techs 32 (2021) 3266-3277. https://doi.org/10.1002/pat.5338.

[185] G. Zhang, W. Wu, M. Yao, Z. Wu, Y. Jiao, H. Qu, Novel triazine-based metal-organic frameworks: Synthesis and mulifunctional application of flame retardant, smoke suppression and toxic attenuation on EP, Materials & Design 226 (2023) 111664. https://doi.org/10.1016/j.matdes.2023.111664.

[186] J. Zhang, Z. Li, X. Qi, W. Zhang, D.-Y. Wang, Size tailored bimetallic metal-organic framework (MOF) on graphene oxide with sandwich-like structure as functional nano-hybrids for improving fire safety of epoxy, Composites Part B: Engineering 188 (2020) 107881. https://doi.org/10.1016/j.compositesb.2020.107881.

[187] J. Zhang, Z. Li, Z.-B. Shao, L. Zhang, D.-Y. Wang, Hierarchically tailored hybrids via interfacial-engineering of self-assembled UiO-66 and prussian blue analogue: Novel strategy to impart epoxy high-efficient fire retardancy and smoke

suppression, Chemical Engineering Journal 400 (2020) 125942. https://doi.org/10.1016/j.cej.2020.125942.

[188] J. Zhang, Z. Li, G.-Z. Yin, D.-Y. Wang, Construction of a novel three-in-one biomass based intumescent fire retardant through phosphorus functionalized metal-organic framework and ß-cyclodextrin hybrids in achieving fire safe epoxy, Composites Communications 23 (2021) 100594. https://doi.org/10.1016/j.coco.2020.100594.

[189] J. Zhang, Z. Li, L. Zhang, J. García Molleja, D.-Y. Wang, Bimetallic metal-organic frameworks and graphene oxide nano-hybrids for enhanced fire retardant epoxy composites: A novel carbonization mechanism, Carbon 153 (2019) 407–416. https://doi.org/10.1016/j.carbon.2019.07.003.

[190] J. Zhang, Z. Li, L. Zhang, Y. Yang, D.-Y. Wang, Green Synthesis of Biomass Phytic Acid-Functionalized UiO-66-NH 2 Hierarchical Hybrids toward Fire Safety of Epoxy Resin, ACS Sustainable Chem. Eng. 8 (2020) 994–1003. https://doi.org/10.1021/acssuschemeng.9b05658.

[191] Y. Zheng, Y. Lu, K. Zhou, A novel exploration of metal–organic frameworks in flame-retardant epoxy composites, J Therm Anal Calorim 138 (2019) 905–914. https://doi.org/10.1007/s10973-019-08267-9.

[192] H.V. Babu, C. Coluccini, D.-Y. Wang, Functional layered double hydroxides and their use in fire-retardant polymeric materials 201–238. https://doi.org/10.1016/B978-0-08-100136-3.00008-X.

[193] D. Basu, A. Das, J.J. George, D.-Y. Wang, K.W. Stöckelhuber, U. Wagenknecht, A. Leuteritz, B. Kutlu, U. Reuter, G. Heinrich, UNMODIFIED LDH AS REINFORCING FILLER FOR XNBR AND THE DEVELOPMENT OF FLAME-RETARDANT ELASTOMER COMPOSITES, Rubber Chemistry and Technology 87 (2014) 606–616. https://doi.org/10.5254/rct.14.86920.

[194] J. Cai, H.-M. Heng, X.-P. Hu, Q.-K. Xu, F. Miao, A facile method for the preparation of novel fire-retardant layered double hydroxide and its application as nanofiller in UP, Polymer Degradation and Stability 126 (2016) 47–57. https://doi.org/10.1016/j.polymdegradstab.2016.01.013.

[195] Calistor Nyambo, Dan Chen, Shengpei Shu, and Charles A. Wilkie, Does organic modification of layered double hydroxides improve the fire performance of PMMA?

[196] Calistor Nyambo, Everson Kandare, and Charles A. Wilkie, Thermal stability and flammability characteristics of ethylene vinyl acetate (EVA) composites blended with a phenyl phosphonate-intercalated layered double hydroxide (LDH), melamine polyphosphate and/or boric acid.

[197] Charles Manzi-Nshuti, Jeanne Hossenlopp, and Charles A. Wilkie, Comparative Study on the Flammability of Polyethylene Modified with Commercial Fire Retardants and a Zinc Aluminum Oleate Layered Double Hydroxide.

[198] F.R. Costa, U. Wagenknecht, G. Heinrich, LDPE/Mg–Al layered double hydroxide nanocomposite: Thermal and flammability properties, Polymer Degradation and Stability 92 (2007) 1813–1823. https://doi.org/10.1016/j.polymdegradstab.2007.07.009.

[199] A. Edenharter, J. Breu, Applying the flame retardant LDH as a Trojan horse for molecular flame retardants, Applied Clay Science 114 (2015) 603–608. https://doi.org/10.1016/j.clay.2015.07.013.

[200] G. Huang, S. Chen, P. Song, P. Lu, C. Wu, H. Liang, Combination effects of graphene and layered double hydroxides on intumescent flame-retardant poly(methyl methacrylate) nanocomposites, Applied Clay Science 88-89 (2014) 78–85. https://doi.org/10.1016/j.clay.2013.11.002.

[201] G. Huang, Z. Fei, X. Chen, F. Qiu, X. Wang, J. Gao, Functionalization of layered double hydroxides by intumescent flame retardant: Preparation, characterization, and application in ethylene vinyl acetate copolymer, Applied Surface Science 258 (2012) 10115–10122. https://doi.org/10.1016/j.apsusc.2012.06.088.

[202] G. Huang, A. Zhuo, L. Wang, X. Wang, Preparation and flammability properties of intumescent flame retardant-functionalized layered double hydroxides/polymethyl methacrylate nanocomposites, Materials Chemistry and Physics 130 (2011) 714–720. https://doi.org/10.1016/j.matchemphys.2011.07.047.

[203] S.-D. Jiang, Z.-M. Bai, G. Tang, L. Song, A.A. Stec, T.R. Hull, Y. Hu, W.-Z. Hu, Synthesis of mesoporous silica@Co-Al layered double hydroxide spheres: layer-by-layer method and their effects on the flame retardancy of epoxy resins, ACS Appl. Mater. Interfaces 6 (2014) 14076–14086. https://doi.org/10.1021/am503412y.

[204] E.N. Kalali, A. Montes, X. Wang, L. Zhang, M.E. Shabestari, Z. Li, D.-Y. Wang, Effect of phytic acid–modified layered double hydroxide on flammability and mechanical properties of intumescent flame retardant polypropylene system, Fire and Materials 42 (2018) 213–220. https://doi.org/10.1002/fam.2482.

[205] E.N. Kalali, X. Wang, D.-Y. Wang, Functionalized layered double hydroxide-based epoxy nanocomposites with improved flame retardancy and mechanical properties, J. Mater. Chem. A 3 (2015) 6819–6826. https://doi.org/10.1039/C5TA00010F.

[206] E.N. Kalali, X. Wang, D.-Y. Wang, Multifunctional intercalation in layered double hydroxide: toward multifunctional nanohybrids for epoxy resin, J. Mater. Chem. A 4 (2016) 2147–2157. https://doi.org/10.1039/C5TA09482H.

[207] C. Li, J. Wan, E.N. Kalali, H. Fan, D.-Y. Wang, Synthesis and characterization of functional eugenol derivative based layered double hydroxide and its use as a nanoflame-retardant in epoxy resin, J. Mater. Chem. A 3 (2015) 3471–3479. https://doi.org/10.1039/C4TA05740F.

[208] Z. Li, Z. Liu, F. Dufosse, L. Yan, D.-Y. Wang, Interfacial engineering of layered double hydroxide toward epoxy resin with improved fire safety and mechanical

property, Composites Part B: Engineering 152 (2018) 336–346. https://doi.org/10.1016/j.compositesb.2018.08.094.

[209] Z. Li, J. Zhang, F. Dufosse, D.-Y. Wang, Ultrafine nickel nanocatalyst-engineering of an organic layered double hydroxide towards a super-efficient fire-safe epoxy resin via interfacial catalysis, J. Mater. Chem. A 6 (2018) 8488–8498. https://doi.org/10.1039/C8TA00910D.

[210] Linjiang Wang, Shengpei Shu, Dan Chen, and Charles A. Wilkie, Variation of anions in layered double hydroxides: Effects on dispersion and fire properties.

[211] C. Manzi-Nshuti, P. Songtipya, E. Manias, M.M. Jimenez-Gasco, J.M. Hossenlopp, C.A. Wilkie, Polymer nanocomposites using zinc aluminum and magnesium aluminum oleate layered double hydroxides: Effects of LDH divalent metals on dispersion, thermal, mechanical and fire performance in various polymers, Polymer 50 (2009) 3564–3574. https://doi.org/10.1016/j.polymer.2009.06.014.

[212] C. Manzi-Nshuti, D. Wang, J.M. Hossenlopp, C.A. Wilkie, Aluminum-containing layered double hydroxides: the thermal, mechanical, and fire properties of (nano)composites of poly(methyl methacrylate), J. Mater. Chem. 18 (2008) 3091. https://doi.org/10.1039/b802553c.

[213] Z. Matusinovic, J. Feng, C.A. Wilkie, The role of dispersion of LDH in fire retardancy: The effect of different divalent metals in benzoic acid modified LDH on dispersion and fire retardant properties of polystyrene– and poly(methyl-methacrylate)–LDH–B nanocomposites, Polymer Degradation and Stability 98 (2013) 1515–1525. https://doi.org/10.1016/j.polymdegradstab.2013.04.007.

[214] C. Nyambo, P. Songtipya, E. Manias, M.M. Jimenez-Gasco, C.A. Wilkie, Effect of MgAl-layered double hydroxide exchanged with linear alkyl carboxylates on fire-retardancy of PMMA and PS, J. Mater. Chem. 18 (2008) 4827. https://doi.org/10.1039/b806531d.

[215] C. Nyambo, D. Wang, C.A. Wilkie, Will layered double hydroxides give nanocomposites with polar or non - polar polymers?, Polymers for Advanced Techs 20 (2009) 332-340. https://doi.org/10.1002/pat.1272.

[216] C. Nyambo, C.A. Wilkie, Layered double hydroxides intercalated with borate anions: Fire and thermal properties in ethylene vinyl acetate copolymer, Polymer Degradation and Stability 94 (2009) 506–512. https://doi.org/10.1016/j.polymdegradstab.2009.02.001.

[217] Y.-T. Pan, J. Wan, X. Zhao, C. Li, D.-Y. Wang, Interfacial growth of MOF-derived layered double hydroxide nanosheets on graphene slab towards fabrication of multifunctional epoxy nanocomposites, Chemical Engineering Journal 330 (2017) 1222–1231. https://doi.org/10.1016/j.cej.2017.08.059.

[218] D.-Y. Wang, A. Das, A. Leuteritz, R.N. Mahaling, D. Jehnichen, U. Wagenknecht, G. Heinrich, Structural characteristics and flammability of fire retarding

EPDM/layered double hydroxide (LDH) nanocomposites, RSC Adv. 2 (2012) 3927. https://doi.org/10.1039/c2ra20189e.

[219] X. Wang, E.N. Kalali, D.-Y. Wang, Renewable Cardanol-Based Surfactant Modified Layered Double Hydroxide as a Flame Retardant for Epoxy Resin, ACS Sustainable Chem. Eng. 3 (2015) 3281–3290. https://doi.org/10.1021/acssuschemeng.5b00871.

[220] X. Wang, Y. Spörer, A. Leuteritz, I. Kuehnert, U. Wagenknecht, G. Heinrich, D.-Y. Wang, Comparative study of the synergistic effect of binary and ternary LDH with intumescent flame retardant on the properties of polypropylene composites, RSC Adv. 5 (2015) 78979–78985. https://doi.org/10.1039/C5RA15565G.

[221] X. Wang, S. Zhou, W. Xing, B. Yu, X. Feng, L. Song, Y. Hu, Self-assembly of Ni–Fe layered double hydroxide/graphene hybrids for reducing fire hazard in epoxy composites, J. Mater. Chem. A 1 (2013) 4383. https://doi.org/10.1039/c3ta00035d.

[222] S. Xu, L. Zhang, Y. Lin, R. Li, F. Zhang, Layered double hydroxides used as flame retardant for engineering plastic acrylonitrile–butadiene–styrene (ABS), Journal of Physics and Chemistry of Solids 73 (2012) 1514–1517. https://doi.org/10.1016/j.jpcs.2012.04.011.

[223] W. Xu, B. Zhang, X. Wang, G. Wang, D. Ding, The flame retardancy and smoke suppression effect of a hybrid containing CuMoO4 modified reduced graphene oxide/layered double hydroxide on epoxy resin, J. Hazard. Mater. 343 (2018) 364–375. https://doi.org/10.1016/j.jhazmat.2017.09.057.

[224] W. Xu, B. Zhang, B. Xu, A. Li, The flame retardancy and smoke suppression effect of heptaheptamolybdate modified reduced graphene oxide/layered double hydroxide hybrids on polyurethane elastomer, Composites Part A: Applied Science and Manufacturing 91 (2016) 30–40. https://doi.org/10.1016/j.compositesa.2016.09.013.

[225] L. Zhang, J. Zhang, D.-Y. Wang, Hierarchical layered double hydroxide nanosheets/phosphorus-containing organosilane functionalized hollow glass microsphere towards high performance epoxy composite: Enhanced interfacial adhesion and bottom-up charring behavior, Polymer 210 (2020) 123018. https://doi.org/10.1016/j.polymer.2020.123018.

[226] Z. Zhang, J. Qin, W. Zhang, Y.-T. Pan, D.-Y. Wang, R. Yang, Synthesis of a novel dual layered double hydroxide hybrid nanomaterial and its application in epoxy nanocomposites, Chemical Engineering Journal 381 (2020) 122777. https://doi.org/10.1016/j.cej.2019.122777.

[227] K. Zhou, R. Gao, X. Qian, Self-assembly of exfoliated molybdenum disulfide (MoS2) nanosheets and layered double hydroxide (LDH): Towards reducing fire hazards of epoxy, J. Hazard. Mater. 338 (2017) 343–355. https://doi.org/10.1016/j.jhazmat.2017.05.046.